MODELLING AND EXPERIMENTAL INVESTIGATION OF ARGET/AGET ATOM TRANSFER RADICAL POLYMERIZATION SYSTEMS

by

Ethan Massicotte
B.Eng, Ryerson University, Toronto ON, 2013

A thesis

presented to Ryerson University

in partial fulfillment of the

requirements for the degree of

Master of Applied Science

in the Program of

Chemical Engineering

Toronto, Ontario, Canada, 2016

AUTHOR'S DECLARATION FOR ELECTRONIC SUBMISSION OF A THESIS

I hereby declare that I am the sole author of this thesis. This is a true copy of the thesis, including any required final revisions, as accepted by my examiners.

I authorize Ryerson University to lend this thesis to other institutions or individuals for the purpose of scholarly research.

I further authorize Ryerson University to reproduce this thesis by photocopying or by other means, in total or in part, at the request of other institutions or individuals for the purpose of scholarly research.

I understand that my thesis may be made electronically available to the public.

ABSTRACT

Modelling and Experimental Investigation of ARGET/AGET Atom Transfer Radical Polymerization Systems

Ethan Massicotte

Master of Applied Science in Chemical Engineering,

Ryerson University, Toronto, 2016

Activators Generated by Electron Transfer (AGET) and Activators Regenerated by Electron Transfer (ARGET) Atom Transfer Radical Polymerization (ATRP) are emerging topics within the polymerization field. These techniques allow for better control over polymer structure and polymer size distributions than conventional polymerizations. However, investigations into these processes are lacking, especially from a modelling point of view. Therefore, a kinetic model of the ARGET ATRP of butyl methacrylate (BMA) in a solution medium and Hybrid Monte Carlo model of the AGET ATRP of butyl acrylate (BA) in a dispersed system were developed and compared with data. In addition, an experimental investigation of the AGET ATRP of BA was carried out to study the kinetic aspects of this polymerization. The results of these studies demonstrate that both models have relatively strong predictive powers, and that different kinetic regimes appear to be available within the dispersed system studied experientially.

ACKNOWLEDGEMENTS

"But the mirror will also show things unbidden, and those are often stranger and more profitable than things which we wish to behold".

-J.R.R.Tolkien, The Lord of the Rings

Over my thesis I have had a great deal of luck in that I have had the help and the support of some wonderful people. I would, therefore, like to take some time to extend my gratitude to them in this section.

Firstly, I would like to thank my professors Dr. Ramdhane Dhib and Dr. Thomas Duever for their patience, kindness, financial support, and guidance throughout a difficult topic. My success achieved over my MASc program is due in no small part to them and their fostering of an environment conducive to my growth.

I would also like to thank the technical staff for all their support in both the minor and dire difficulties I experienced. With their help I managed to avoid important impediments which would have surely resulted in further delays in my project.

To my lab mates I would like to express my gratitude for their help during my project. In particular, my colleague and friend Kishor Regmi, whose advice helped me countless times.

I would also like to thank my girlfriend Naadia for her support and love, as well as for her help in editing my thesis, as well as my friends, especially Tony, Vincent, Alex, Mike, and Lenny for their support and the times we have shared together.

Finally, I would like to extend my deepest thanks to my family. I owe the greatest debt to them for their constant support. I would not be where or who I am if it was not for them.

Thank you all!

CONTENTS

LIST OF FIGURES

LIST OF TABLES

LIST OF APPENDICES

CHAPTER 1 : INTRODUCTION

1.1 Overview

Polymers and the chemical industries leading to their production, have become an integral part of contemporary society. With numerous applications, ranging over a wide set of fields, such as automotive, energy, paint, electronic, biomedical, etc. (Chanda and Roy, 2009), it is not at all surprising that polymers have come to assume this role. However, irrespective of this success the polymerization field is continually evolving, and new chemical techniques and technologies are expanding the materials attainable from polymerization processes. Of these advances, one of the most recent and exciting was the development of the controlled (living) radical polymerization (CLRP) methods, which allow for the synthesis of a plenitude of polymers, under relatively mild conditions, with precise chemical architecture and narrow molecular weight distributions (Braunecker and Matyjaszewski, 2007). This breakthrough provided a staunch demarcation between conventional radical polymerization and CLRP, as this level of control over the polymer structure and distribution was unheard of for radical polymerization, and had only previously been attainable in living anionic polymerization.

Owing to its advantages over the conventional radical polymerization process, CLRP has received a lot of attention in both academic and industrial sectors. In this regard, three principle version of the CLRP system have emerged: Nitroxide Mediated Radical Polymerization (NMRP or NMP), Atom Transfer Radical Polymerization (ATRP), and Reversible Addition-Fragmentation Chain Transfer (RAFT) Polymerization. Currently efforts have been undertaken to advance all of these fields in terms of knowledge of their mechanisms, improvements to their core processes, their environmental impact, and their industrial applications. Now while the various CLRP methods have advanced significantly in all these areas, further improvements are still possible, as evidenced in some recent papers; (Destarac, 2010; Monteiro and Cunningham, 2012; Oh, 2008). Of particular importance in this context is fostering a deeper understanding of the CLRP processes in various media.

Consequently, this work will attempt to elucidate some of the phenomenon at play in various ATRP systems. ATRP being selected for study, due to its ability to generate high purity block

copolymers, its good end group functionality, and large range of applicable monomers. This system will be investigated in three main ways: modelling the Activators Regenerated by Electron Transfer Atom Transfer Radical Polymerization (ARGET ATRP) of butyl methacrylate in a solution medium, modelling of the Activators Generated by Electron Transfer Atom Transfer Radical Polymerization (AGET ATRP) of butyl acrylate in a two-stage dispersed medium, and the experimental investigation of the AGET ATRP of butyl acrylate in a two-stage dispersed system. Thus, this thesis will be broken into three parts one for each of the studies given above. It is hoped that through this effort, new knowledge will become available describing the major phenomenon present within these systems.

1.2 Objectives

The main objective of this thesis is to provide further insights into the ATRP process. To accomplish this end, three major studies of the ATRP system will be carried out. From the perspectives of each of these studies the goals of this thesis are specifically:

1. Kinetic modelling of the ARGET ATRP of butyl methacrylate in a solution medium:

- Develop a model to simulate the ARGET ATRP of butyl methacrylate in solution media, providing details on the conversion and molecular weight distributions.
- Compare model predictions with experimental data in open literature and attempt to enhance the quality of the model predictions.
- Use the model to draw conclusions about the nature of the system

2. Modelling of the activators generated by electron transfer atom transfer radical polymerization (AGET ATRP) of butyl acrylate in a two-stage dispersed system:

- Develop a model to simulate the AGET ATRP of butyl acrylate in a two stage dispersed system using a Hybrid Monte Carlo algorithm

- Compare model predictions to experimental data in open literature and modify it such that it is able to capture the general trends of the system.
- Use the model to draw conclusions about the nature of the system

3. Experimental investigation of the AGET ATRP of butyl acrylate in a two-stage dispersed system:

- Determine process conditions under which a controlled radical polymerization occurs.
- Extract data which provides information about the nature of the AGET ATRP process.
- Provide qualitative insights into the behavior of the system.

1.3 Thesis Organization

- Chapter 2 provides background information, as well as a literature review of conventional radical polymerization, controlled radical polymerization, ATRP, dispersed systems, butyl acrylate polymerization, and the use of advanced ATRP systems for polymerization in dispersed mediums;
- Chapter 3 presents the kinetic based modelling work done on the ARGET ATRP of BMA in a solution medium;
- Chapter 4 presents the Hybrid Monte Carlo modelling work done on the AGET ATRP of BA in a two-stage dispersed system;
- Chapter 5 discusses the experimental work done on the AGET ATRP of BA in a two-stage dispersed system. The main focus of this chapter is to explain the experimental trends found within the data;
- Chapter 6 provides an overview of the most important conclusions of this thesis and offers suggestions for future work.

CHAPTER 2 : BACKGROUND AND LITERATURE REVIEW

In this chapter the background necessary to understand the topics of this thesis is given. This requires that a couple of subjects within the polymerization field be introduced. The first subset of these are the characteristics and mechanism of conventional radical polymerization, controlled (living) radical polymerization, and atom transfer radical polymerization (including its modifications). With these details one can form an idea of how the solution ARGET ATRP of butyl methacrylate will evolve, and understand the basic kinetic mechanism underlying the AGET ATRP of butyl acrylate in a two-stage dispersed system. However, as there are some further characteristics which arise as a result of the nature of dispersed systems, a summary of ATRP in emulsified systems, as well as information regarding the unique features of the ATRP of butyl acrylate and its characteristics within dispersed systems will be given.

2.1 Conventional Radical Polymerization

Conventional radical polymerization is one of the oldest and most widely used polymerization techniques (Braun, 2009; Chanda and Roy, 2009). It is classified under the subgroup of polymerization termed chain-growth polymerization. Being grouped as such, it shares a relatively common feature with other chain-growth polymerization reactions, which is that its mechanism can be broken into three elementary parts: initiation, propagation, and termination. Often however in addition to these reactions, radical polymerizations tend to have transfer reactions, wherein a radical transfers its activity to some other molecule. Shown below in Table 2.1 is the general mechanism for the free radical polymerization process. The mechanism as depicted below is only meant to include the main reactions commonly involved in the process.

Table 2.1: Standard Chemical Mechanism for Conventional Free Radical Polymerization

1. Initiation	$I \xrightarrow{k_d} 2R_0^{\cdot}$	(Dissociation/Decompostion of initiator)
	$R_0^{\cdot} + M \xrightarrow{k_i} R_1^{\cdot}$	(Initiation)
2. Propagation	$R_n^{\cdot} + M \xrightarrow{k_p} R_{n+1}^{\cdot}$	(Propagation)
3. Transfer	$R_n^{\cdot} + T \xrightarrow{k_{trt}} P_n + T\cdot$	(Transfer to transfer agent)
4. Termination	$R_n^{\cdot} + R_m\cdot \xrightarrow{k_{tc}} P_{n+m}$	(Combination)
	$R_n^{\cdot} + R_m^{\cdot} \xrightarrow{k_{td}} P_n + P_m$	(Dispropotionation)

Where *I*: initiator, $R_0^{\cdot}$: primary radical generated from the initiator, *M*: monomer, *T*: Transfer agent, $R_1^{\cdot}$: propagating radical of chain length 1, $R_n^{\cdot}$: propagating radical of size n; where n≥1, $R_m^{\cdot}$: propagating radical of size m; where m≥1, $P_{n+m}/P_n/P_m$: are dead polymers of length n+m, n, and m respectively.

As can be seen above the polymerization process begins with the generation of initiator radicals, or as they are also known primary radicals. The primary radicals now active in the media can react with monomer molecules to start the polymerization process in a step called initiation. A very important feature of this reaction is that the newly formed molecules still keep the radical chain end functionality of their predecessor. Due to this conservation of functionality with the addition of monomer, the radicals can continue to grow by consecutively adding monomer units in a step called propagation. It is this step in the polymerization that provides the polymer molecules with their extreme size.

Interestingly, however, there is a limit to the growth of these radicals beyond that set by the amount of monomer present, as chain growth ending reactions such as termination and transfer[1] occur concurrently with propagation. These reactions while serving to end the growth period also have distinct effects on the reaction process. For instance, the effect of termination is that the total number of radicals in the system is reduced below that produced by the initiator, and the polymer

[1] While most transfer reactions result in the formation of dead chains there are some, such as backbiting, which do not.

size can be greatly extended, if the combination mechanism of termination is dominant. However, in the case of transfer reactions, the number of radicals in the system may not be diminished, and in certain circumstances these reactions can result in branching.

With this picture of the free radical system in mind, some of the major advantages and disadvantages of the process can now be pointed out. Its advantages, owing mainly to the nature of the radicals involved, are that it can form large molecules relatively quickly, it has good chemo- and regio-selectivity, can be easily adapted to different polymerization media, is a relatively fast process, and has a large range of applicable monomers (Braunecker and Matyjaszewski, 2007). However, the system still suffers from some significant disadvantages such as the radicals lose their functionality upon irreversibly terminating, the reactions have poor stereo-selectivity, and little control is attainable over the individual polymers or their population (Braunecker and Matyjaszewski, 2007). To circumvent these disadvantages, attempts to improve the free radical process have been made. In the next section, some of the most successful modifications are outlined.

2.2 Controlled (Living) Radical Polymerization (CLRP)

Recently, attempts have been made to enhance the conventional free radical polymerization process. Often it was hoped that with these modifications, better control over individual polymers and their populations could be obtained, and that the final polymer products could be made to have good chain end functionality (reactivity). Of these attempts some the most successful have been the methods that fall into the category termed controlled (living) radical polymerization.

At their core, the controlled (living) radical polymerization techniques all share the common feature of establishing a dynamic equilibrium between growing radicals and a dormant species - or more explicitly, a radical which has reversibly lost its activity. CLRP techniques, thus, add an additional step to the radical polymerization process in the form of an equilibrium. Shown below in Table 2.2 is the general mechanism of the CLRP processes. It is important to note that this mechanism only includes reactions which commonly occur in these processes; also, the reaction outlined in the dotted box is the main equilibrium step that differentiates these controlled polymerizations from the conventional radical polymerization.

Table 2.2: General Mechanism for a Controlled (Living) Radical System

1. Initiation[2,*]	$I \xrightarrow{k_d} 2R_0^{\cdot}$	(Dissociation/Decompostion of initiator)
	$R_0^{\cdot} + M \xrightarrow{k_i} R_1^{\cdot}$	(Initiation)
2. Propagation	$R_n^{\cdot} + M \xrightarrow{k_p} R_{n+1}^{\cdot}$	(Propagation)
3. Transfer	$R_n^{\cdot} + T \xrightarrow{k_{trt}} P_n + T\cdot$	(Transfer to transfer agent)
4 Radical Equilibrium[1,*]	$R_n - X + Agent \underset{k_{deact}}{\overset{k_{act}}{\rightleftharpoons}} Agent - X + R_n^{\cdot}$.	
5. Termination	$R_n^{\cdot} + R_m^{\cdot} \xrightarrow{k_{tc}} P_{n+m}$	(Combination)
	$R_n^{\cdot} + R_m^{\cdot} \xrightarrow{k_{td}} P_n + P_m$	(Dispropotionation)

The variables used above are defined as follows: I: initiator, $R_0^{\cdot}$: primary radical generated from the initiator, M: monomer, T: Transfer agent, $R_1^{\cdot}$: propagating radical of chain length 1, $R_n - X$: dormant polymer of chain length n; where n≥1, $R_n^{\cdot}$: propagating radical of size n; where n≥1, $R_m^{\cdot}$: propagating radical of size m; where m≥1, $P_{n+m}/P_n/P_m$: are dead polymers of length n+m, n, and m respectively. The Agent term above can represent different chemicals depending on the particular version of CLRP selected. For a more detailed discussion of the most popular CLRP methods see (Braunecker and Matyjaszewski, 2007; Matyjaszewski and Tsarevsky, 2014; Nicolas et al., 2013)

Notes:

[1,*] This equilibrium reaction is slightly more complicated in the case of reversible addition-fragmentation chain-transfer polymerization (RAFT), but the general function of it still holds; i.e. establishing an equilibrium between dormant and active radicals.

[2, *] During these controlled radical polymerizations different initiation methods may be used, but a standard free radical initiation technique is shown here for simplicity.

The idea behind introducing this equilibrium is that it can be set up in a way that creates a strong tendency for radicals to exist in a dormant state, but importantly still provides them with the ability to become active again. This means that at any given instant the majority of the radicals in the system exist in a reversible dormancy, which reduces reactions such as termination and transfer, while still allowing these radicals to become active at any given instant. Polymers in this system

are thus claimed to have a higher livingness, as chain ending reactions are significantly diminished, and the majority of the radicals in the system can continue to grow once activated from their dormant state. This provides the user of these techniques with a significantly increased control over chain features and the size of individual molecules.

On top of this, two other interesting features arise from the establishment of the equilibrium. The first of these is that radicals in a state of dormancy can be made to have good chain end functionality depending on the type equilibrium used. If this can be established, this is an amazing property to have as it allows for further modification of the polymers after the reaction has finished (owing to the fact that the majority of the polymer chains exist in this dormant state at the end of the reaction). For example, macromolecules of such a kind can be used as the starting materials in CLRP systems, which can lead to the generation of interesting structures like block copolymers (Gody et al., 2015; Li et al., 2016; Zaremski et al., 2015). Also these final polymer products may- if compatible- be used with other reaction techniques such as click chemistry, generating other fascinating molecular architectures(Cao et al., 2016; Gozgen et al., 2009; Jeong et al., 2015).

Aside from this previous feature, another intriguing characteristic may be attained in these systems. This attribute arises from the careful tuning of the rate of initiation and the rate of exchange between dormant and active radicals. By carefully tuning these rates, while remembering that the equilibrium should at all points strongly favour the dormant species, control over the breadth of the molecular weight distribution can be obtained. How this occurs can be gleaned if one considers what modification of each of these rates induces. The rate of initiation for instance determines how close the starting of growth periods for polymers are in regards to each other, as its value fixes the speed at which polymeric radicals are generated. The rate of dynamic exchange, on the other hand, determines how equally distributed growth periods are between polymers in the system, as its value determines how quickly one radicals chance to grow will end and another's will start. It thus is the case that by varying the speed of initiation (how closely spaced the starting of the growth periods are to each other) and the rate of exchange of the equilibrium (how equally distributed the growth opportunities are in the system), control over the molecular weight distribution of the polymers can be achieved. It can therefore be envisaged that with proper tuning of these rates, not only will control over polymer architecture and improvements to chain end functionality be realizable, but also a greater control over polymer populations should be attainable.

With all of this in mind there are however some major drawbacks to the CLRP methods. These drawbacks are that these processes often occur at a much slower rate, they require additional chemicals, and the final polymers usually have a more involved purification process when compared with the conventional radical polymerization. Additionally, the benefits gained from using CLRP methods to generate general commodities seem minimal at present (Destarac, 2010; Oh, 2008). It therefore currently seems to be the case that conventional radical polymerization is unlikely to be replaced by CLRP in their production. Nonetheless even with these faults the CLRP methods seems to have a bright future ahead of them, as they make available new polymer architectures, and therefore material properties.

2.3 Atom Transfer Radical Polymerization (ATRP)

Of all the CLRP methods arguably the most promising currently is atom transfer radical polymerization (ATRP), specifically because it has some significant advantages over the other major methods: NMRP and RAFT. In particular, it is more versatile when forming block copolymers and the formed polymers can often be easily chemically modified (Braunecker and Matyjaszewski, 2007; Matyjaszewski and Tsarevsky, 2014). In addition, versions of the ATRP reaction can be started and stopped at will, and in comparison to NMRP it has a large range of applicable temperatures and monomers (Braunecker and Matyjaszewski, 2007; Matyjaszewski and Tsarevsky, 2014). It does however have its disadvantages when compared to both of the other major methods. These disadvantages are that it has a smaller range of applicability, slower speed, and can not generate molecules as large as those found in RAFT; and it is not as environmentally friendly or as biocompatible as NMRP (Braunecker and Matyjaszewski, 2007). However even with these relative disadvantages, due to significant control it provides over polymer structure and distribution, as well as the control it provides over the process as a whole, a case can definitely be made for ATRP being the most promising of the three methods. For this reason, the ATRP system was chosen as a focus point for this thesis.

2.3.1 General Features and Initiation Systems

The ATRP process was first reported in 1995 independently by two groups: Kato et al. (1995), and Wang and Matyjaszewski (1995a, b). As with the other CLRP methods it involves the establishment of an equilibrium between an active radical and a dormant species. In the ATRP system this equilibrium is established through use of an appropriate catalyst. This catalyst is conventionally a transition metal complex (Matyjaszewski and Tsarevsky, 2014), but can also take on other forms, as was the case in a recent study (Treat et al., 2014). Independent however of the type of catalyst used, the catalyst in its activator form is able to remove capping agents from a dormant species forming a deactivator species and an active radical. It then can in its deactivator form go on to cap active radicals and form once again the dormant species and the activator. In this way, it establishes an equilibrium between dormant species and active radicals. Below in Table 2.3 the general mechanism for the original ATRP process is presented.

Table 2.3: General Mechanism of the original ATRP process

(Activation of initiator)	$I-X+A \underset{k_{deact0}}{\overset{k_{act0}}{\rightleftarrows}} R_0^{\cdot}+D$
(Initiation)	$R_0^{\cdot}+M \overset{k_i}{\rightarrow} R_1^{\cdot}$
(Propagation. Where n≥1)	$R_n^{\cdot}+M \overset{k_p}{\rightarrow} R_{n+1}^{\cdot}$
(Transfer)	$R_n^{\cdot}+T \overset{k_{trt}}{\longrightarrow} P_n+T\cdot$
(Equilibrium)	$R_n-X+A \underset{k_{deact}}{\overset{k_{act}}{\rightleftarrows}} R_n^{\cdot}+D$
(Termination)	$R_n^{\cdot}+R_m^{\cdot} \overset{k_{tc}}{\longrightarrow} P_{n+m}$
	$R_n^{\cdot}+R_m^{\cdot} \overset{k_{td}}{\longrightarrow} P_n+P_m$

Where *I*: initiator, *M*: monomer, *X*: halogen, *A*: Activators, *D*: Deactivators, $R_0^{\cdot}$: primary radical, *T*: Transfer agent, $R_1^{\cdot}$: radical of chain of length 1, $R_n^{\cdot}$: radical of size n; where n≥1, $R_m^{\cdot}$: radical of size m; where m≥1, R_n-*X*: halide capped radical, and $P_{n+m}/P_n/P_m$: are dead polymers of length n+m, n and m respectively.

In this original form the ATRP process starts once activators have stripped a halide atom from alkyl halide initiators forming a primary radical and the deactivator species. The primary radicals are assumed to then carry on the reaction in a manner similar to the conventional radical process, while the catalysts would help to establish an equilibrium between dormant and active radicals (See Table 2.3). Now while all ATRP systems share some common features with this original process, there have been a large number of modifications made. This is because some major issues associated with the system were able to be addressed through simple modifications of the process.

The first of these to be tackled was the fact that the catalyst, in its activator form, was not stable in the presence of oxygen, and as it was used as a starting reagent a difficult synthetic procedure had to be carried out before each reaction. It was thus desirable to find a way to avoid this difficult synthetic procedure. An early answer to this was to use conventional initiators to generate the necessary primary radicals, instead of using alkyl halides and the unstable activators. This modification, called reverse ATRP, allowed the process to start with the stable deactivators and conventional radicals, allowing the activators to be generated later in the process via the equilibrium step, and thus simplifying the synthetic procedures greatly. However, this alteration to the ATRP system stripped it of its ability to use macro-initiators (polymer halides) as starting materials, as only conventional initiators were used. For this reason, often both conventional and alkyl halide initiators were used together in a process coined simultaneous reverse and normal initiation (SR&NI) ATRP.

However, with the advent of these systems a new problem unfortunately emerged. It was that pure block copolymers could no longer be generated, as the conventional radicals in these new systems could lead to the formation of homopolymer impurities. For this reason, in an attempt to avoid the use of conventional radicals a novel system called AGET (activators generated by electron transfer) ATRP was created. This process utilized reducing agents which avoided radical generation, and performed the necessary reduction of deactivators to activators. In this manner the system was not only able to start with the oxidatively stable deactivator, but also was able to form pure block copolymers by using alkyl halide macro-initiators as the only source of primary radicals in the system.

Subsequently, further improvements were made to the system by tackling the issue of the large amounts of catalyst necessary for the reaction. In solving this problem, it was realized that if the

ratio of the deactivator to the activator at equilibrium could be kept at a reasonable level, only catalytic amounts of the catalyst would be needed. This however was unattainable in the earlier systems due to the buildup of deactivators because of the irreversible termination of radicals (the persistent radical effect). Luckily, through use of additional agents, other reaction systems were devised whereby the activators could be regenerated from the deactivators. The first of these systems termed initiators for continuous activator regeneration (ICAR) used radicals derived from conventional initiators to battle the persistent radical effect and establish the necessary ratios. It however, similarly to the reverse and SR&NI ATRP, pure block copolymers could not be generated. For this reason, it was opted that once again alternative reducing agents be used, as was the case in AGET ATRP, and a process termed ARGET (activators regenerated by electron transfer) ATRP was devised for use with catalytic amounts of catalyst[2].

Pressing forward from these achievements, attempts have recently been made to modify the process in ways that reduce the need for purification. This has been achieved in two main ways. The first of these is through the complete elimination of transition metal catalyst from the process (Treat et al., 2014). These metal free ATRPs are still in their infancy, but may completely replace the old methods of ATRP which required the use of toxic chemicals. The second way on the other hand in which this has been achieved is through the elimination of the reducing agent from the ATRP system. This is achieved by using electrochemistry or radiation, rather than a reducing species to bring about the transformation of deactivators to activators (Dadashi-Silab et al., 2014; Magenau et al., 2013). Interestingly these methods also had the ability to switch the polymerization process on an off at will. This pleasant surprise would provide the user of such processes with an interesting avenue for control over the system.

With a description of these last updates an overview of the basic chemical mechanism of the ATRP process has been given. Interestingly, the major phenomenon described above reasonably approximate the main features of these processes when carried out in bulk and solution (Though the solvent can have some effects on the kinetic parameters, and if it is not carefully selected can result in some slightly different reaction pathways such as transfer to solvent). Thus, due to its simple kinetic structure and its use of the solution media the ARGET ATRP of butyl methacrylate

[2] Reverse ATRP is chemically identical to ICAR ATRP, and AGET ATRP is chemically identical to ARGET ATRP. The only difference between these systems is the amount of catalyst used.

studied in this thesis is reasonably described by the ideas described so far. However, in order to flesh out the details needed to discuss the second part of this thesis, the dispersed polymerization of butyl acrylate by AGET ATRP, some additional details need to be described. For this reason, in the next section a look at some topics introducing the complications associated with this polymerization will be given.

2.4 Complications Associated with Application of ATRP to Dispersed Media

2.4.1 Dispersed Media and Their Features

In order to facilitate an understanding of ATRP in dispersed media a brief discussion of the three most prevalent types of dispersed media is given here: emulsion, miniemulsion, and microemulsion. Each of these are distinguished either by unique kinetic features and/or differences in their final products. Below a brief description of the main features of each process is given.

2.4.1.1 Emulsion Polymerization

Starting with the most popular of these dispersed systems, the emulsion system is a dispersion in which monomer is emulsified in a continuous phase. Most commonly this takes on the form of an oil in water emulsion, thus resulting in the monomer being dispersed in a continuous aqueous phase. In any case, emulsifying of monomer in the amounts typical of emulsion systems results in the creation of three distinct regions at the start of the polymerization. These regions are monomer swollen micelles, monomer droplets, and a continuous phase. Below in Figure 2.1 a depiction of this is given. Where within the figure the small circles represent monomer swollen micelles, the large circles represent monomer droplets, and the grey background represents the continuous aqueous phase.

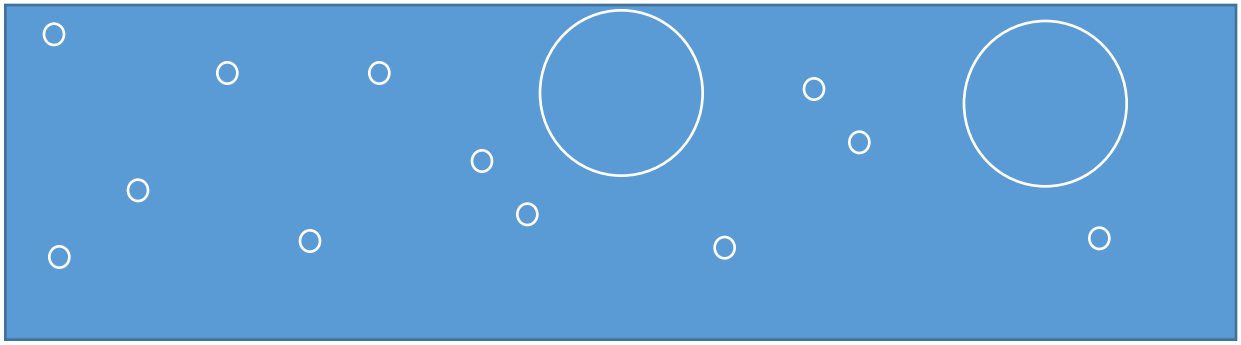

Figure 2.1: Initial state of the emulsion system

From this initial state, polymerization proceeds mainly in discrete polymer particles, which have been generated from either micellar, homogeneous, and/or coagulation nucleation mechanisms (Chern, 2009; Van Herk, 2013). As these particles are small and discrete in nature, they simultaneously result in a reduction in the rate of bimolecular reactions (such as termination) due to isolation of molecules in different particles, and an increase in this rate because molecules trapped in the same particles are within close proximity. Interestingly within these particles it also seems to be the case that for a large portion of the reaction the concentration of monomer remains relatively constant. This is owing to the fact that monomer droplets within this system act as monomer reservoirs until they are depleted. Adding further to this complex nature, phenomenon such as the gel effect also seem to be operative in these systems at high conversions. All of these phenomena when brought together with the standard chemical kinetics of the radical system, form what is known as an emulsion polymerization, and generally result in polymer particles in the size range of 50-500nm.

2.4.1.2 Microemulsion Polymerization

This process while sharing some similar characteristics with the emulsion process differs from it quite drastically. To begin, microemulsion polymerizations make use of a much larger amount of surfactant than emulsion systems and in some cases even use some cosurfactant. What this allows for is the complete elimination of monomer droplets from the system and enclosing of all monomer within monomer swollen micelles. As can be imagined, this drastically alters the mechanism of

the process, and the resulting latex. A depiction of the initial state of the microemulsion system is given below in Figure 2.2. Where within this figure the small circles are meant to represent small monomer swollen micelles and the grey background the continuous phase.

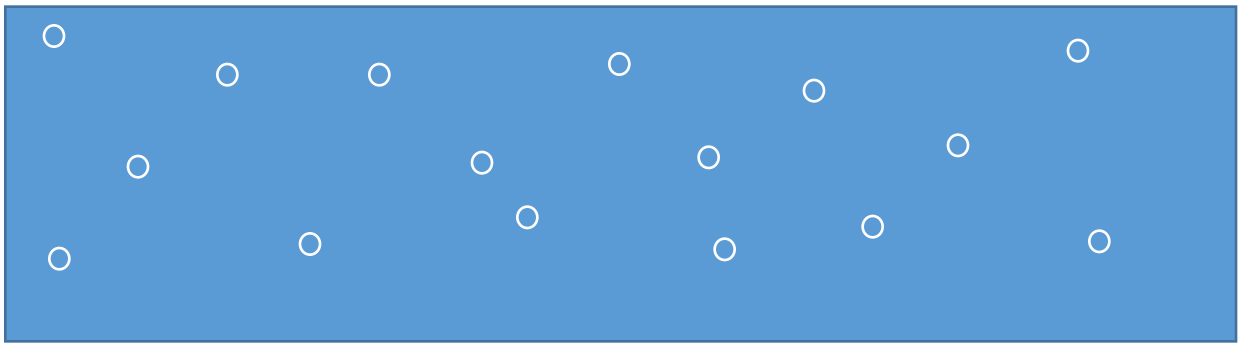

Figure 2.2: Initial state of microemulsion system

In this system, polymerization occurs within discrete polymer particles which are generated by either micellar, homogeneous, and/or coagulation mechanisms (Chern, 2009; Van Herk, 2013). These particles, similarly to those generated in emulsion, result in the compartmentalization of species and thus the two effects discussed above. However, differing from emulsion systems, these particles have a constant monomer concentration within them for a relatively short period of time (Guo et al., 1992). This is owing to the lack of monomer droplets within this system which normally act as monomer reservoirs. In addition to this, as the size of these particles are generally in the range of 10-50nm in diameter, further dramatic shifts in the kinetics of these processes away from emulsion occur. For instance in these systems the gel effect is negligible as particles often only contain one radical at a time. Moreover due to the small size of these particles, the main chain ending reactions become transfer reactions, and desorption of radicals out of these particles is greatly enhanced. This has a dramatic effect on the system as for instance high molecular weight polymers on the order of 10^6-10^7 g/mol in size are formed due to the chain ending process occurring mainly through transfer reactions. For these reasons the microemulsion process, while sharing similar characteristic with the emulsion system, must be considered its own distinct entity.

2.4.1.3 Miniemulsion Polymerization

Finally the miniemulsion system takes quite a different approach to the dispersion process of monomer in a heterogeneous system. In these systems surfactant and costabilizers are used in combination with high shear forces to generate a dispersion of submicron sized monomer droplets within a continuous phase. In their ideal form these miniemulsion systems should not contain any monomer swollen micelles, but in systems where the surfactant level is above a critical concentration (its critical micellar concentration) they often can. A depiction of the initial state of an ideal miniemulsion system is given below in Figure 2.3. Where within this figure the circles represent monomer droplets and the grey background the continuous phase.

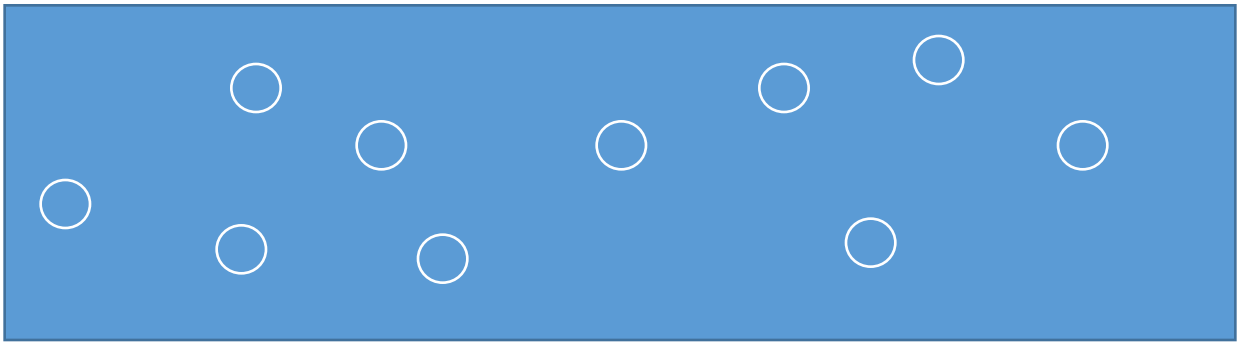

Figure 2.3: Initial state of miniemulsion system

Miniemulsion polymerizations starts with a nucleation stage which generates the polymer particles (Similar to that of microemulsion and emulsion). Differently however from emulsion and microemulsion systems the nucleation process can occur by not only micellar (if micelles are present), homogeneous and coagulation mechanisms, but also by transformations of droplets into particles. This new nucleation process is what gives miniemulsion polymerizations their distinct features. These features are that the particles within the system behave like an isolated submicron reactor, particles generated can be on the order of 1-10µm in size, and the gel effect is pertinent due to the size of the particles generated. Droplet nucleation also makes the miniemulsion systems very good candidates for the polymerization of extremely hydrophobic monomer. This is because there would be no need to transport these monomers across the aqueous phase, as all the necessary components should be contained within the submicron sized miniemulsion droplets. For the above

reasons miniemulsion polymerization can be considered as distinct from both emulsion and microemulsion polymerizations.

2.4.2 ATRP in Dispersed Media

While the ATRP system, within the last two decades, has become quite mature in bulk and solution mediums, the dispersed version of this system has lagged behind due to its complicated nature. Both from a theoretical and experimental point of view the complexities of this system have mustered up quite a challenge for researchers in this field. With that being said, a lot of progress has been made recently. This includes both experimental advances of the systems (Min et al., 2006; Stoffelbach et al., 2008; Wei et al., 2014; Wu et al., 2015) and an increased understanding of the processes governing them (Kagawa et al., 2007; Thomson and Cunningham, 2010; Tobita, 2010; Zetterlund, 2010). Through these advances, successful application of ATRP to the three main types of dispersed media mentioned above have been obtained.

However, in order to accomplish this, great difficulties associated with adapting the ATRP process to dispersed media first had to be overcome. To start with, within these systems, catalyst would often partition between both the aqueous and organic phases; losing its activity upon dissociation in the aqueous phase. To prevent this from happening extremely hydrophobic ligands were used[3], but this had the downside of making it almost impossible to transport the catalysts across the aqueous phase. On top of this most anionic surfactants, which had worked well in conventional dispersed systems, could not be used in ATRP systems due to their interactions with the catalysts.

Interestingly the miniemulsion polymerization provided solutions to these problems via its very nature, as within these systems there is no need for transport of species throughout the reactor. Instead polymerization occurs in isolated submicron sized droplets. Thus, through combination of this characteristic of miniemulsion and appropriate selection of the surfactant (non-ionic or cationic), ATRP was relatively easily adapted to the miniemulsion system. These systems however required the generation of the miniemulsion through a shear induced process (often sonification) thus complicating the synthetic procedure and limiting their applications in industry.

[3] This also technically required that the transition metal be strongly bonded to the ligand, as if it were not it would often partition to the aqueous phase leaving the ligand behind.

Similar to this the microemulsion process was also able to adapt the ATRP system reasonably well to dispersed media. This was achieved because its mechanisms did not require a large amounts of catalyst to be transported through the aqueous phase and appropriate surfactants (non-ionic or cationic) could easily be chosen for use in these systems. It however unlike the miniemulsion process does require some transport of these species through the aqueous phase, as often a large number of micelles within the system are left unpolymerized and instead act as reservoirs. Further in these systems due to the small size of the particles generated, if any partitioning occurs it can have a dramatic effect on the polymerization, even to such an extent as to create bimodal molecular weight distributions (Min and Matyjaszewski, 2005). That being said the AGET ATRP process, with appropriate selection of catalyst and surfactant, has been proven to work quite well in this dispersed system and has led to generation of well controlled polymer structures, with good particle and molecular weight distributions. These systems however do suffer from the requirement of a high surfactant concentration relative to the monomer, which results in a more rigorous purification process.

For the emulsion polymerization process on the other hand, the success of the previous two systems was not mimicked directly. This was because large oil droplets within these systems trapped a large portion of the initiator and catalyst within them. This resulted in issues associated with the transport of catalyst/initiator across the aqueous phase to the polymer particles (reaction loci), and droplet nucleation in the case of normal ATRP. Attempting to avoid these problems, Min et al. (2006) developed a two-step procedure in which a microemulsion polymerization is transformed to an emulsion polymerization by the injection of monomer. In doing this they were able to avoid the issue of transportation of catalyst and initiator in the system by successfully enclosing these species in the particles and monomer swollen micelles of the microemulsion system. Using this technique in combination with the AGET ATRP initiation method they were able to obtain a successful emulsion system. This system, while not exactly a pure ab initio emulsion system, has piqued the interest of researchers due to its possible uses in industry.

Concurrent with this experimental development, advances in our understanding and modelling capabilities in regards to these systems have also occurred. To begin the idea of compartmentalization, which was originally developed for radicals, has been extended to include other components such as the catalyst. Thus in the ATRP system, the discrete nature and size of

the particles not only has an effect on the bimolecular rate of reaction between radicals, but also between radicals and catalysts (More generally this is true for any species undergoing a bimolecular reaction). Studies using models to account for this new phenomenon have revealed new insights such as the fact that there may be possible regions in these systems where the rate of polymerization is larger than those in the bulk case, while the control over polymer architecture has also increased (Thomson and Cunningham, 2010; Tobita, 2010).

On top of this, further advances have also been seen in subjects such as the effect of diffusion controlled reactions, as well as the relations governing the partitioning of chemical species. In terms of the diffusion controlled reactions, through use of simulation it was found that no significant effects appear to be operative below 60% conversion (Zetterlund, 2010). However, at higher conversions, due to diffusional limitations associated with the deactivation reaction, it is believed that an increase in the rate of polymerization and a decrease in the control over radicals in the system can be seen. Interestingly, it was shown in a recent study that this decrease in control may be compensated for at higher conversions, as at these conversions residual deactivation due to propagation can greatly increase control over the polymerization (Rabea and Zhu, 2015). Partitioning on the other hand has been investigated from an experimental and modelling point of view in attempts to improve available knowledge of the system. Two major results were obtained from these studies (Kagawa et al., 2007; Qiu et al., 2000b): conditions and reagents used in dispersed systems needed to be selected carefully, otherwise partitioning effects could be significant; and even with a hydrophobic ligand, the transition metal could still partition to the aqueous phase, if extracted by water from the complex. These were both crucial results as they showed the importance of selecting both conditions and reagents.

These advances in theoretical and experimental settings have greatly contributed to the development of the ATRP process in dispersed media. For instance, all three of the major dispersed systems have been made compatible with the ATRP process. Further models of the systems have progressed in their descriptive power with developments in the theoretical understanding of the system. There is however still a need for further investigation within these systems. In particular experimental attempts to improve upon faults in the processes above, or creation of improved models of both microemulsion and emulsion systems, are both subsections of this area of research which could still use attention.

2.5 Complications Associated with Butyl Acrylate

The behavior of butyl acrylate adds complexity to the system beyond that found with most other monomers. This is owing to the variations it causes in the basic kinetic structure of ATRP, as well as the kinetics of dispersed systems; both of which play a crucial role in determining not only the systems evolution, but also its final product. For this reason, in what follows, an attempt to detail the most consequential features of butyl acrylate polymerization in ATRP and dispersed systems is given.

2.5.1 Butyl Acrylate Kinetics during ATRP

With the addition of butyl acrylate to the system, the kinetics of the ATRP process becomes modified. This is owing to the generation of a species not commonly found in other systems, tertiary radicals. These radicals differ from the commonly found secondary radicals, as secondary radicals have their functionalities located at the ends of polymer chains, whereas tertiary radicals have them located in the interior. This change in the location of the functional group results in different reactivity's for secondary and tertiary radicals, because of differences in the groups surrounding them. Due to this fact, within systems employing butyl acrylate as a monomer a doubling of the possible radical reactions occurs, as secondary and tertiary reactions need to be considered separately. It is this as well as the complications associated with the generation and consumption of these tertiary radicals that creates the complex chemical kinetics in butyl acrylate systems. Below in Table 2.4 the general mechanism for the ATPR of butyl acrylate is given.

Table 2.4: Mechanism of the ATRP of butyl acrylate

(Activation of initiator)	$I - X + A \underset{k_{deact,s,0}}{\overset{k_{act,s,0}}{\rightleftarrows}} R_{s,0}^{\cdot} + D$
(Initiation)	$R_{s,0}^{\cdot} + M \xrightarrow{k_i} R_{s,1}^{\cdot}$
(Backbiting)	$R_{s,n}^{\cdot} \xrightarrow{k_{bb}} R_{t,n}^{\cdot}$
(Propagation. Where n≥1)	$R_{s,n}^{\cdot} + M \xrightarrow{k_{p,s}} R_{s,n+1}^{\cdot}$
	$R_{t,n}^{\cdot} + M \xrightarrow{k_{p,t}} R_{t,n+1}^{\cdot}$
(Transfer to transfer agent)	$R_{s,n}^{\cdot} + T \xrightarrow{k_{trt,s}} P_n + T\cdot$
	$R_{t,n}^{\cdot} + T \xrightarrow{k_{trt,t}} P_n + T\cdot$
(Equilibrium)	$R_{s,n} - X + A \underset{k_{deact,s}}{\overset{k_{act,s}}{\rightleftarrows}} R_{s,n}^{\cdot} + D$
	$R_{t,n} - X + A \underset{k_{deact,t}}{\overset{k_{act,t}}{\rightleftarrows}} R_{t,n}^{\cdot} + D$
(Termination)	$R_{s,n}^{\cdot} + R_{s,m}^{\cdot} \xrightarrow{k_{tc,ss}} P_{n+m}$
	$R_{s,n}^{\cdot} + R_{s,m}^{\cdot} \xrightarrow{k_{td,ss}} P_n + P_m$
	$R_{s,n}^{\cdot} + R_{t,m}^{\cdot} \xrightarrow{k_{tc,st}} P_{n+m}$
	$R_{s,n}^{\cdot} + R_{t,m}^{\cdot} \xrightarrow{k_{td,st}} P_n + P_m$
	$R_{t,n}^{\cdot} + R_{t,m}^{\cdot} \xrightarrow{k_{tc,tt}} P_{n+m}$
	$R_{t,n}^{\cdot} + R_{t,m}^{\cdot} \xrightarrow{k_{td,tt}} P_n + P_m$

Where *I*: initiator, *M*: monomer (butyl acrylate), *X*: halogen, *T*: Transfer Agent, *A*: Activators , *D*: Deactivators, $R_{s,0}^{\cdot}$: primary radical, $R_{s,1}^{\cdot}$ ·: secondary radical of chain of length 1, $R_{s,n}^{\cdot}$: secondary radical of size n; where n≥1, $R_{t,n}^{\cdot}$: tertiary radical of size n; where n≥1, $R_{s,n}$-*X*: halide capped secondary radical, $R_{t,n}$-*X*: halide capped tertiary radical , and P_{n+m}/P_n/P_m: are dead polymers of length n+m, n and m respectively.

As can be seen above the generation of tertiary radicals occurs through a process called backbiting. In the backbiting reaction, secondary radicals undergo an intramolecular transfer process of their radical activity to another location along their chain. Generally this transfer occurs to the fifth carbon back from the secondary radical in a 1, 5 hydrogen shift process (Cuccato et al., 2013; Yu and Broadbelt, 2012), with shifts further back into the chain also being possible from this point. In any case a tertiary radical is generated which can undergo any of the reactions available to its secondary radical predecessor; importantly though with an often reduced activity. Keeping this in mind, it will continue to participate in these reactions up until the point where it undergoes a propagation reaction and once again forms a secondary radical. This direct change of a tertiary radical back to a secondary one is still the subject of debate (Nikitin and Hutchinson, 2009), but currently is the most widely used representation of the system. Nevertheless with this final reaction, the main complexities added due to the unique butyl acrylate kinetics have been laid out.

Beyond these kinetic features the generation of tertiary radicals also affects the final polymer product. This is because every time a tertiary radical propagates a short chain branch is created as well. These short chain branches often result in reduction of the stiffness and tensile strength at yield, while resulting in increases in the ultimate tensile strength and tensile impact values of the polymers created (Mortimer, 1971)[4]. Branching of this kind can therefore drastically affect the properties of the final polymer product. With this in mind, an interesting effect that arises in the ATRP system is that the fraction of branches on the chain, which result from tertiary radical propagation, can be significantly reduced from that of conventional polymerization (Ahmad et al., 2009; Ballard et al., 2014). ATRP thus presents a possible route to the generation of poly(butyl acrylate) structures with drastically different properties.

Thus as can be clearly seen above the use of butyl acrylate as a monomer can add some significant complexity to the system. This is owing to the tertiary radicals generated during its polymerization. These radicals not only affect the kinetics of the system, but also have an effect on the final polymer product. This situation unfortunately can become even more complicated in dispersed systems

[4] These short chain branches are also known to affect physical properties such as crystallinity, melting point, modulus, the hardness of polymeric materials, as well as the properties under an external flow field (As was stated in the work of Kim and Baig (2016)).

where partitioning of butyl acrylate helps to determine the kinetics of the process. In the next section a brief overview of these added complications is given.

2.5.2 Butyl Acrylate in Dispersed Media

In dispersed polymerizations the monomer used has a large effect on the kinetic mechanism of the system. This is because the hydrophilicity of the monomer and the polymer formed can greatly affect which mechanisms are dominant. In the case of butyl acrylate, both the monomer and the polymer tend to be quite hydrophobic. For this reason in these systems the monomer and polymer preferentially stay in the organic phase. Ergo the most significant kinetic mechanisms of this system are those which favour hydrophobic behavior.

To begin with, in conventional dispersed polymerizations of butyl acrylate the micellar nucleation mechanism, which involves the absorption of a radical by a micelle, is most likely to be the only form of nucleation operative (if coagulation nucleation is ignored, as its prevalence in the system only depends on the amount of surfactant). This is because in dispersed polymerization of butyl acrylate, the polymeric radicals in the system are not likely to spend too much time in the aqueous phase. Thus the homogeneous mechanism of nucleation, which requires radicals to grow to a certain length in the aqueous phase and then curl up into particles, is highly unlikely. On top of this, reactions in the aqueous phase are likely negligible. This is because radicals in these systems are much more likely to be absorbed than desorbed and monomer is preferentially located in the organic phase.

Though these kinetic changes may not seem to be important, they can dramatically affect the evolution and products of the system. For instance the type and number of particles generated in these systems can drastically differ from those in which homogeneous nucleation is operative. This difference can be even more pronounced in the case of ATRP, as homogeneous nucleation may result in loss of control of polymer product. Moreover in general, hydrophilic polymers could result in aqueous phase reactions and loss of control in ATRP systems, as the hydrophobic catalysts would not be able to access these reactions. It is for these reasons that it is important that these features be considered, as if they are not, a proper description of the system will not be given.

2.6 Summary

In this chapter the basic topics required to understand both the solution and dispersed polymerizations studied in this thesis have been laid out. This includes details on the general chemical kinetics of these systems, as well as some of the complications associated with the more complex dispersed system. Thus topics ranging from the mechanisms of the underlying processes to the features of dispersions have been covered.

CHAPTER 3 : MODELLING OF THE SOLUTION ARGET ATRP OF BUTYL METHACRYLATE

3.1 Introduction

ARGET ATRP (Activators Regenerated by Electron Transfer Atom Transfer Radical Polymerization) is a reaction which is gaining a lot of traction in the polymerization field. At a fundamental level, it shares a lot in common with the original ATRP reaction, including the use of a transition metal complex as a mediating agent and alkyl halides as initiators. However, it deviates from this original system in regard to its initial feed and by the addition of a reducing agent in large excess relative to the transition metal complex. These changes to the original ATRP reaction are beneficial, as they allow for a more oxidatively stable initial feed and allow the transition metal complex concentration to be reduced to the ppm range. With these advantages the ARGET ATRP process can be used to produce polymers of higher purity (possibly reducing the need for purification), and reduce the demand on handling the initial components of the system. It is for these reasons that the ARGET ATRP reaction is alluring from an academic and possibly even industrial perspective.

Now while research into the experimental side of ARGET ATRP has been vigorously carried out, the modeling and simulation of its kinetic behavior is lagging behind. This is evidenced by the fact that only two major papers have currently been published on this specific topic, one by Li et al. (2011) and the other by Payne et al. (2013) . Now even though these two studies have illuminated important details of the ARGET ATRP reaction, further development and research into this area of study is required. In the current work an attempt is made to contribute to this area of research by building upon the work mentioned above. Interestingly, simply by combining the models developments by Li et al. (2011) and Payne et al. (2013), using a mathematical framework involving differential equations and the method of moments, insights not yet seen in either work may be obtainable.

It is therefore one the goals of this thesis to build on the work of Payne et al. (2013) and Li et al. (2011) and develop a representative model for the batch version of this system. This as mentioned above will differ slightly from both of these previous works. In the case of Payne et al. (2013) it

will differ in that it will model the system using differential equations and the method of moments. In comparison with the work of Li et al. (2011) on the other hand it will differ in that it includes a second reduction reaction and is simulating a monomer not considered within their work. It is hoped that with these changes important insights will arise and that this subject can be further illuminated.

3.2 Process Description

The process studied in this chapter is a simple modification of the original ATRP process shown in Chapter 2, Table 2.3. In order to properly modify the process, two reduction reactions involving tin(II) 2-ethylhexanoate and the transfer to monomer reactions are added to this original reaction scheme. While seemingly small modifications, both of these additions have a significant effect on the process. For instance the addition of the reduction reactions allows for the generation of activators from deactivators, and thus also the possibility of using the deactivator as a starting reagent. The transfer to monomer reactions on the other hand provide another route of radical generation and polymer termination in the system. With this in mind, a depiction of the full mechanism of the ARGET ATRP process is given below in Table 3.1.

Table 3.1: Chemical Mechanism of the Solution ARGET ATRP of BMA.

Reduction of Deactivator species	$Red^{II} + D \xrightarrow{k_{r1}} Red^{III} + A$
	$Red^{III} + D \xrightarrow{k_{r2}} Red^{IV} + A$
Activation of initiator	$I + A \underset{k_{deact,0}}{\overset{k_{act,0}}{\rightleftharpoons}} R_0^{\cdot} + D$
Initiation	$R_0^{\cdot} + M \xrightarrow{k_p} R_1^{\cdot}$
Propagation. Where n≥1	$R_n^{\cdot} + M \xrightarrow{k_p} R_{n+1}^{\cdot}$
Equilibrium of Macro-radical	$R_n - X + A \underset{k_{deact}}{\overset{k_{act}}{\rightleftharpoons}} R_n^{\cdot} + D$
Transfer with monomer	$R_n^{\cdot} + M \xrightarrow{k_{trm}} P_n + M \cdot$

Equilibrium of Monomer Radical	$M - X + A \underset{k_{deact,0}}{\overset{k_{act,0}}{\rightleftharpoons}} M\cdot + D$
Propagation of Monomer Radical	$M\cdot + M \overset{k_p}{\rightarrow} R_1^{\cdot}$
Termination	$R_n^{\cdot} + R_m^{\cdot} \overset{k_{tc}}{\rightarrow} P_{n+m}$
	$R_n^{\cdot} + R_m^{\cdot} \overset{k_{td}}{\rightarrow} P_n + P_m$

Where I: initiator (ethyl 2-bromoisobutyrate), M: monomer (butyl methacrylate), X: halogen (Bromine), A: Activators (copper (I) bromide tris[(2-pyridyl)methyl]amine complex) , D: Deactivators ((copper (II) bromide tris[(2-pyridyl)methyl]amine complex), Red^{II}: Reducing Agent in its first oxidation state (Tin (II) 2-ethylhexanoate), Red^{III}: Reducing Agent in its second oxidation state (Tin (III) 2-ethylhexanoate), Red^{IV}: Reducing Agent in its third oxidation state (Tin (IV) 2-ethylhexanoate), $R_0^{\cdot}$: primary radical, $R_1^{\cdot}$: radical of chain of length 1, $R_n^{\cdot}$: radical of size n; where n≥1, $R_{s,n}$-X: halide capped secondary radical, and $P_{n+m}/P_n/P_m$: are dead polymers of length n+m, n and m respectively.

3.3 Model

3.3.1 Overview

In modelling this solution polymerization, differential equations were used to develop the necessary mathematical framework. The required equations were easily derived for reactants with uniform sizes, via population balances, however the equations describing the dynamics of polymeric species were more difficult to obtain. This was because in order to acquire a fuller set of data describing the polymeric species present, the method of moments was used. This involved developing population balance equations for the zeroth, first, and second moments of the polymeric species in regards to their length; where the zeroth moments provided information on concentration profiles, and appropriate ratios of the zeroth, first and second moments provided information on the molecular weight distribution. Derivation of these equations however was a trying process, necessitating some form of infinite summation of population balance equations for the various polymer chain lengths within the system. Nevertheless, finite forms of these equations were developed (For more details on how this was done, see (Mastan and Zhu, 2015)). The equations describing molecules of both mono- and polydisperse sizes are as follows:

Monodisperse molecule balances:

$$Monomer\ Balance$$

$$\frac{d[M]}{dt} = -k_p[M]([R_0.] + [\lambda_0] + [M.]) - k_{trm}[M][\lambda_0] \tag{3.1}$$

$$Reducing\ Agent\ (II) Balance$$

$$\frac{d[Red^{II}]}{dt} = -k_{r1}[Red^{II}][D] \tag{3.2}$$

$$Reducing\ Agent\ (III) Balance$$

$$\frac{d[Red^{III}]}{dt} = k_{r1}[Red^{II}][D] - k_{r2}[Red^{III}][D] \tag{3.3}$$

$$Reducing\ Agent\ (IV) Balance$$

$$\frac{d[Red^{IV}]}{dt} = k_{r2}[Red^{III}][D] \tag{3.4}$$

$$Deactivator\ Balance$$

$$\frac{d[D]}{dt} = -k_{r1}[Red^{II}][D] - k_{r2}[Red^{III}][D] + k_{act,0}([I] + [M - X])[A] - k_{deact,0}([R_{s,0}.] + [M.])[D] + k_{act}[A][\delta_0] - k_{deact}[D][\lambda_0] \tag{3.5}$$

$$Activator\ Balance$$

$$\frac{d[A]}{dt} = k_{r1}[Red^{II}][D] + k_{r2}[Red^{III}][D] - k_{act,0}([I] + [M - X])[A] + k_{deact,0}([R_0.] + [M.])[D] - k_{act}[A][\delta_0] + k_{deact}[D][\lambda_0] \tag{3.6}$$

$$Initiator\ Balance$$

$$\frac{d[I]}{dt} = -k_{act,0}[I][A] + k_{deact,0}[R_0.][D] \tag{3.7}$$

$$Primary\ Radical\ Balance$$

$$\frac{d[R_0.]}{dt} = -k_p[M][R_0.] + k_{act,0}[I][A] - k_{deact,0}[R_0.][D] \tag{3.8}$$

Monomer Radical Balance

$$\frac{d[M.]}{dt} = k_{trm}[M][\lambda_0] - k_p[M][M.] + k_{act,0}[M-X][A] - k_{deact,0}[M.][D] \tag{3.9}$$

Dormant Monomer Balance

$$\frac{d[M-X]}{dt} = -k_{act,0}[M-X][A] + k_{deact,0}[M.][D] \tag{3.10}$$

Polydisperse Molecule Equations (Polymeric Equations):

Macroradical Zeroth Moment Balance

$$\frac{d[\lambda_0]}{dt} = k_p[M]([R_0.] + [M.]) + k_{act}[A][\delta_0] - k_{deact}[D][\lambda_0] - k_t[\lambda_0][\lambda_0] - k_{trm}[M][\lambda_0] \tag{3.11}$$

Macroradical First Moment Balance

$$\frac{d[\lambda_1]}{dt} = k_p[M]([R_0.] + [M.] + [\lambda_0]) + k_{act}[A][\delta_1] - k_{deact}[D][\lambda_1] - k_t[\lambda_1][\lambda_0] - k_{trm}[M][\lambda_1] \tag{3.12}$$

Macroradical Second Moment Balance

$$\frac{d[\lambda_2]}{dt} = k_p[M]([R_0.] + [\lambda_0] + [M.] + 2[\lambda_1]) + k_{act}[A][\delta_2] - k_{deact}[D][\lambda_2] - k_t[\lambda_2][\lambda_0] - k_{trm}[M][\lambda_2] \tag{3.13}$$

Dormant Species Zeroth Moment Balance

$$\frac{d[\delta_0]}{dt} = -k_{act}[A][\delta_0] + k_{deact}[D][\lambda_0] \tag{3.14}$$

Dormant Species First Moment Balance

$$\frac{d[\delta_1]}{dt} = -k_{act}[A][\delta_1] + k_{deact}[D][\lambda_1] \tag{3.15}$$

Dormant Species Second Moment Balance

$$\frac{d[\delta_2]}{dt} = -k_{act}[A][\delta_2] + k_{deact}[D][\lambda_2] \tag{3.16}$$

Dead Polymer Zeroth Moment Balance

$$\frac{d[\mu_0]}{dt} = \frac{1}{2}k_{tc}[\lambda_0][\lambda_0] + k_{td}[\lambda_0][\lambda_0] + k_{trm}[\lambda_0][M] \tag{3.17}$$

Dead Polymer First Moment Balance

$$\frac{d[\mu_1]}{dt} = k_{tc}[\lambda_1][\lambda_0] + k_{td}[\lambda_1][\lambda_0] + k_{trm}[\lambda_1][M] \tag{3.18}$$

Dead Polymer Second Moment Balance

$$\frac{d[\mu_2]}{dt} = k_{tc}([\lambda_2][\lambda_0] + [\lambda_1]^2) + k_{td}[\lambda_2][\lambda_0] + k_{trm}[\lambda_2][M] \tag{3.19}$$

$$With\ [\lambda_X] = \sum_{n=1}^{\infty}[R_n \cdot]\ n^X, [\delta_X] = \sum_{n=1}^{\infty}[R_n - X]\ n^X, [\ \mu_X] = \sum_{n=1}^{\infty}[P_n]\ n^X, \tag{3.20-3.22}$$

End Polymer Product Properties relation to moments

$$M_n = \left(\frac{\lambda_1 + \mu_1 + \delta_1}{\lambda_0 + \mu_0 + \delta_0}\right)\left(M_{wt,mon}\right) \tag{3.23}$$

$$M_w = \left(\frac{\lambda_2 + \mu_2 + \delta_2}{\lambda_1 + \mu_1 + \delta_1}\right)\left(M_{wt,mon}\right) \tag{3.24}$$

$$PDI = \frac{M_w}{M_n} \tag{3.25}$$

These equations were solved using MATLABs built in solver for stiff ordinary differential equations, ode15s, which is a quasi-constant step size implementation in terms of backward differences of the Klipfenstein-Shampine family of numerical differentiation formulas of orders 1-5. Using this method of simulation times on the order of 20s would be obtained.

In any case by solving both the algebraic and the differential equations above a complete simulation of reactant concentration dynamics and molecular weight data was obtained. This allowed one to study reactant specific phenomenon within the system, as well as changes brought about in either reactant dynamics or molecular weight data by changes in initial conditions. The model therefore had the potential to allow for some important insights to be uncovered. However, one had to be careful about conclusions drawn from these results, as the model was not perfect,

and made certain simplifying assumptions about the process. In the next section these simplifying assumptions are outlined.

3.3.2 Model Assumptions

Certain simplifying assumptions were made about the process. This was done in order to reduce the mathematical complexity of the system, while importantly still maintaining sufficient accuracy. Thus the following assumptions were made about the process:

1. Diffusional effects were neglected.
2. High temperature reactions such as β-Scission and thermal initiation were ignored.
3. Termination of radical with copper catalyst is negligible.
4. Termination events between macro-radicals and primary radicals, as well as between two primary radicals are ignored.
5. Chain length dependency of radical reactions is negligible.
6. All radicals derived from initiators are secondary.
7. Initiator and monomeric radicals react with monomer with the same rate as polymeric radicals.

3.4 Results and Discussion

3.4.1 Original Parameters

In its original form the model developed in this work was kinetically similar to that of Payne et al. (2013). It therefore did not take into account the reactions associated with the transfer of radical activity to monomer, and made use of the kinetic parameters available within their work; where the reactions associated with the transfer of radical activity to monomer were the transfer to monomer, equilibrium of monomer radical, and propagation of monomer radical reactions shown in Table 3.1. Unfortunately, however use of a model of this form resulted in poor fits of the experimental data provided by Payne et al. (2013). This was at first believed to be caused by the fact that diffusional effects affecting the rate of termination, but since in the work of Payne et al.

(2013), reasonable fits seemed to be obtainable using a constant rate of termination, this hypothesis was discarded. As no other possible cause seemed evident to explain such a phenomenon, these deviations between the two models were assumed to be due to differences resulting from the method of simulation used in their work and the current work (Monte Carlo and kinetic equations, respectively. The results obtained using this original form of the model, as well as the parameters used in its simulation can be found below in Figure 3.1, and Table 3.2 respectively.

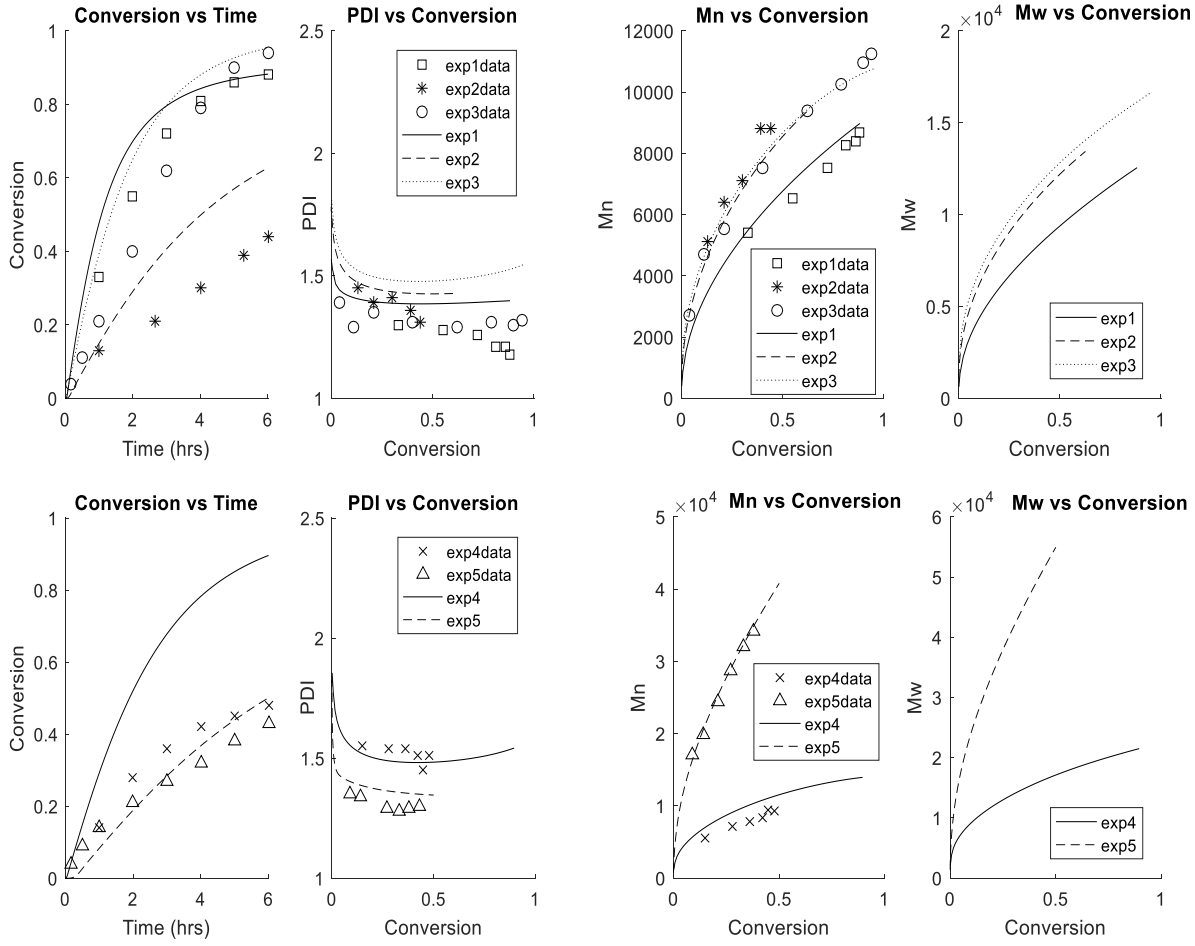

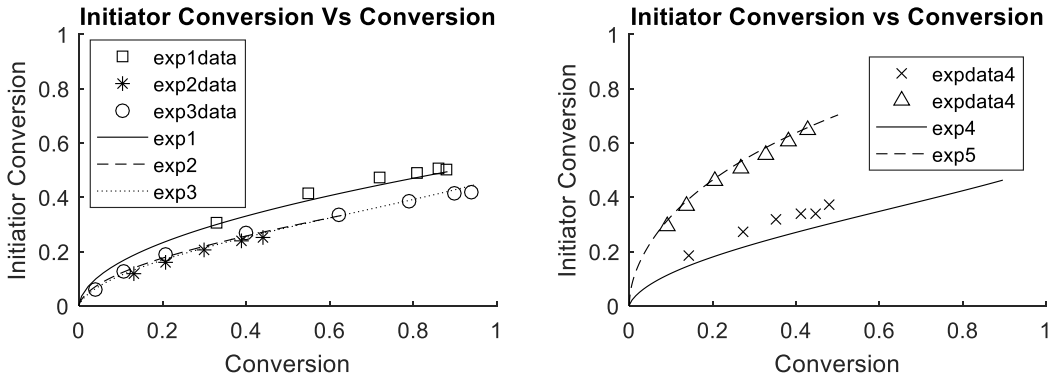

Figure 3.1: Plots comparing model predictions to the experimental values of Payne et al. (2013).

Note: For initial conditions of the simulation see the experimental conditions in Appendix A.

Table 3.2: Kinetic parameters originally used in simulation

Rate Constant	Original A ($L\ mol^{-1}\ s^{-1}$)	Original E_a (J/mol)	Reference
k_{r1}	5.55×10	1.49×10^4	(Payne et al., 2013)
k_{r2}	1.87×10^2	1.49×10^4	(Payne et al., 2013)
$k_{act,0}$	5.38×10^4	2.77×10^4	(Payne et al., 2013)
$k_{deact,0}$	3.94×10^8	7.98×10^3	(Payne et al., 2013)
k_p	3.80×10^6	2.29×10^4	(Beuermann et al., 2000; Payne et al., 2013)[3,*]
k_t[4,*]	N/A[1,*]	N/A[1,*]	(Payne et al., 2013)
k_{deact}	1.97×10^8	7.98×10^3	(Payne et al., 2013)

k_{act}	3.99×10^{6}	2.77×10^{4}	(Payne et al., 2013), (Seeliger and Matyjaszewski, 2009; Tang and Matyjaszewski, 2007)[2,*]

Notes:

[1,*]Instead of provided values for the activation energy and frequency of the reaction a constant value of $k_t=9.0\times10^{7}$ L mol^{-1} s^{-1}was given in the work of Payne et al. (2013); This value was only applicable at 70 °C.

[2,*]Found in work of Payne et al. (2013) using data of Tang and Matyjaszewski (2007) and Seeliger and Matyjaszewski (2009).

[3,*] Same parameter used as (Payne et al., 2013); initial source was (Beuermann et al., 2000).

[4,*] Termination is assumed to occur 90% of the time by disproportionation, as was assumed by Payne et al. (2013).

3.4.2 Model Improvements

In an attempt to improve the quality of the model, two modifications were made to it. The first of these was to include the contribution of the transfer to monomer reactions in the model. Where, again, the transfer reactions are the transfer to monomer, equilibrium of monomer radical, and propagation of monomer radical reactions shown in Table 3.1. However, this addition had only a very small impact on the kinetics. In fact, a complete overlap was obtained with the model originally developed in terms of kinetic predictions; expect for a slight deviation between the two in terms of predictions of M_n and PDI when the targeted chain length (TCL) was quite large (~400). Nonetheless even with this negligible effect under most conditions, it was opted that these reactions should be included, as they still theoretically occur.

Thus, with only minor changes evident from the addition of the transfer reactions, a second attempt had to be made to improve the model. This second attempt to improve the model took a different

approach and assumed instead that the parameters estimated in the work of Payne et al. (2013) were not compatible with the model developed in this work. A parameter estimation was therefore carried out. This was done by minimizing a cost function that accounted for differences between predicted and experimental values of conversion, M_n, and PDI for a given set of kinetic parameters. The cost function used is depicted below.

$$\min_{\boldsymbol{A}\ \&\ \boldsymbol{Ea}} \left[\sum_{i=1}^{3} \left(\sum_{\substack{All\ data\ points \\ for\ experiment}} \left(\frac{\boldsymbol{y_{i,predicted}}}{\boldsymbol{y_{i,experiment}}} - \mathbf{1} \right)^{2} \right) + \sum_{i=6}^{7} \left(\sum_{\substack{All\ data\ points \\ for\ experiment}} \left(\frac{\boldsymbol{y_{i,predicted}}}{\boldsymbol{y_{i,experiment}}} - \mathbf{1} \right)^{2} \right) \right] \tag{3.26}$$

Where:

$\boldsymbol{A} = [\, \boldsymbol{A_{kr1}}, \boldsymbol{A_{kr2}}, \boldsymbol{A_{kt}}, \boldsymbol{A_{kact,0}}, \boldsymbol{A_{kdeact,0}}, \boldsymbol{A_{kact}}, \boldsymbol{A_{kdeact}}, \boldsymbol{A_{kp}}, \boldsymbol{A_{ktrm}}]$

$\boldsymbol{Ea} = [\boldsymbol{Ea_{kr1}}, \boldsymbol{Ea_{kr2}}, \boldsymbol{Ea_{kt}}, \boldsymbol{Ea_{kact,0}}, \boldsymbol{Ea_{kdeact,0}}, \boldsymbol{Ea_{kact}}, \boldsymbol{Ea_{kdeact}}, \boldsymbol{Ea_{kp}}, \boldsymbol{Ea_{ktrm}}]$

$\boldsymbol{y} = \boldsymbol{Conversion, PDI, or\ Mn}^{*}$

$\boldsymbol{y_{i,predicted}}$: is the predicted value of a given output for the ith experiment.

$\boldsymbol{y_{i,experimental}}$: is the experimental value of a given output for the ith experiment.

By using this cost function and as an initial guess the parameters of Payne et al. (2013), the optimal parameters were obtained for the model, and are given in Table 3.3. These parameters resulted in a much closer fit than was obtainable originally, which can be seen from the results presented within Figure 3.2 below.

Table 3.3: Optimal kinetic parameters for model developed in this work

Rate Constant	Optimal A ($mol\ s^{-1}\ L^{-1}$)	Optimal E_a (J/mol)	Reference
kr_1	50.5	1.63×10^4	This work
kr_2	106	1.78×10^4	This work
$kact_{,0}$	7.34×10^4	2.80×10^4	This work
$kdeact_{,0}$	1.96×10^8	9.22×10^3	This work
kp	4.38×10^6	2.57×10^4	This work
kt*	5.70×10^9	1.58×10^4	This work
kdeact	2.08×10^8	8.01×10^3	This work
kaact	7.00×10^6	2.55×10^4	This work
ktrm	2.32×10^3	3.21×10^4	This work

*Termination is assumed to occur 90% of the time by disproportionation, as was assumed by Payne et al. (2013).

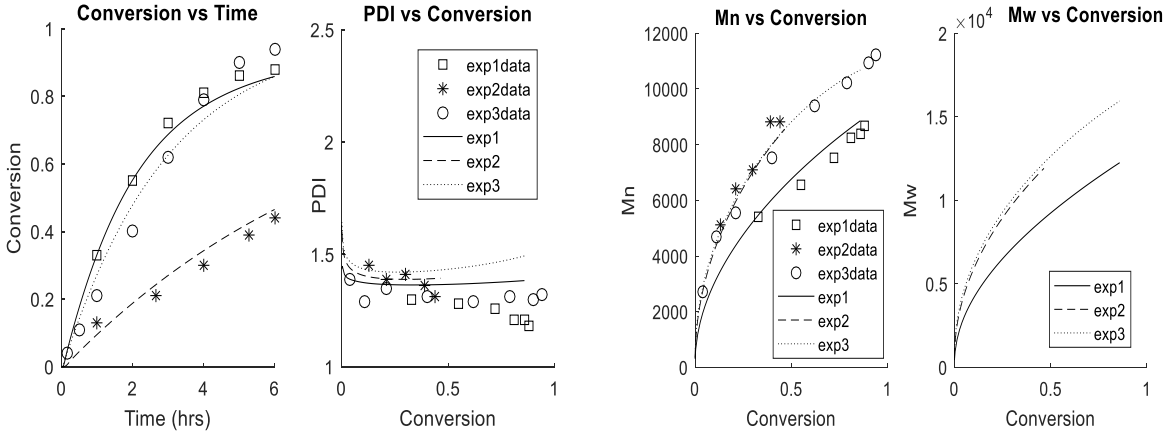

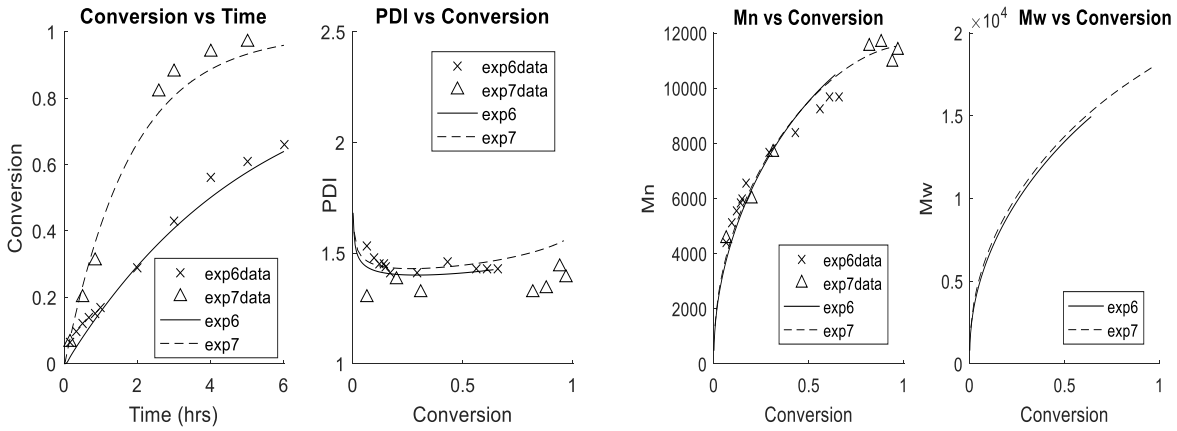

<u>Figure 3.2</u>: Plots comparing optimal-model predictions to the experimental values of Payne et al. (2013) for experiments 1-3, 6, & 7

Note: For initial conditions of the simulation see the experimental conditions in Appendix A.

Now while the simulation results seem to be quite close to the experimental data, some deviations between predicted and experimental values occurred. For instance, at high conversions the model predictions of the conversion trends deviated slightly from the values obtained experimentally. Further slight differences exist between the predicted values of PDI and the experimental values for experiments 1, 3, & 7. A likely explanation for this is that some sort of diffusional phenomenon is occurring within the system, as generally these effects would increase the rate of polymerization and slightly reduce the PDI, at high conversions (Rabea and Zhu, 2015).

With that in mind a reasonable fit does seem to be obtainable for the remaining values being compared above. It is important to note however that these values were used in the optimal fitting process, and are therefore expected to provide some of the best fits to the data. For this reason, they alone do not provide a rigorous test of the model accuracy. Instead a better test would be to use data which was not used in this parameter estimation process. For this purpose, some of the data points, those associated with experiment 4 & 5, as well the initiator conversion for all of the experiments, were set aside. Below in Figure 3.3 a comparison of these data points to the values predicted by the model is given.

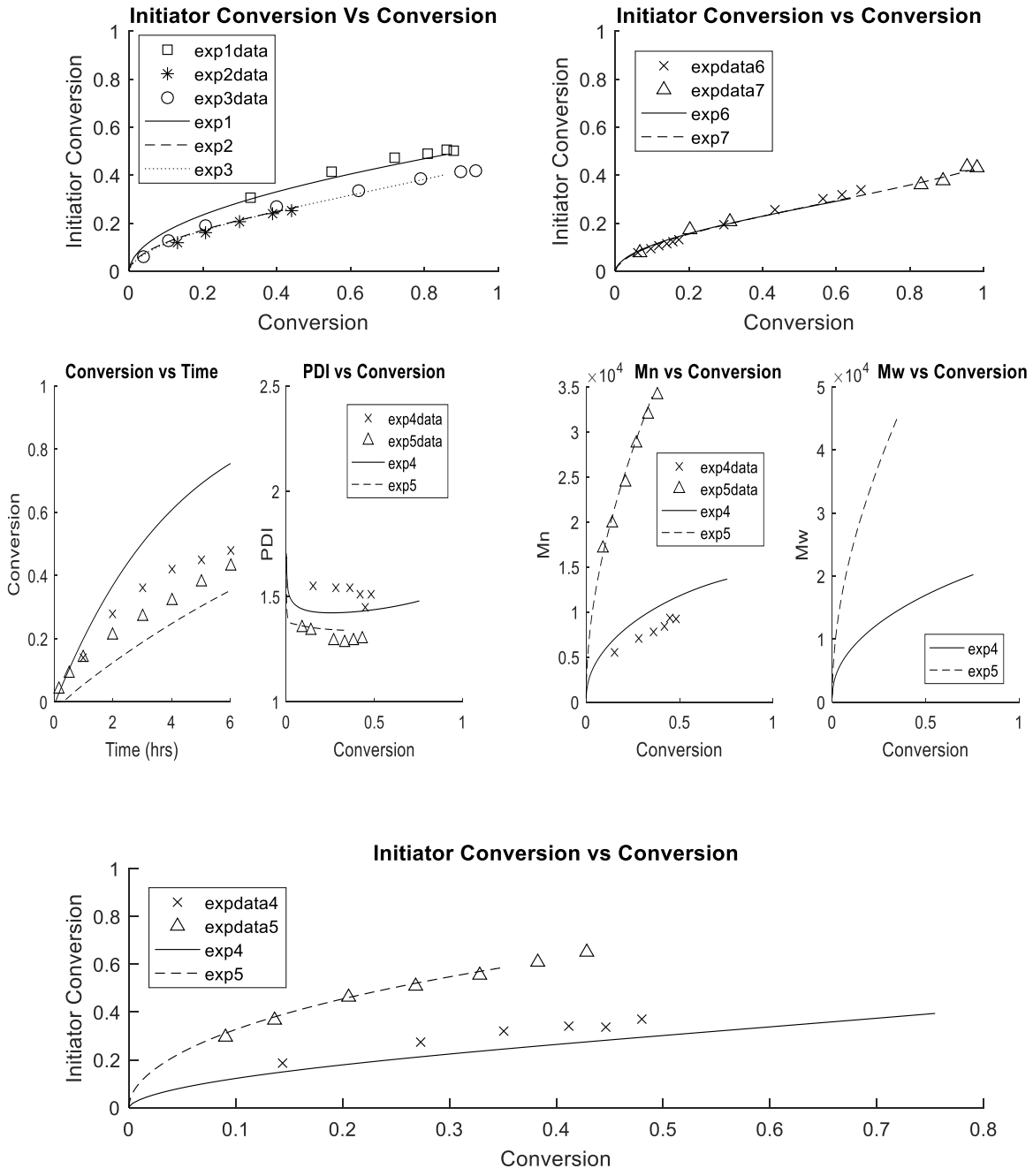

<u>Figure 3.3</u>: Plots comparing optimal-model predictions to the experimental values of Payne et al. (2013)

Note: For initial conditions of the simulation see the experimental conditions in Appendix A.

As can be seen above, reasonable prediction of the experimental values is obtained by the model. However, there are noticeable differences between the predicted and experimental values when it comes to the conversion trends of experiments 4 and 5. These discrepancies between model and

experimental values were seen in the work of Payne et al. (2013), and were thus not wholly unexpected; that being said, they still call for an explanation. At present, the most plausible causes for these deviations seem to be a chain length dependency associated with the rate constants and diffusional effects. These phenomena are likely explanations for the deviations, as in experiments 4 and 5 the TCL was increased to 50 and 400 respectively, and thus large chain phenomenon was feasibly more relevant at these conditions. With this in mind, in the future it would be interesting to develop a model over a wide range of TCL, to try to see if the trends of the data can be approached by a combination of the phenomenon mentioned above.

3.5 Conclusions

From the results given above it can be seen that adequate predictions of the experimental trends were obtained through use of the model. Importantly however deviations from the experimental data of Payne et al. (2013) existed. In particular, noticeable deviations from the conversions trends of experiments 4 and 5 were found. This as discussed above could be due to the fact that chain length dependency and diffusional effects were not taken into account. In the future it would be interesting to see how well the model developed in this work performs over a large TCL range, and if inaccurate, what additional features need to be added to it to account for the phenomenon present in this system.

CHAPTER 4 : MODELLING OF THE AGET ATRP OF BUTYL ACRYLATE IN A TWO-STAGE DISPERSED SYSTEM

4.1 Introduction

Models of dispersed polymerization systems have progressed significantly since their inception early in the 20th century. This is evidenced by the fact that models can now capture trends such as conversion, molecular weight distribution, and even particle size distributions for systems undergoing conventional radical polymerization (Feeney et al., 1984; Gao and Penlidis, 2002; Pladis et al., 2014). That being said, the natures of many topics within the field of emulsion remain ambiguous and are not captured within current models. Of these, some of the most recent and unexplored problems have arisen from the application of the CLRP methods to dispersed systems. These topics require careful attention, as often the rich phenomenon within dispersed systems are exceedingly complex due to the additional components required to perform this form of polymerization.

Nevertheless, basic models have been developed to shed light on the complex kinetics of emulsion polymerizations. Usually these come in the form of either statistical models (Monte Carlo) or approximate population balance model, since finite differential models which fully describe the system have proven difficult to obtain. These models nonetheless have provided important insights into the system, showing the potential effects of compartmentalization, diffusion-controlled reactions, and partitioning effects. Their use however is mainly limited to miniemulsion CLRPs, with extensions to other dispersed systems only being approximate in nature. There thus seems to be a gap in current knowledge when it comes to the application of these ideas to emulsion systems.

For this reason, in the current work an attempt to develop a model for a two-stage emulsion CLRP will be made. It is hoped that this model will be able to capture trends in conversion and molecular weight data. Thus as a comparison, experimental data will be used as a benchmark against model predictions. This attempt is importantly only meant to be qualitative in nature and only the general trends will likely be captured. Nevertheless important insights into some of the phenomenon occurring in these systems is hoped to be gleaned.

4.2 Process Description

The dispersed process studied in this thesis is the AGET ATRP of butyl acrylate (BA) in a two-stage dispersed system; with use of Copper (II) Bromide/Bis(2-pyridylmethyl)octadecylamine ($CuBr_2$/BPMODA) as a deactivator (catalyst), Ethyl 2-bromoisobutyrate (EBiB) as an initiator, ascorbic acid (AA) as a reducing agent, and polyoxyethylene (20) oleyl ether (Brij 98) as a surfactant. In order to properly understand this process one has to consider two features associated with it: the chemical mechanism and the nature of the mediums used. These features help to determine how the process progresses and its main characteristics. In what follows a description of the process as a whole is given by providing details on the nature of these two features.

Beginning this discussion with the mediums adopted for this process, a few subjects need to be tackled. To start, the place of each of the mediums used and their functions within the process should be specified, so as to allow the reader to understand the role of each medium. On top of this as both of the mediums utilized are dispersed systems, the key features distinguishing them from homogenous polymerizations should be illustrated (this helping to make clear some of the shifts that can be expected to the chemical kinetics within these systems). Finally, since two distinct forms of dispersed media are used, the differences in the phenomena at play in both of these systems should be given. In the paragraphs that follow a brief description of these characteristics is provided.

Starting with the place and purpose of each of the mediums within the process a couple of topics can be discussed. To begin, the process itself involves a transformation of a microemulsion to an emulsion via the injection of additional monomer to the system. This transformation is desired as it allows for a reduction in the surfactant content relative to the monomer content, and increases the solid content of the polymerization process. Now as the end goal of this procedure can be seen to be the generation of an emulsion, one might wonder why an ab initio emulsion was not used instead. The reason for this is that early attempts to perform an ab initio emulsion were unsuccessful, resulting in systems with higher molecular weights than those predicted (Jousset et al., 2001; Qiu et al., 1999). This was believed to be caused by the use of extremely hydrophobic ligands, which while importantly preventing catalyst dissociation in the aqueous phase, had the disadvantageous result of hindering transportation of catalyst from monomer droplets to the reaction loci. Therefore to overcome this issue, Min et al. (2006) developed a two-stage emulsion

procedure, which allowed the catalyst (and initiators) to become trapped in the polymer particles generated during the microemulsion phase. This system, which has been shown to successfully carry out the AGET ATRP process (Min et al., 2006), allows one to circumvent the problem of the previous systems. It also presents clear roles for both the microemulsion and emulsion mediums within this process; with the microemulsion serving to enclose species in desirable locations within the reaction environment, while the injection of monomer and associated transformation of the system to an emulsion serves to bring the process to a desirable state.

Keeping these purposes of both of the microemulsion and emulsion in mind, the discussion can now be focused on the major features which distinguish a dispersed system from a standard homogenous medium. These features are the discrete nature of the reaction loci and the partitioning of species throughout the different phases of the system. Beginning this discussion with the discretization of the reaction loci, it can be seen that this phenomenon has a significant effect on the nature of bimolecular reactions within the system. This effect is importantly mixed. The discretization prohibits the reaction of molecules in different reaction loci, lowering the bimolecular rate, while increasing the rate of bimolecular reaction due to either confined space or relatively large fluctuations in the number of these molecules in different reaction loci (Tobita, 2010). Through the interplay of these discretization effects, bimolecular reactions in this system gain their unique properties. For instance, often the rate of termination is dramatically decreased due to the significant effect of segregation of radicals when compared to the other rate increasing effects. However in the case of other bimolecular reactions, this interplay can often become more complicated, and both reductions and increases in the reaction rates are possible depending on conditions. The determining factor in whether an overall increase or decrease in rate occurs often has to do with the size of the reaction loci, as well as the partitioning behavior of the species involved in the reaction. Nevertheless, it can be concluded that discretization can have a significant effect on a plethora of the reactions in a process.

On top of this the partitioning behavior found in both the microemulsion and emulsion systems further complicates the kinetics. In both of these systems certain components partition themselves throughout the different phases. In the current process being considered these species are butyl acrylate (monomer), $CuBr_2$ and CuBr (Copper portions of catalyst). Due to this behavior, only a portion of these species are available for reaction at any given instant. This significantly changes

the rates of reaction and the dynamics of the process. Importantly however not all species in the system behave in this manner, and some species cannot partition, at least to any appreciable degree. This results in these species being trapped in their current location in the reaction media. In the current system the species of this kind are polybutylacrylate, BPMODA, Ascorbic acid and EBiB. Due to this entrapment care must be taken to ensure that these species are found in the appropriate location within the system for a reaction to occur. This is particularly important in the case of the EBiB and BPMODA, as in emulsion systems they can become trapped within large monomer droplets away from the desired reaction loci, resulting in poor reaction conditions. For these reasons the partitioning behavior can also become quite important in these dispersed systems.

Finally on top of the complications introduced above, system specific complications can be introduced. These intricacies often have to do with the size of the particles in the system and changes in the partitioning behavior due to changes in the relative amounts of species present. In the case of the emulsion system, larger particle sizes and an excess of monomer can be found. The excess of monomer keeps the reaction loci saturated with monomer for the majority of the reaction, though not all of it, while the large particles allow phenomenon such as the gel effect to occur (For more details see the emulsion section). In the case of the microemulsion system on the other hand, smaller particle sizes and a comparatively smaller amount of monomer are present. This results in different monomer partitioning behavior in microemulsion systems, and for instance a negligible gel effect (For more details see the microemulsion section). Thus due to these resulting differences between these systems, these system specific considerations can also can be seen to be quite important.

With this last remark an exposition of the physical qualities of the system has been given. At this point it therefore becomes possible to begin a description of the chemical mechanism active within this process. Now while this mechanism shares some attributes in common with the standard ATRP process (depicted above in Table 2.3), the chemical mechanism of this polymerization differs quite significantly. This is owing to the changes brought about when shifting to an AGET ATRP process, the complexities of butyl acrylate radical polymerization, the use of dispersed media, and the specific reagents used. Shown below in Table 4.1 is the full chemical mechanism of this process.

Table 4.1: Mechanism for the AGET ATRP of butyl acrylate

(Reduction)	$Red^{I}{}_{(aq)} + CuBr_{2(aq)} \xrightarrow{k_{red1}} Red^{II}{}_{(aq)} + CuBr_{(aq)}$
	$Red^{II}{}_{(aq)} + CuBr_{2(aq)} \xrightarrow{k_{red2}} Red^{III}{}_{(aq)} + CuBr_{(aq)}$
(Activation of initiator)	$I - Br + CuBr/BPMODA \underset{k_{deact,s,0}}{\overset{k_{act,s,0}}{\longleftrightarrow}} R_{s,0}\cdot + CuBr_2/BPMODA$
(Initiation)	$R_{s,0}^{\cdot}: + M \xrightarrow{k_p} R_{s,1}^{\cdot}$
(Backbiting)	$R_{s,n}^{\cdot} \xrightarrow{k_{bb}} R_{t,n}^{\cdot}$
(Propagation. Where n≥1)	$R_{s,n}^{\cdot} + M \xrightarrow{k_{p,s}} R_{s,n+1}^{\cdot}$
	$R_{t,n}^{\cdot} + M \xrightarrow{k_{p,t}} R_{s,n+1}^{\cdot}$
(Equilibrium)	$R_{s,n} - Br + CuBr/BPMODA \underset{k_{deact,s}}{\overset{k_{act,s}}{\longleftrightarrow}} R_{s,n}\cdot + CuBr_2/BPMODA$
	$R_{t,n} - Br + CuBr/BPMODA \underset{k_{deact,t}}{\overset{k_{act,t}}{\longleftrightarrow}} R_{t,n}\cdot + CuBr_2/BPMODA$
(Transfer with monomer)	$R_{s,n}^{\cdot} + M \xrightarrow{k_{trm,s}} P_n + R_{s,1}\cdot$
	$R_{t,n}^{\cdot} + M \xrightarrow{k_{trm,t}} P_n + R_{s,1}\cdot$
(Transfer with polymer)	$R_{s,n}^{\cdot} + P_m \xrightarrow{k_{trp,s}} P_n + R_{t,m}^{\cdot}$
(Termination)	$R_{s,n}^{\cdot} + R_{s,m}^{\cdot} \xrightarrow{k_{tc,ss}} P_{n+m}$
	$R_{s,n}^{\cdot} + R_{s,m}^{\cdot} \xrightarrow{k_{td,ss}} P_n + P_m$
	$R_{s,n}^{\cdot} + R_{t,m}^{\cdot} \xrightarrow{k_{tc,st}} P_{n+m}$
	$R_{s,n}^{\cdot} + R_{t,m}^{\cdot} \xrightarrow{k_{td,st}} P_n + P_m$
	$R_{t,n}^{\cdot} + R_{t,m}^{\cdot} \xrightarrow{k_{tc,tt}} P_{n+m}$
	$R_{t,n}^{\cdot} + R_{t,m}^{\cdot} \xrightarrow{k_{td,tt}} P_n + P_m$

Where *I-Br*: Ethyl 2-bromoisobutyrate, *M*: monomer, *CuBr/BPMODA*: Activators (Catalyst in its lower oxidation state), $CuBr_{2(aq)}$ copper (II) bromide in the aqueous phase), $CuBr_{(aq)}$ copper (I) bromide in the aqueous phase, *CuBr₂/BPMODA*: Deactivators (Catalyst in its higher oxidation state), $Red^{I}{}_{(aq)}$: Reducing agent in its first oxidation state, $Red^{II}{}_{(aq)}$: Reducing agent in its second oxidation state, $Red^{III}{}_{(aq)}$: Reducing agent in its third oxidation state, $R_{s,0}\cdot$: primary radical, $R_{s,1}\cdot$: secondary radical of chain of length 1, $R_{s,n}\cdot$: secondary radical of size n; where n≥1, $R_{t,n}\cdot$: tertiary radical of size n; where n≥1, $R_{s,n}$-*X*: halide capped secondary radical, $R_{t,n}$-*X*: halide capped tertiary radical , and $P_{n+m}/P_n/P_m$: are dead polymers of length n+m, n and m respectively.

As can be seen above in Table 4.1, this process begins in a fashion quite different from that of the standard ATRP process, with a percentage of the copper, which makes up the metal complex (catalyst), partitioning to the aqueous phase and reacting with ascorbic acid. This complication, which arises due to the nature of these metal complexes in dispersed systems, results in the reaction mechanism being split between the two phases. This manifests in the reduction reactions taking place within the aqueous phase (Ascorbic acid is water soluble), and the remainder of the reactions occurring within the organic phase.

Keeping this is mind, the process – as was stated above - begins with the oxygen unstable copper (I) bromide being generated from the oxygen stable copper (II) bromide by reaction with ascorbic acid. Due to the nature of the dispersed media, these species then partition throughout the different phases of the system. From here, with some of both of the copper species now present in the organic phase, the polymerization carries on in a fashion similar to that of standard ATRP, though with added complexities associated with the AGET ATRP process, butyl acrylate polymerization, and dispersed media. Thus similarly to the standard ATRP radicals are generated through an equilibrium with alkyl halide initiators, which can then go on to participate in propagation, termination, transfer, and the associated equilibrium reactions. However as mentioned above there are some added complexities. For instance in this process the reduction reactions which had played an integral role in the start of the polymerization, also can occur throughout the process. These reactions thus not only allow for the use of the oxygen stable copper (II) species at the start of the polymerization, but also for less catalyst to be used in general, as the copper (I) can now be partially regenerated from the copper (II) species. On top of this, reactions associated with butyl acrylate radical polymerization also further complicate the kinetics. As was mentioned in the previous chapter the formation of tertiary radicals, which can participate in the majority of the reactions accessible to secondary radicals, results in a near doubling of the possible reactions. This doubling of the reactions, also doubles the possible pathways within the process, thus increasing its complexity dramatically. Further complications also arise from the nature of the dispersed media used. To start the partitioning behavior of the different species (see description above) determine the location of the reactions within the system and how prevalent they will be. To make matters worse the monomer droplets, which act as monomer reservoirs for a portion of the process, are eventually depleted resulting in more convoluted partitioning behavior (i.e. non-saturated partitioning behavior). On top of this the discrete nature of the reaction loci in the system further

enhance rates in the process, resulting in sometimes unexpected kinetic behavior. Thus only by taking into account all of these added complexities, as well as the features of the standard ATRP process can a full picture of the chemical mechanism be formed.

With the aggregation of both the chemical and media specific features of this system, the underlying nature of the process can be illustrated. Importantly these individual features of this system are strongly linked. For instance the media specific properties have a direct effect on the mechanism in that they modify rates or - as was the case with the copper species - slightly modify the mechanisms. This causal relationship can also be seen to flow in the other direction, as the chemical mechanism of the system determines how chemical compounds will be consumed, and thus when changes to the physical nature of the system will occur (for instance the depletion of monomer droplets). They therefore must be considered jointly, as otherwise the interaction effects between them will be completely missed. This however results in a rather complicated framework for the workings of the system. Nonetheless without this rigorous depiction of the process, important insights into its evolution and characteristics will not be given.

4.3 Model

The modelling of the AGET ATRP process in a dispersed medium is by no means simple. This is because not only does one have to deal with the complicated nature of the chemical kinetics, but also understand the main effects of phenomenon such as compartmentalization and partitioning of species. As a direct result of this, it has proven to be quite difficult to obtain a compact differential model of this system[5]. On top of this, approaches with simpler mathematical frameworks, such as the Monte Carlo method, also appear to struggle in simulating such physio-chemical processes; often only obtaining results after long simulation times. In fact, a pure Monte Carlo method without any careful tailoring would likely result in an algorithm which is far too cumbersome for much practical use. In an attempt to circumvent these problems, in the current work, a hybrid model of both the Monte Carlo and differential algorithms is used, so as to incorporate the best qualities of

[5] Interestingly some approximate population balance models have been made. One work that contains a model of this form is that done by Van Steenberge et al. (2014).

both of each approach into the final algorithm. In the paragraphs that follow a breakdown of this model will be given.

Beginning this discussion with the differential portion of the algorithm, it can be seen that its main use is in the simulation of the aqueous phase reactions. The reactions occurring in this phase are the reduction reactions involving the copper species and ascorbic acid. These reactions are both easily and quickly represented using the differential method of simulation. This would be contrasted if one were to make use of a Monte Carlo method to simulate these reactions, as this would likely result in a slow simulation time, and due to the large volume of the aqueous phase, a more complicated algorithm. For this reason, it was decided that the simulation of aqueous phase reactions would be best handled by taking a kinetic modelling approach, and specifically using equations of the following form to describe the dynamics of the aqueous phase:

$$\frac{d[Red^{I}]}{dt} = -k_{red1}[Red^{I}][CuBr_2] \tag{4.1}$$

$$\frac{d[Red^{II}]}{dt} = k_{red1}[Red^{I}][CuBr_2] - k_{red2}[Red^{II}][CuBr_2] \tag{4.2}$$

$$\frac{d[Red^{III}]}{dt} = k_{red2}[Red^{II}][CuBr_2] \tag{4.3}$$

$$\frac{d[CuBr_2]}{dt} = -k_{red1}[Red^{I}][CuBr_2] - k_{red2}[Red^{II}][CuBr_2] \tag{4.4}$$

$$\frac{d[CuBr]}{dt} = k_{red1}[Red^{I}][CuBr_2] + k_{red2}[Red^{II}][CuBr_2] \tag{4.5}$$

Where: $[Red^{I}]$ is the concentration of the reducing agent in its first oxidation state, $[Red^{II}]$ is the concentration of the reducing agent in its second oxidation state, $[Red^{III}]$ is the concentration of the reducing agent in its third oxidation state, $CuBr_2$ is the concentration of the copper (II) bromide in the aqueous phase, $[CuBr]$ is the concentration of the copper (I) bromide in the aqueous phase.

It is important to note that the time (t) as used within these equations should be considered separate from those used in the Monte Carlo. These equations were solved by the ode45 function in MATLAB, which is an implementation of the explicit Runge-Kutta (4,5) pair of Dormand and Price called DP54.

The Monte Carlo algorithm, on the other hand, is used to simulate the reactions occurring in the organic phase. This is done to avoid the complicated mathematics associated with the compartmentalization of species within discrete polymer particles. At its core the algorithm makes use of the scheme developed by Tobita and Yanase (Tobita, 1995; Tobita and Yanase, 2007). What this means is that the algorithm relies on the generation of hypothetical time periods until occurrence for any realizable process, and uses these times to make decisions about which process has occurred at any given instant. For the processes dealt with in this model, it was assumed that the necessary times could be generated by exponential distributions of the form of equation (4.1). Exponential distributions of this form are easily simulated, through use of a computer and equations (4.2) and (4.3).

$$P\left(t_{react,occur}\right) = \frac{1}{t_{react,avg}} e^{\left(-\frac{t_{react,occur}}{t_{react,avg}}\right)} \tag{4.6}$$

$$t_{react,occur} = t_{react,avg} \ln\left(\frac{1}{U}\right) \tag{4.7}$$

$$t_{react,avg} = \frac{1}{\rho N_{av} V_{part}} \tag{4.8}$$

Where: $P\left(t_{react,occur}\right)$ is the probability of a specific time until occurrence, U is a random number taken from a continuous uniform distribution from 0 to 1, $t_{react,occur}$ is the hypothetical time until a reaction occurs or the time selected randomly from an exponential distribution representing the reaction, $t_{react,avg}$ is the average time until a reaction occurs, ρ is the rate of a particular event in mol L^{-1} s^{-1}, N_{av} is Avogadro's number, and V_{part} is the volume of the reaction loci.

After generating these times, the algorithm then works by using them to make a decision about which process has occurred by selecting the process with the smallest time until occurrence as the event which has transpired. The system is then moved forward appropriately by adjusting the amounts of reactants and increasing the simulation time by the amount selected.

However, in the case of propagation, these reactions must be accounted for in a different manner. This is because the propagation reactions occur quickly and frequently in the system, and thus would drastically slow down the algorithm. Therefore, to avoid this slowdown, the propagation

reactions are instead accounted for by using a Poisson distribution for a given time interval. These distributions are generated from the equations shown below.

$$\bar{r} = k_p[M]_p \Delta t \tag{4.9}$$

$$P(r) = \frac{\bar{r}^r e^{-\bar{r}}}{r!} \tag{4.10}$$

Where: $\bar{r}$ is the expected number of monomer units added during the interval, k_p is the rate constant for propagation, $[M]_p$ is the concentration of monomer in the particle, Δt is the difference between the time at which the reaction currently selected by the algorithm will occur and that of the previous reaction selected by the algorithm, r is the actual amount of monomer units added, and $P(r)$ is the probability of adding r monomer units. It is important to note that while the above equations describe the Poisson distribution of the process, they do not provide the numerical technique used to obtain the random values. The method used to obtain values randomly from this distribution was that used by the built-in MATLAB function poissrnd; i.e. the waiting time method for small values of $\bar{r}$ and Ahren's and Dieter's method for larger values of $\bar{r}$.

As may be seen, the advantage of these Poisson distributions is that in any given time interval the number of propagation events can be accounted for by randomly selecting a number from these distributions. This greatly increases the speed of the algorithm, while still allowing for the propagation events to be appropriately considered. That being said for the sake of simplicity a couple of assumption are made about this process. These assumption are that all radicals that are active in a given interval are assumed to have grown by the same amount, and only one particle is assumed to have an active radical at any given instant. These assumptions while actually fallacious do provide a reasonable approximation to the true system. This is because often only one radical is active in a particle, and particles are rarely active at the same time due to the nature of this controlled radical polymerization.

In any case after accounting for the propagation reactions by appropriately updating the amount of monomer within the particle, as well as the size of the polymers and their corresponding distribution properties (M_n, M_w, and PDI), all the necessary dynamics of the organic phase will have been taken into account, and this process as a whole can be repeated. Using this approach

Tobita and Yanase (2007) were able to simulate the miniemulsion process for various CLRP systems. However, in order to properly simulate the AGET ATRP of butyl acrylate in the two-step emulsion system studied an extended version of this Monte Carlo method had to be created. This is because in this system one has to account for the interplay between macroscale and nanoscale phenomenon, and also account for partitioning effects, which conveniently provide a link between the differential and Monte Carlo parts of the algorithm. Therefore two major extensions to this original Monte Carlo were needed.

The simpler of these two extensions was to develop a way to account for the partitioning effects occurring in the system. This was done through use of a modified version of the Morton/Vanzo equations (Morton et al., 1954; Vanzo et al., 1965) suggested by Maxwell et al. (1992) and partitioning coefficients. The modified Morton/Vanzo equation was used to account for the monomer partitioning, while the partition coefficients were used to account for copper(I) and copper (II) partitioning behavior. However, besides these equations, mole balance equations were also needed to account for the total amount of monomer, copper(I), and copper (II) remaining in the system at any given instant. Below these partitioning equations, as well as the related mole balance equations are given:

Monomer Partitioning:

When the aqueous phase is saturated with monomer:

$$\ln(1-\Phi_p)+\Phi_p-0.5956=0 \tag{4.10}$$

Once the aqueous phase is no longer saturated with monomer:

$$\ln\left(\frac{[M]_{aq}}{[M]_{aq,sat}}\right)=\ln(1-\Phi_p)+\Phi_p-0.5956 \tag{4.11}$$

$$[M]_{aq}=\frac{\left(\frac{N_M-V_{p,tot}(1-\Phi_p)\rho_M}{Mw_M}\right)}{V_{aq}} \tag{4.12}$$

$$N_M=(1-x)N_{M,0} \tag{4.13}$$

Where the monomer concentration in the particle could be determined from:

$$\Phi_m\approx 1-\Phi_p \tag{4.14}$$

$$[M]_p = \frac{\Phi_m \rho_M}{Mw_M} \tag{4.15}$$

Copper (I) Partitioning:

$$K_{Cu(I)} = \frac{[Cu^I]_{org}}{[Cu^I]_{aq}} \tag{4.16}$$

$$N_{Cu(I)} = [Cu^I]_{org} V_{org} + [Cu^I]_{aq} V_{aq} \tag{4.17}$$

Copper (II) Partitioning:

$$K_{Cu(II)} = \frac{[Cu^{II}]_{org}}{[Cu^{II}]_{aq}} \tag{4.18}$$

$$N_{Cu(II)} = [Cu^{II}]_{org} V_{org} + [Cu^{II}]_{aq} V_{aq} \tag{4.19}$$

Where: $[M]_{aq}$ is the concentration of monomer in the aqueous phase, $[M]_p$ is the concentration of monomer in the particle or organic phase, Φ_p is the volume fraction of polymer in polymer particles, Φ_m is the volume fraction of the monomer, ρ_M is the density of monomer, Mw_M is the molecular weight of monomer, V_{aq} is the volume of the aqueous phase, N_M is the number of moles of monomer remaining the system, $N_{M,0}$ is the initial number of moles of monomer in the system, x is the conversion of monomer, $K_{Cu(I)}$ is the partition coefficient for copper (I) species, $[Cu^I]_{org}$ is the concentration of copper (I) in the organic phase, $N_{Cu(I)}$ is the number of moles of copper (I) remaining in the system, $[Cu^I]_{aq}$ is the concentration of copper (I) in the aqueous phase, $K_{Cu(II)}$ is the partition coefficient for copper (II) species, $[Cu^{II}]_{org}$ is the concentration of copper (II) in the organic phase, $N_{Cu(II)}$ is the number of moles of copper (II) remaining in the system, $[Cu^{II}]_{aq}$ is the concentration of copper (II) in the aqueous phase, V_{org} is the volume of the entire organic phase, and $V_{p,tot}$ is the total volume enclosed by all the particles.

Note: The Morton/Vanzo equation given above is applicable for temperatures in the neighbourhood of 50 °C, but is assumed to work at 80 °C. It was solved using the fsolve function in MATLAB, which used the trust-region-dogleg algorithm to solve a set of nonlinear equations.

With these relations a complete description of the partitioning behavior in the system can be given, as all other components are assumed not to partition between the various phases. Importantly these partition/mole balance equations also serve the crucial role of providing a link between the Monte Carlo and differential portions of the algorithm, in that they link the organic phase reactions to the aqueous phase reactions. Thus by taking advantage of this link, the Monte Carlo and differential algorithms can maintain appropriate levels of communication with each other through updates made to the mole balances/partitioning equations at regular intervals.

In practice this communication occurs by first taking a relatively large step forward (though small enough to ensure numerical accuracy) with the differential algorithm to account for the aqueous phase behavior in that step period. Then using the Monte Carlo portion of the algorithm the organic phase behavior is accounted for by allowing it to run through the duration of that step. Once this is done the link is established between the algorithms by updating the overall quantities of the monomer, activator, and deactivator in the system using both differential and Monte Carlo algorithms, and then appropriately partitioning these species between the phases according the equations given above. In this fashion one is able to appropriately track the total amount of these species which are shared between the phases, and thus ensures that both algorithms are working together consistently.

With this in mind there was still a second update to the model required. This update allowed one to account for the interplay between the macroscale and nanoscale phenomenon, and required a careful use of averages and proportions. Properties that need to be accounted for in this manner are the rate of polymerization, rate of consumption of each of the copper species, the average volume of the particles, and the proportion of nucleated micelles. These properties can be broken into two groups. The first, simply need to be known at a single point. These are the average volume of the particle and the proportion of nucleated micelles. The other form of average however needs to be known over an interval. These averages correspond to the reaction rates and are found by calculating the mean value of the reaction rates over the considered interval. Below in Figure 4.1 a look at these two different types of averages is given. Where in this figure Rp_{avg} is the average rate of polymerization, R_{CuBr} is the average rate of consumption of CuBr consumption, R_{CuBr2} is

the average rate of $CuBr_2$ consumption, $V_{p,avg}$ is the average volume of the particles, and A_{avg} is the proportion of active particles.

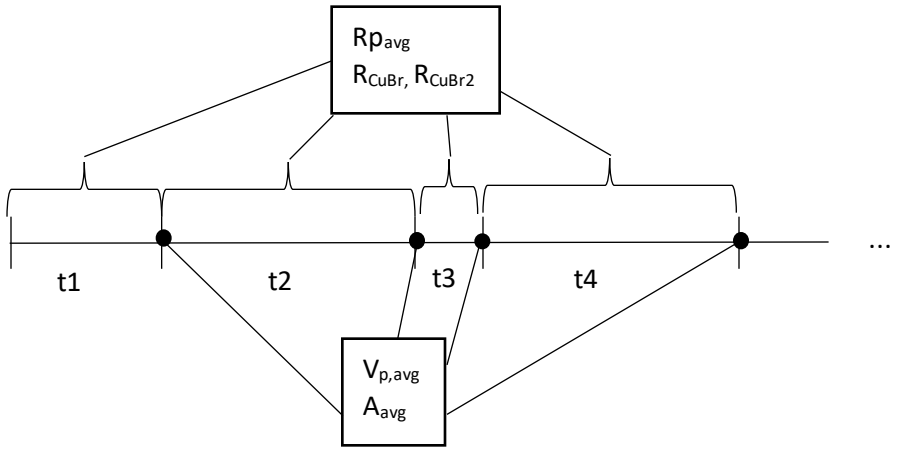

Figure 4.1: Different averages accounted for in the model

With the addition of these two extensions to the algorithm of Tobita and Yanase (Tobita, 1995; Tobita and Yanase, 2007), as well as a differential framework for accounting for aqueous phase reactions, a working simulator of the system is obtained. This simulator is however approximate in nature; owing to the manner in which estimates of the macroscale properties of the system were obtained, as well as assumptions used to simplify the model. Nonetheless it should be able to qualitatively describe the behavior of the system and provide important insights into its nature.

4.4 Model Assumptions

The following assumptions were made about the process:

1. The copper species and monomer were the only species which partitioned to any appreciable extent between the phases.
2. The deactivator and activator molecules are assumed to partition as a whole, even though in reality only the copper species partition to the aqueous phase. This neglects the

reformation and separation processes as the transition metal moves to and from ligands in the system.

3. The volume of the particle could be found from the mass of the polymer held within it as follows:

$$\boldsymbol{V_{part}} = \frac{\boldsymbol{m_{poly}}}{\boldsymbol{\rho_p} \cdot \boldsymbol{\Phi_p}}$$

Where: $\boldsymbol{V_{part}}$ is the volume of the particle, $\boldsymbol{m_{poly}}$ is the mass of polymer within the particle, $\boldsymbol{\rho_p}$ is the density of the polymer, and $\boldsymbol{\Phi_p}$ is the volume fraction of the polymer within the particle.

4. The behavior of large particles which are formed through coagulation could be modelled solely by simulating the reaction dynamics in the precursor particles that formed them; i.e. large particles can be modelled by breaking them into their component parts.
5. β-Scission, thermal initiation, primary radical termination, and termination due to catalyst are ignored.
6. Primary radicals are assumed to react at the same rate as polymeric radicals when reacting with monomer.
7. Reduction reactions occur solely in the aqueous phase.
8. Diffusional effects and chain length dependency of reactions are ignored.
9. All radicals derived from initiator are secondary.
10. The initiation equilibrium proceeds at the same rate as its macromolecule counterpart

4.5 Results and Discussion

The model developed in this work was able to capture the major features of this system. This included not only the trends in "livingness"[6], but also trends associated with the molecular weight distributions. That being said, model predictions importantly still showed some deviations in behavior from that seen in the experiments conducted by Min et al. (2006). This was particularly noticeable for the PDI trends obtained, as well as the "livingness" profiles at relatively high values

[6] For a definition of livingness please see the nomenclature section.

(>0.9). Below in Figures 4.2-4.4, a visual comparison between model predictions and the data of Min et al. (2006) is given.

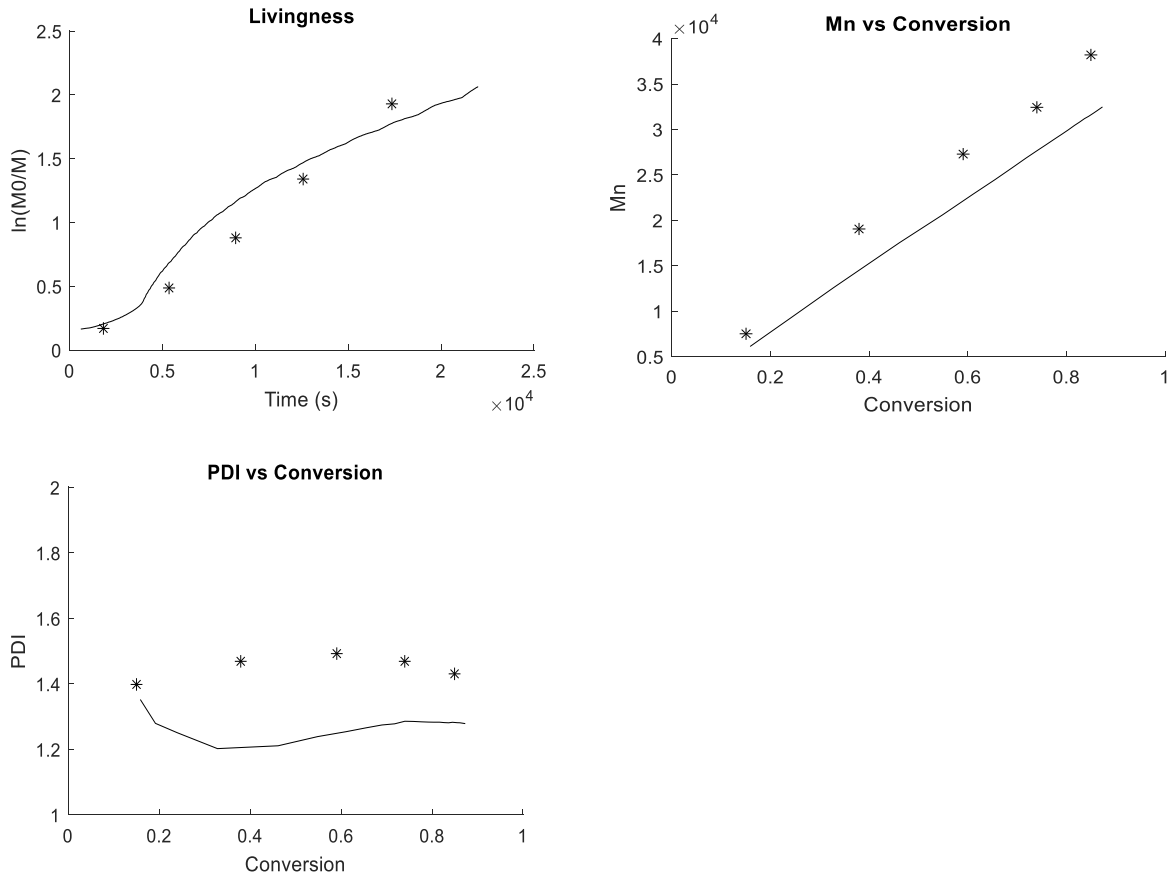

<u>Figure 4.2</u>: Visual comparison of the data of Min et al. (2006) and Hybrid Monte Carlo predictions: Experiment 1.

Note:

1. Initial conditions were the experimental conditions for experiments 1 as carried out in the work of Min et al. (2006) and given in Appendix B.
2. The parameters used within the model can be found in Appendix C.
3. Multiple runs were carried out to ensure numerical stability.

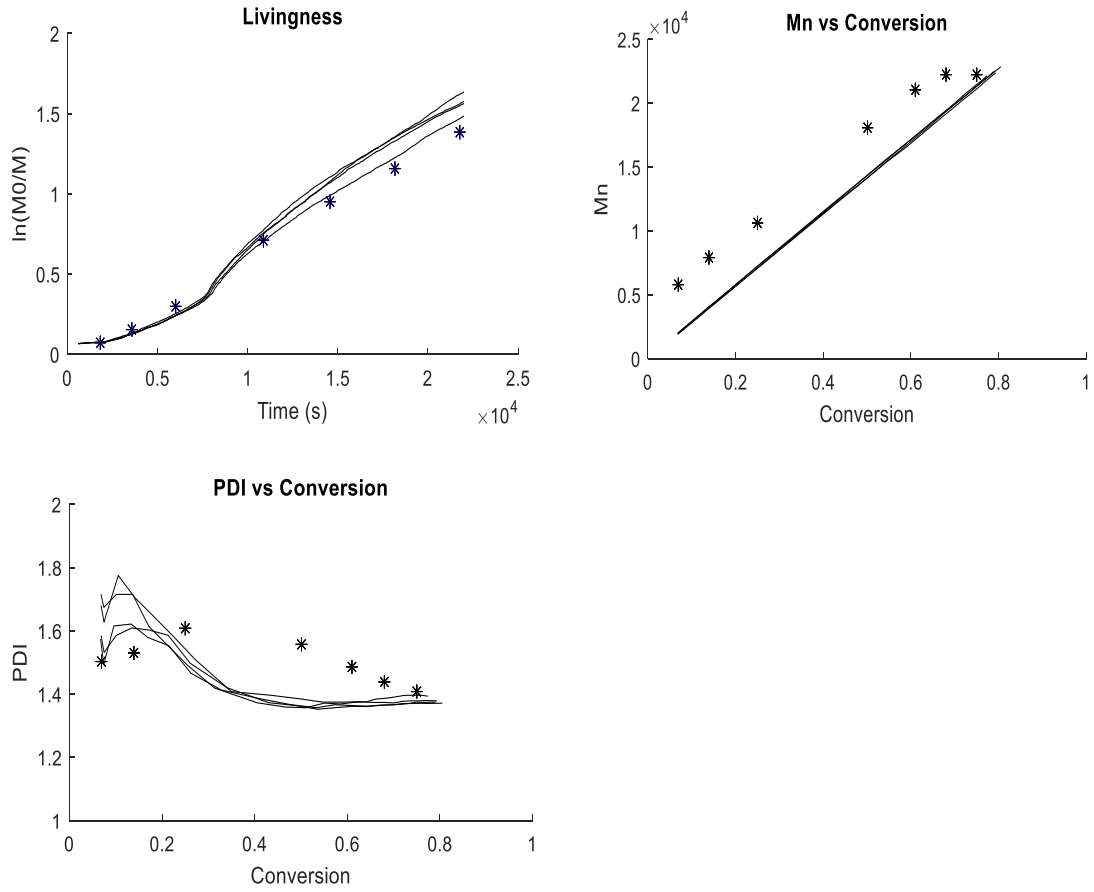

Figure 4.3: Visual comparison of the data of Min et al. (2006) and Hybrid Monte Carlo predictions: Experiment 2.

Note:

1. Initial conditions were the experimental conditions for experiments 2 as carried out in the work of Min et al. (2006) and given in Appendix B.
2. The parameters used within the model can be found in Appendix C.
3. Multiple runs were carried out to ensure numerical stability.

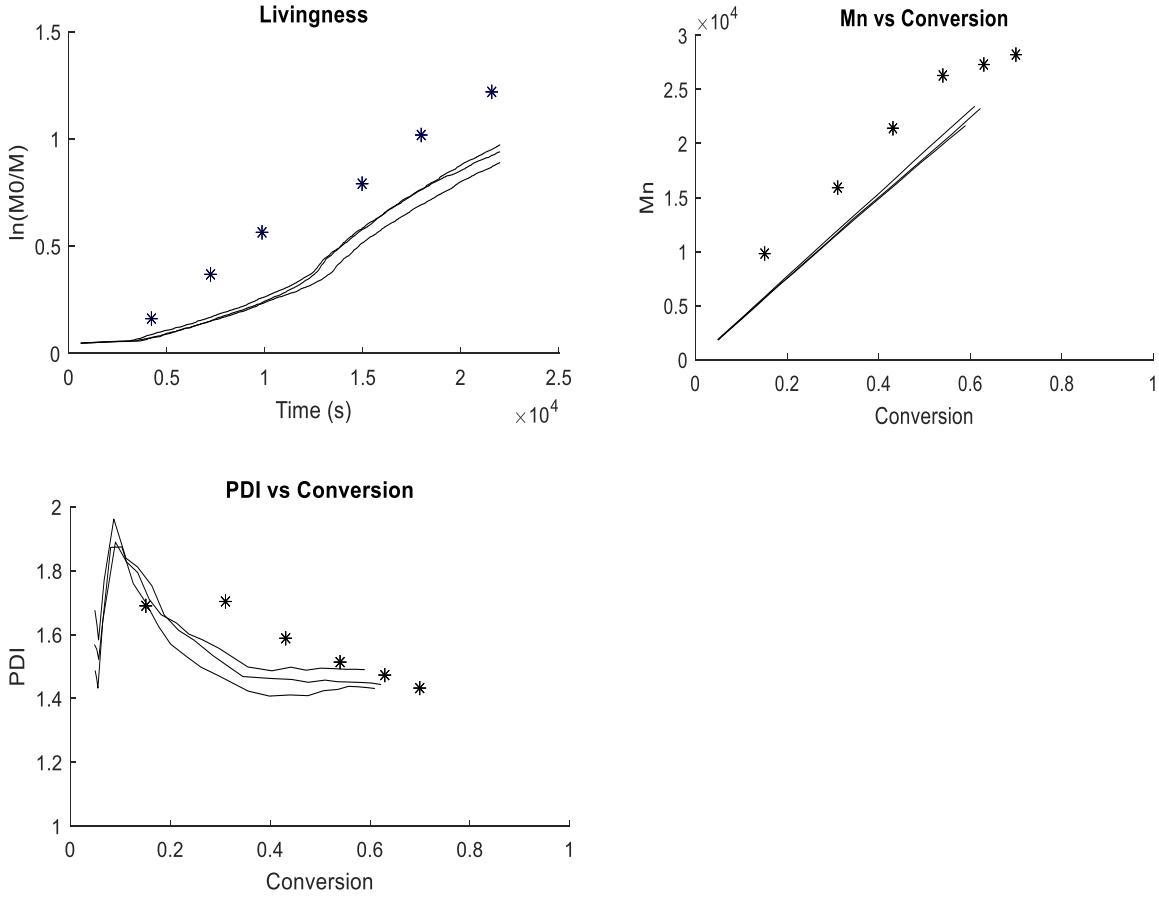

<u>Figure 4.4</u>: Visual comparison of the data of Min et al. (2006) and Hybrid Monte Carlo predictions: Experiment 3.

Note:

1. Initial conditions were the experimental conditions for experiments 3 as carried out in the work of Min et al. (2006) and given in Appendix B.
2. The parameters used within the model can be found in Appendix C.
3. Multiple runs were carried out to ensure numerical stability.

Now while the original goal of this study was only to develop a model which qualitatively captured the trends of the system, something which seems to have been obtained above, providing reasons for the deviations between predicted and experimental values may prove fruitful. In particular, discourse of this sort, may allow one to understand some of the phenomenon which appears to be present within the system. Nevertheless, before discussing any of the possible mechanistic reasons for these deviations, a simple reason must first be presented. This simple reason is that the differences between model predictions and experimental trends may be in a part due to insufficient knowledge of the kinetic parameters of the system; a point which is particularly relevant in dispersed systems, where vast quantities of parameters are required, and where experimental measurements are difficult to obtain. This situation is even worse in the current system, as the AGET ATRP process has not been studied extensively within these dispersed systems, and even very basic rate constants are not available. As a consequence of these circumstances, in works like this one, approximations of a large portion of the rate constants have to be made[7]. This need unfortunately then leaves one uncertain as to whether model predictions could simply be improved by better parameter estimates. For instance, it may have been the case that most of the deviation seen in the above plots were explainable simply as the result of poor parameter approximation.
With that in mind, it is nonetheless still likely that mechanistic reasons for the deviations are at least in part responsible for the dissimilarities found between model and experimental trends. This is because in the current model, certain phenomenon which are known to occur, and also have an effect within the system, have been neglected in order to simplify the simulation process. For example, diffusional effects on radicals, the catalyst, and the monomer, at high conversions have been neglected, even though these have been shown to play important roles at these conversions (Rabea and Zhu, 2015; Zetterlund, 2010). Further some advanced dispersed/chemical phenomenon such as concentration dependent catalyst partitioning coefficients, coagulation of particles, and activation/deactivation rates for initiator molecules which deviate from those of macromolecules, have been assumed negligible; this being in spite of the fact that these are also likely to have an impact on the dynamics of the system.

The presents of these phenomenon also seems to be supported by data. For example, diffusional effects within dispersed controlled radical polymerizations are expected to result in plots of

[7] Concurrent adjustment of these rate constants were made –within a reasonable range-to provide better fits of the data.

"livingness" which have an increased linearity, as well as trends in PDI vs conversion which are concave in nature (Rabea and Zhu, 2015; Thomson and Cunningham, 2010; Zetterlund, 2010). By looking at the visual comparison above, it becomes obvious that if the model were to gain these features, better fits of the experimental data would be obtained; thus being suggestive of diffusional phenomenon. Similarly, the small polymer particle sizes simulated (~3 nm in radius), relative to those obtained experimentally (~45-60 nm in radius), are suggestive of coagulative effects within the system; this being especially telling, when one considers the fact that the only other known mechanism for growth of these particles, the growth of polymer molecules, has already been taken into account.

For the remaining phenomenon mentioned above, direct evidence of this sort, however does not exist. There is nevertheless experimental evidence of their presence and effect in literature. For instance, in the case of concentration dependent partition coefficients, experimental evidence for their variation with concentration is given by (Elsen et al. (2012) and Qiu et al. (2000b); while work demonstrating the importance of the exact partition value at any given instant is given by Kagawa et al. (2007). On the other hand, differences in rate constants for macro-radicals and primary radicals in regards to the main ATRP equilibrium, have been evidenced both experimentally and from a modelling point of view in the work of Payne et al. (2013).

In summary, while the model developed in this work adequately captures the qualitative features of the system, some gaps still exist. As pointed out above, these gaps seem to be indicative of diffusional effects at high conversion, coagulation of polymer particles, and perhaps other less obvious phenomenon such as concentration dependent partition coefficients, as well as different values of k_{act}/k_{deact} for initiator molecules. By accounting for these phenomenon within the system, it is believed that differences between model predictions and experimental values can be narrowed down. However as was importantly noted above, the deviations between model predictions and experimental data may be in part a result of poor parameters estimates. It therefore is also quite relevant that future attempts be made to improve estimates of these values, so that kinetic models can be more adequately validated.

4.6 Conclusions

From the results obtained above it seems that the Hybrid Monte Carlo model developed for this system adequately described some of the major phenomenon within it. This included both trends in "livingness" and molecular weight distributions. Nonetheless there were still some important deviations between model predictions and experimental data, such as deviations in PDI trends, "livingness" at high conversion, and particle size predictions. This as discussed above could have been indicative of diffusion, coagulative, partitioning, or initiation effects, as well as from a non-mechanistic point of view, poor parameter estimates. In the end, this model thus not only illustrated the strength of the model under certain assumptions, but also pointed out some important areas in which it could possibly be improved.

CHAPTER 5 : EXPERIMENTAL INVESTIGATION OF THE AGET ATRP OF BUTYL ACRYLATE IN A TWO-STAGE EMULSION SYSTEM

5.1 Introduction

Atom Transfer Radical Polymerization (ATRP) occurring within an emulsion system is a relatively new topic within the polymerization field. It has mainly been pursued due to the fact that the emulsion media is favoured in industry for the production of nanoparticles. Unfortunately however it has proven to be quite difficult to adapt the ATRP process to emulsion systems. This is because issues such as coagulation of particles, the reaction of anionic surfactant with catalyst, and partitioning effects have hindered this process. Nevertheless, some systems have been developed to successfully carry out ATRP in emulsion.

To date, the most successful of these approaches has been the two-stage AGET ATRP emulsion developed by Min et al. (2006). This two-stage procedure avoids issues associated with previous systems such as poor initiation efficiency and/or droplet nucleation. It accomplishes this through use of both a microemulsion and emulsion stage. In particular, the polymerization process first proceeds in a microemulsion, which when sufficiently polymerized (~30% conversion) is then transformed into an emulsion by injection of monomer. This is a crucial feature of the process as it avoids the transport/droplet nucleation issues of the previous systems by enclosing catalyst and initiator within polymer particles formed during the microemulsion stage.

Experimental studies of this system currently are nevertheless lacking and further investigation into this subject is required. For this reason, part of this thesis is dedicated to an experimental investigation of this system. In particular a look at a slightly altered version of this process, which makes use of a different catalyst from that of Min et al. (2006) and is not completely air free, is made. The purpose of this work is to help illuminate some of the features of this process, and also to clarify its limitations or possibilities.

5.2 Materials

n-Butyl acrylate (BA, ≥98%, stabilized by 50 ppm 4-methoxy phenol; purchased from VWR) was purified by passing it through an inhibitor remover column (purchased from Sigma Aldrich). The chemicals Polyoxyethylene (20) oleyl ether (Brij 98), L-Ascorbic Acid (AA, 99%), 4,4'-Dinonyl-2,2'-Dipyridyl (dNbpy, 97%), THF (HPLC grade, ≥99.9%) were purchased from Sigma Aldrich, while Ethyl 2-bromoisobutyrate (EBiB, 98%) and Copper (II) Bromide ($CuBr_2$, 99%), methanol (ACS grade, ~99.8%) were purchased from VWR. All chemicals above were used as received unless stated otherwise.

5.3 Experimental Setup

5.3.1 Reactor and Associated Equipment

Depicted below in Figure 5.1 is the general setup used for reactions. This setup made use of a 2L stainless steel PARR reactor. This reactor contained a dip-tube for sampling and nitrogen gas entry, a stirring rod with a 45° pitched blade impeller, a cooling pipe, a thermocouple for temperature measurement, a pressure gauge, and a gas vent located near the top of the reactor. The main purpose of this reactor was to provide a closed environment for the process to occur. However alongside this reactor, some other equipment was necessary for running the reaction. This equipment was the controller/computer, nitrogen tank/ gas outlet valve, the pressure gauge, and the external cooling system. These accessories and the reactor allowed one to construct a well-controlled environment to carry out the reaction.

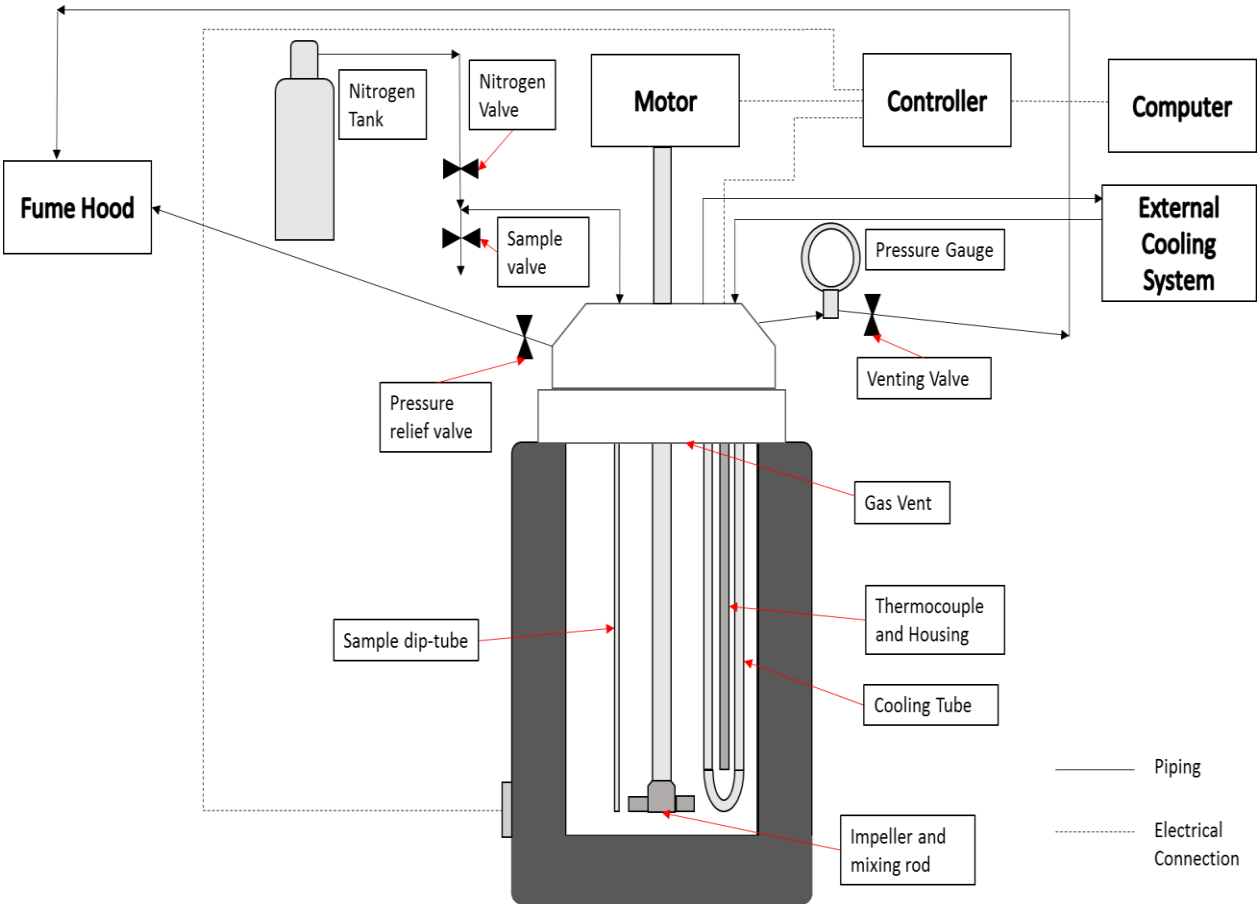

Figure 5.1: Reactor setup

5.4 Experimental Procedure

5.4.1 General Procedure

The first step in the experimental procedure was to confirm that the reactor was clean. This was accomplished by a visual/touch inspection of any accessible portion of the reactor, followed by a check for clogs in the pipes or unreachable locations through use of pressurized air. This check generally was not necessary, as the reactor should have been cleaned directly after any previous reactions, but was a good practice as it prevented possible faults.

In any case, once clean, the next step in the procedure was the preparation of the chemicals. This began by first measuring out the appropriate amounts of $CuBr_2$ and dNbpy into a beaker. The $CuBr_2$ was measured to the nearest 0.2mg directly into this container using a PTFE coated spatula, as this would not react with the $CuBr_2$. The dNbpy on the other hand was measured to the nearest 0.1mg on to a piece of blank paper using a stainless steel spatula and then transferred into the beaker ensuring the paper was thoroughly jostled to remove any remnants. The blank piece of paper was then reweighed to check if all of the dNbpy was transferred from the paper (At least all measurable quantities thereof). From here, a small magnetic stir rod and monomer were transferred to the vial for the formation and dissolution of the copper complex, with the monomer transfer occurring through use of a 10mL pipette with graduations of 0.1 mL. The beaker containing these ingredients was then sealed with aluminum foil and placed on a heating plate and brought to a temperature of approximately 60 °C to form and dissolve the copper complex within the monomer solution. This resulted in a brown solution upon complete dissolution of the complex (a green paste was seen prior to dissolution).

In the meantime- as this dissolution process took quite some time to complete- a solution of Brij 98 and water was made to the concentration desired for the microemulsion. This was done by first measuring out the Brij 98 into a small 25mL beaker, with this mass measurement made accurate to the nearest 1mg. This surfactant was then transferred to a 500 mL beaker containing distilled water in the amounts required, and which had been measured out using a 250 mL graduated cylinder with graduations of 2 mL. The 25 mL beaker which now contained some remnants of the Brij 98 was filled with a portion of the distilled water from the 500 mL beaker. At this point the

500mL, 25 mL beaker, and the utensils used during the transfer process (ends being inserted into the 25mL beaker) were then placed on the hot plate until any remaining Brij 98 dissolved.

At this point, the copper complex was completely dissolved in the monomer, and in a separate beaker the initiator, EBiB, could be measured out; often this was only done to the nearest 10mg, but in some cases was done right to the nearest 0.1 mg. This compound was appreciably volatile, so it was immediately mixed with the copper complex solution and quickly sealed. This transfer had to be done as fast as possible using a preheated pipette as the copper complex precipitated quickly once cooled and EBiB is again quite volatile. From here, after giving the components of both this organic and the aqueous Brij 98 solutions some time to dissolve, the two solutions were combined to form the microemulsion solution by using a heated pipette to quickly transfer the organic mixture into the Brij 98 solution under mixing. This microemulsion was then given time to equilibrate.

Once this process was complete the microemulsion was poured into a 2L PARR stainless steel reactor and sealed therein. The mixture was then purged 4 times with nitrogen (99.998% purity) in order to clear the headspace of the reactor and remove some of the dissolved oxygen from the system. Four purges were selected, as this resulted in the expected oxygen in the headspace being reduced to below 0.01 in mole fraction, while importantly preventing the loss of too much of the volatile components. This fact is exemplified below in Figure 5.2, where a plot of the relation between the current mole fraction of oxygen in the headspace and the number purges is given. This plot was generated using the relation $y_j = y_0 \left(\frac{P_L}{P_H}\right)^j$; where: y_j is the mole fraction after the jth purge, y_0 is the initial mole fraction, P_L is the ambient pressure, P_H is the pressure when the vessel is pressurized with nitrogen, j is the number of purges. This relation is derived from the well known ideal gas law. For more information see Appendix E and (Crowl and Louvar, 2011).

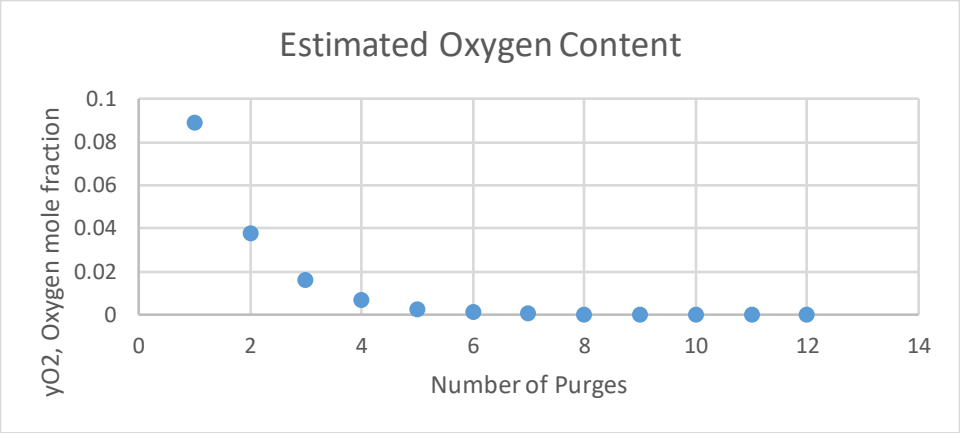

Figure 5.2: Oxygen vapor mole fraction versus number of purges

In any case, after removing this portion of oxygen from the system the reaction mixture was then heated up to the reaction temperature and the stirrer was operated at an appropriate speed (Often 250 rpm controller). Now while the system and the controller were equilibrating to the set point, an aqueous solution of ascorbic acid was prepared in a 40 mL beaker. This was done by first measuring out the desired amount of ascorbic acid and then dissolving it into 30 mL of distilled water. The ascorbic acid was then left to dissolve in a cupboard away from a light source as it was light sensitive.

Once the system had equilibrated and the ascorbic acid fully dissolved, the reaction was started by injecting the ascorbic acid solution into the vessel. The microemulsion polymerization was then allowed to carry on for 10 minutes total, with a sample being collected at the 5-minute mark to characterize some of the behavior of this reaction. At the 10-minute mark the system was transformed from a microemulsion to an emulsion polymerization by the injection of additional monomer. At this point more ascorbic acid was also added to compensate for the small amounts of oxygen entering the system during the injection processes. The system was then allowed to carry on in this fashion until the end of the reaction with samples being taken at regular intervals. These samples were exposed to air and cooled in order to quench the polymerization.

After the reaction had completed the system was disassembled and exposed to air to end the reaction. The reactor was then cleaned using soap, water, and pressurized air. This involved scrubbing all accessible regions with a brush and soapy water, and use of pressurized air to clear pipes and unreachable areas. Once cleaned in this fashion the reactor was closed with its container

nearly full of distilled water. It was then placed under high pressure and stirring, and the distilled water removed from pipes to help remove any residual materials within the system. This was then repeated a second time, after which the reactor was left to dry.

5.4.2 Intermittent Procedures

5.4.2.1 Monomer Purification

For any given experiment at least 50 mL of purified monomer had to be ready for use. Purified monomer was produced by passing the monomer through an inhibitor remover column, purchased through Sigma Aldrich. This was accomplished by adding the monomer dropwise to the column via a 250 mL separatory funnel. During this purification it was ensured that the flowrate through the column was not in excess of 120 mL per hour, as this was the recommended maximum flowrate. Further, due to butyl acrylates sensitivity to light, the equipment was wrapped in aluminum foil and some of the lights were turned off, so as to avoid light induced reactions. This being said, once the monomer had eluted and was purified, it was stored within a refrigerator until use. The column was then washed with methanol, dried, and stored sealed inside the refrigerator (This washing procedure could only be repeated a few times before the column packing material had to be completely changed).

5.4.2.2 Leak Testing

To ensure the system remained free of leaks a periodic leak test was done. This leak test involved filling the reactor (almost full) with distilled water, sealing it, and placing it under a blanket of nitrogen at high pressure; this minimized the amount of nitrogen needed for the test, and also allowed some of the possible residue within the system to be dissolved within the distilled water. The test then began by first creating a soap/water solution by mixing tap water with soapy mixture. The soap/water solution was then sprayed over possible areas of leakage on the closed reactor. If any bubble appeared, adjustments to the reactor were then made until the point where upon retesting bubble formation did not occur.

5.4.2.3 Controller Tuning

In order to establish proper control over the temperature and stirring speed within the reactor the controller had to be intermittently tuned. This was generally done using the automatic tuning procedure specified by the manufacturer PARR. The procedure involved first filling the reactor with distilled water to the volume to be used during the true reaction. The reactor and its accompanying accessories were then turned on, in order to mimic the reaction conditions. At this point the controller was turned on and the autotune setting was selected. The controller would then try to reach the desired setpoint and disturb the system until it had found parameters which worked reasonably well. Once this was done the controller changed its parameters to these values and the system was ready for a reaction to be carried out. This procedure was repeated for any changes of the reaction volume, or setpoints of the controlled variables.

5.5 Experimental Analysis

Samples collected from the experiments were analyzed to obtain conversion and molecular weight distributions. The conversion was determined gravimetrically, whereas the molecular weight was determined using GPC/SEC. In what follows the details of these analysis techniques is given. This includes both the necessary formulas and procedures used. It is hoped that after reading this section, a clear idea of how to perform these techniques will be provided.

5.5.1 Conversion

The monomer conversion was determined by the gravimetric method. This method makes use of mass fractions which are known within the system and the mass fraction of the overall solid content to obtain a value for the conversion. This is accomplished via the following formulas (these are specific to this system):

$$Conv = \frac{(F_{sol} - F_{CuBr_2} - F_{dNbpy} - F_{AA} - F_I)}{F_M} = \frac{F_{sol} - (F_{sol} - F_{poly})}{F_M} = \frac{F_{poly}}{F_M} \quad (5.1)$$

$$F_{sol} = \frac{(m_{dry,cup} - m_{empty,cup})}{(m_{wet,cup} - m_{empty,cup})} \quad (5.2)$$

Where F_{sol}: mass fraction of solids, F_{poly}: Mass fraction of polymer, F_x: initial mass fraction of compound x in solution, $CuBr_2$: copper(II) bromide, dNbpy: 4,4'-dinonyl-2,2'-dipyridyl, AA: ascorbic acid, I: initatior (ethyl 2-bromoisobutyrate), M: monomer (butyl acrylate), and $m_{y,cup}$: mass of cup in state y.

Now as the values of all the mass fractions other than F_{sol} are known, a value of the conversion can be obtained by taking the measurements: $m_{dry,cup}$, $m_{wet,cup}$, and $m_{empty,cup}$. These measurements are obtained by finding the mass of a dry cup, the mass of the cup with an aliquot of sample in it, and the mass of this cup once the sample has been allowed to dry; with the drying process occurring in a vacuum oven at 40-50 °C over a period of 24 hrs. Once these measurements were taken the conversion of the sample was then determined using the formulas provided above. This measurement procedure while quite simple is also one of the best methods for determining conversion.

5.5.2 Molecular Weight

Measurements of the polymer molecular weights on the other hand were determined using a Viscotek GPCmax VE2001 solvent/sample module and Viscotek TDA 302 Triple detector array. In order to properly characterize samples using this machine a careful procedure had to be carried out. This procedure began first with the purification of the polymer samples to be run. This was necessary, as impurities such as the copper catalyst could possibly interfere with the detection devices of the column, while those such as the surfactant could broaden the molecular weight

distribution found. Thus to ensure a sufficient level of purity, extraction of the polymer by either drying of an emulsion sample in the oven or precipitation using methanol, was followed by repeated washes with methanol. These washes ensured the polymers were stripped of any impurities, and had an accompanying visual change from white/pink to transparent.[8]

In any case once the polymer had been purified, the GPC samples could then be made by dissolving the polymer in THF such that its concentration fell in an acceptable range, 1-10mg/mL. These samples were then transferred to 2 mL sample vials via a polycarbonate syringe, filtering the liquid through a 0.2µm polypropylene filter to ensure the removal of all large undissolved particles. Along with these samples two standards were prepared for calibration and verification purposes. This involved similarly dissolving the necessary sample in THF and filtering them into a 2 mL sample vial. With the preparation of all of these samples the GPC could then be run.

The GPC measurement procedure consisted of first running a narrow standard to calibrate the GPC. Calibration with one sample was possible due to the use of the triple detection array within the GPC used. This array of detectors was made up of an RI detector, right angle light scattering detector, low angle light scattering detector, and a viscometer. The combination of information obtained from these detectors could be used to calibrate the machine and provide measurements of molecular weight distributions without the standard procedure which requires the generation of calibration curves. Thus simply by running a narrow standard, at the operating conditions specified in Table 5.1, through the column and using the OmniSec software a calibration of the system could be obtained.

Table 5.1: GPC operating conditions

Operating Variable	Value
Temperature (Detector)	22°C
Temperature (Column)	22°C
Flow Rate (mL/min)	1 mL/min (Generally; though sometimes changed if higher resolution was required)
Solvent	THF
Laser wavelength (nm)	670 nm

From here a broad standard could then be run through the column using the operating conditions of Table 5.1, to ensure proper calibration. If the resulting data matched with the values expected

[8] Often this washing was done far above the polymer glass transition temperature (~-49°C), greatly improving the purification process.

for the broad standard the remainder of the samples could be run at the conditions of Table 5.1, with intermittent running of the broad standard to check for drift. In this way reliable data on the molecular weight distribution of the samples was obtained.

5.6 Results and Discussion

The results obtained within this study were very different from those first expected. This was because in a similar system to this, that of Min et al. (2006), control over polymers, dispersion stability, and an initiator efficiency closer to their predicted behaviors were obtained. In the current system however this combination of factors seemed to be allusive. This was likely due to the use of a different ligand within this study, which was chosen over that used by Min et al. (2006) due to its commercial availability. The strange behavior of this system can be seen below in Figures 5.3-5.6, which provide results for experiment 1-4 respectively, while the conditions used in these experiments can be found in Table 5.2.

Table 5.2: Experimental conditions used to study the AGET ATRP of BA in a two-stage dispersed system

Exp	T (°C)	P (psig)	RPM	$CuBr_2$ (g)	L (g)	I (g)	S (g)	RA_1 (g)	M_1 (g)	RA_2 (g)	M_2 (g)	$H_20,_1$(g)	V_{tot} (mL)
1	70	20-40	250	0.0252	0.0927	0.2273	8.9429	0.2003	3.576	0.1504	42.9	520	572
2	70	20	250	0.0274	0.1005	0.1592	6.2591	0.0323	3.576	0.0078	28.61	350	386
3	70	20	250	0.0277	0.1007	0.1598	6.2600	0.0122	3.576	0.0061	28.61	345	381
4	70	20	250	0.0277	0.1010	0.1609	6.2608	0.0081	3.576	0.0081	28.61	346	382

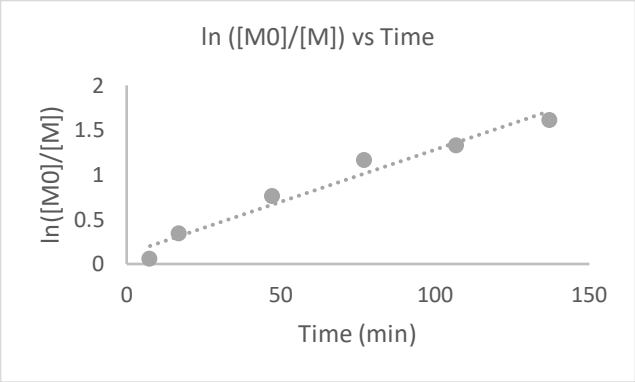

Experiment 1: Waterloo GPC			
Sample	**Mn**	**Mw**	**PDI**
4	1.27×10^{6}	2.19×10^{6}	1.73
4	1.26×10^{6}	2.06×10^{6}	1.64
5	3.54×10^{6}	4.50×10^{6}	1.41
5	2.56×10^{6}	4.74×10^{6}	1.85
MMA STD 1500K	1.05×10^{6}	1.15×10^{6}	1.12

Figure 5.3: Results of Experiment 1

Note: This experiment deviates from the ones given below in a few respects, the most important of these is the large amount of ascorbic acid used relative to the catalyst. This is because when ascorbic acid is in excess, to the extent in the above experiment, this results in a system which follows conventional radical polymerization behavior.

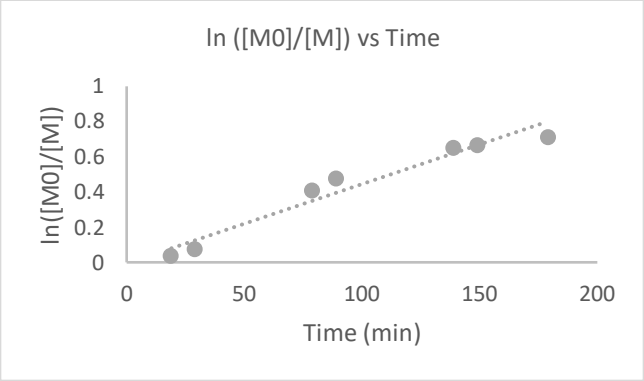

Experiment 2: Polyanalytik GPC			
Sample	**Mn**	**Mw**	**PDI**
5	1.38×10^{5}	2.01×10^{5}	1.46
5	1.32×10^{5}	1.91×10^{5}	1.45
8	1.34×10^{5}	1.92×10^{5}	1.43
8	1.36×10^{5}	1.92×10^{5}	1.42
PS stand-Mw=99K	9.26×10^{4}	9.91×10^{4}	1.07
PS stand-Mw=135K	8.07×10^{4}	1.36×10^{5}	1.69

Figure 5.4: Results of Experiment 2

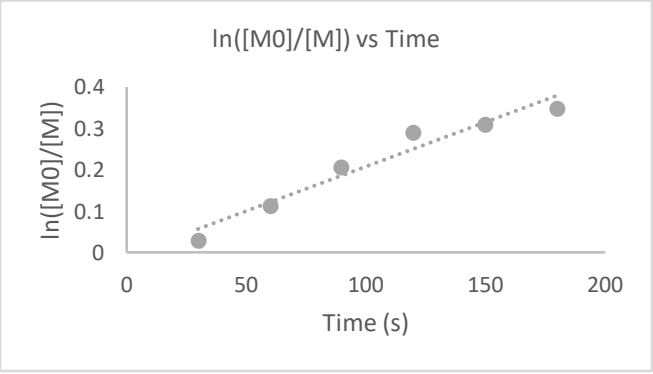

Experiment 3: Ryerson GPC			
Sample	**Mn**	**Mw**	**PDI**
4	6.75×10^{4}	1.27×10^{5}	1.88
4	6.68×10^{4}	1.25×10^{5}	1.86
7	7.18×10^{4}	1.25×10^{5}	1.75
7	7.65×10^{4}	1.33×10^{5}	1.74
PSBS- Mw=147K	8.51×10^{4}	1.40×10^{5}	1.64
PSBS- Mw=147K	8.76×10^{4}	1.47×10^{5}	1.67

Figure 5.5: Results of Experiment 3

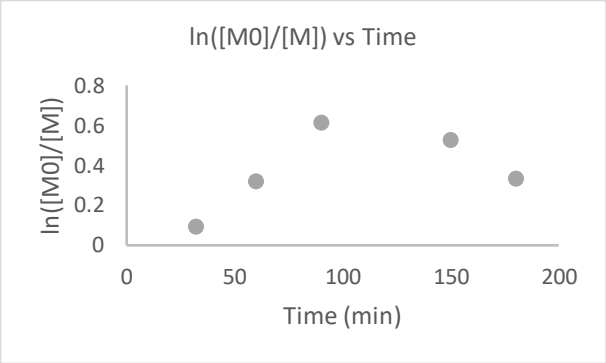

Experiment 4: Ryerson GPC			
Sample	**Mn**	**Mw**	**PDI**
3	1.10×10^5	1.66×10^5	1.51
3	1.05×10^5	1.60×10^5	1.51
4	1.42×10^5	2.12×10^5	1.49
4	1.36×10^5	2.04×10^5	1.5
PSBS- Mw=147K	8.53×10^4	1.43×10^5	1.68
PSBS- Mw=147K	8.71×10^4	1.47×10^5	1.69

Figure 5.6: Results of Experiment 4

Note: For this experiment the plot of the ln(M0/M) vs Time went into a region where coagulation caused measurements to be inaccurate, hence the decrease in value.

Within these figures the numerous behaviors available in this system make themselves evident. To start, as can be seen for the results of experiment 1 in Figure 5.3, the system has a conventional free radical polymerization regime which can be reached simply by using a sufficient amount of reducing agent (ascorbic acid). In this region, the polymerization is characterized by high and relatively conversion invariant molecular weights, broad molecular weight distributions (high PDI), and fast polymerization times; characteristics which are typical of a standard conventional radical polymerization in dispersed systems. It is important to note that this regime is theoretically obtained at high reducing agent concentrations, and that when the reducing agent concentrations are lowered sufficiently, one expects to find systems undergoing a controlled radical polymerization.

However, when the reducing agent concentration was lowered from that found within this conventional regime, the results showed some characteristics combining the behavior of both the conventional and controlled radical polymerizations. This region, exemplified by the results of experiments 2 and 3, which are shown in Figure 5.4 and 5.5 respectively, could have varying attributes depending on the conditions under which the reaction occurred. For instance, in experiment 2 lower molecular weights, a larger reaction time, and a size distribution narrower than those of a conventional free radical system were found; as would be expected in a controlled radical polymerization system. It however still, in a manner similar to a conventional radical polymerization, maintained a conversion invariant molecular weight. Alternatively experiment 3, while having low-valued/conversion dependent number average molecular weights, and large

polymerization times, features expected in controlled systems, also had distributions that were broad in a fashion similar to conventional radical polymerization. Thus the characteristics of the system within this regime appears to be quite varied, though still apparently split in their behavior between the conventional and controlled radical regimes.

That being said, upon further lowering of the reducing agent concentration a controlled regime was obtained. This regime, which can be personified here by experiment 4 (Figure 5.6), has the characteristics of low molecular weights which increase with conversion (ideally in linear fashion), and narrow size distributions. Unfortunately however, at least with the chemicals and conditions used in this study, coagulation of polymer particles occurred concurrently with these other phenomenon. This is believed to occur due to the slow rate of formation of large polymers within this system, which normally effectively stabilize dispersions (Oh, 2008). In any case with this final regime, it can be seen that three regions appear to exist within this system and can be obtained by varying the ascorbic acid concentration. A visualization of this fact is given below in Figure 5.7. In this figure the pictures in the upper portion of the figure are meant to depict the stability of the dispersions and the lower pictures are meant to depict the size distributions of the polymers.

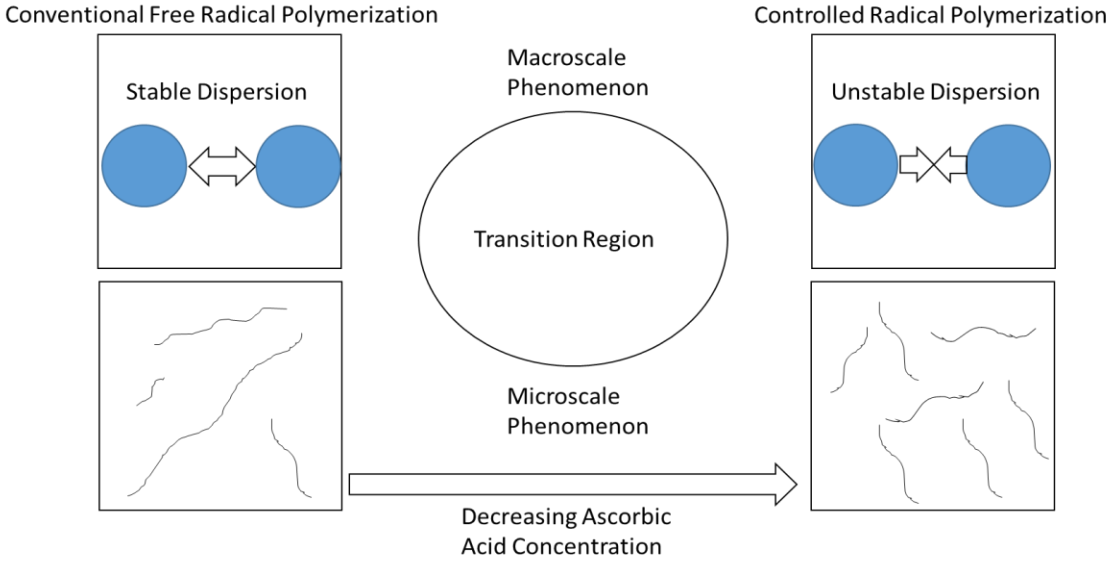

Figure 5.7: Regimes found in the AGET ATRP of BA in an emulsion system

Now while these three regimes of polymerization could possibly be expected, the manner in which the transition from an uncontrolled to a controlled polymerization occurred was quite surprising. For instance the large amount of variability found within this region and the fact that only some of the features of the living system became active at any given condition is unusual. Further only unimodal molecular weight distributions were found within this region, but generally in this type of mixed system you would expect bimodal distributions (One peak generated for components undergoing free radical polymerization and one for those undergoing controlled radical polymerization). For these reasons the system was considered to exhibit some very strange behavior.

Now although difficult to pinpoint any given cause for the behavior of this region, it maybe assumed that it is due to the dispersed system used. This is because the heterogeneous conditions found of these dispersed systems lead to a highly complicated process and thus appears to be conducive to the variability found in this transition region. In any case, it is important to realize that the variability of this region may allow one to access some rich behavior within this system. For example it may be possible to use appropriate conditions within this region to obtain a sufficient level of livingness, but still gain some of the benefits of an uncontrolled polymerization, such as better dispersion stability. Determining conditions of this sort would greatly improve the process and for this reason it may prove profitable to further investigate the nature of this transition region.

That being said there are still some complicating details of this system, which may deter users. The first of these was that poor initiation efficiency unavoidably manifested itself in all the experiments. This was believed to be in part due to the extreme volatility of the initiator (EBiB) used. However, compounding this, and likely the dominant reason for the poor initiation efficiency was the partitioning behavior of the copper catalyst used in this study. This partitioning behavior reduced the initiator efficiency because a large portion of the copper catalyst partitioned itself to the aqueous phase (as was evidenced for a similar system studied by Qiu et al. (2000b)) resulting in a slow rate of activation for initiators. That being said, while having this unfortunate effect, it should also be noted that the catalyst partitioning behavior may also be partly responsible for the rich phenomenon observed within the transition region of this system. Thus if upon further study,

this region provides auspicious conditions for polymerization, a sacrifice between initiation efficiency and richer polymerization conditions may have to be made.

On top of this however there is another deterrent associated with the system studied, which is that the rate polymerization appears to drastically decrease as the reaction goes on. In some reactions this decrease in rate can be explained through the coagulation of particles, which results in an inaccurate measurement of conversion; as was the case in experiment 4. Further in some cases the polymerization ceases due either to the glass effect or diffusion controlled activation, as was the case in experiment 7. However in some systems this decrease in rate occurs at a conversion much too low for diffusion events to be important and is not accompanied by any significant coagulation. It thus must occur because of some other phenomenon within the system. Of the possible causes for this behavior, the best explanation appears to come from the phenomenon termed the persistent radical effect. This effect is the accumulation of deactivator species within the system due to irreversible termination events between radicals. This serves to reduce the rate of polymerization, as the accumulation of deactivator species results in a shifting of the radical equilibrium towards dormancy. It therefore can have the unfortunate effect of slowing the rate of polymerization to a value much lower than that expected. That being said, the persistent radical effect may also be responsible for some of the rich behavior of the transition region, such as the lower polydispersity achievable within it. Its importance in this polymerization must be weighed against its negative effect of slowing down the reaction.

Naturally, it is not always possible to get a perfect controlled polymerization. However, a transition region may provide conditions whereby one can obtain a good balance between controlled and uncontrolled polymerizations. In the best case this would come in the form of a highly living system, with dispersion stability, and a tunable distribution. It therefore may be able to provide a sufficient incentive to use this system, even with its undesirable accompanying traits, however further investigation is still needed to further prove the existence of this region and its traits.

5.7 Conclusions

Keeping all of the above in mind a rich picture of the system can be painted. To begin it can be seen that three distinct regimes exist within the system studied. These regimes were the uncontrolled, controlled, and transition regimes, all of which have unique features associated with their products and kinetics. Of these, the transition regime seems to be the most interesting as a rich variety of phenomenon appears to be available within it, and which importantly has the characteristic of often sharing both features of the controlled and uncontrolled regimes. That being said under the conditions studied this often comes with the negative effects of a slow reaction time and poor initiation efficiency. Nevertheless, once experimentally established, this region could be of great value in the future as if a fine balance between the controlled and uncontrolled regimes can be found, improved kinetics or final polymer properties may be obtainable.

CHAPTER 6 : CONCLUSIONS AND RECOMMENDATIONS

6.1 Concluding Remarks

In this work the ARGET ATRP of butyl methacrylate in solution and the AGET ATRP of butyl acrylate in a two-stage dispersed system were investigated. Three main investigations were carried out:

1. A study of the ARGET ATRP of butyl methacrylate in solution from the perspective of modelling and simulation. In particular, a kinetic model was developed and the accuracy of its predictions under certain assumptions was determined. Rate equations were therefore derived from the reactions present in the process, and the method of moments was used to determine the evolution of average polymer molecular weights and polydispersity.

   It was found that the model predictions using the parameters and kinetic scheme of Payne et al. (2013) did not produce good predictions of the data. Therefore, two modifications were made in this study to improve upon the model. The first of these was the addition of the transfer to monomer reactions. These reactions unfortunately however had a negligible effect on the overall kinetics under the conditions studied; only slightly changing the values of number average molecular weight and PDI when the ratio of monomer to radicals in the system was high (High TCL). Thus another attempt to improve model predictions was made through a second modification.

   Realizing the discrepancy could be removed by alteration of the parameters provided by Payne et al. (2013), a new set of parameters were estimated to provide optimal fits to the data. This was achieved by optimizing a normalized cost function, whose value depended on the squared difference between model predictions and experimental data. The results of the optimization were good in that predictions allowed for the majority of the experimental trends to be captured. Nevertheless, there still existed some gaps between model predictions and experimental values suggesting the model deviations may be due to other terms such as diffusional effects, chain length dependency, and/or copper catalyzed termination. However, as was pointed out in Chapter 3, more experimental data is needed to further improve the model quality.

2. Modelling work done on the AGET ATRP of butyl acrylate in a two stage dispersed system. In this study, a hybrid Monte Carlo model was developed to qualitatively capture the trends present in the system of Min et al. (2006). The model made use of rate equations to simulate the aqueous phase, and the Monte Carlo method developed by Tobita and Yanase (Tobita, 1995; Tobita and Yanase, 2007) to simulate the organic phase.

   In modelling the dispersed system a qualitative fit of the data was obtained. This was considered to be good result, as no comparable models existed in literature, and the one developed in this work seemed at least to provide a reasonable fit of the trends seen in this system. However, there were a few discrepancies between model predictions and experimental data. These model discrepancies appeared to directly suggest the presence of diffusional effects at high conversion, as well as coagulation of polymer particles, while indirectly hinting at the presence of concentration dependent partition coefficients and different rates of activation/deactivation for initiator molecules. Importantly however this discrepancy is also likely in part due to inaccurate prediction of parameters, as crude estimates of a large number of parameters in the system had to be made.

3. An experimental study of the AGET ATRP of butyl acrylate using the catalyst $CuBr_2$/2dNbpy, initiator EBiB, surfactant Brij 98, and reducing agent ascorbic acid. In the exploration of this polymerization process, data on the monomer conversion and polymer molecular weight were collected.

   The results obtained within this study were relatively unexpected. A mixed region between controlled and uncontrolled radical polymerization was found. In this region the polymerization shared some characteristics of both controlled and uncontrolled polymerization, though in a surprising manner, as characteristics suggestive of these two processes simply occurring concurrently were not found within this system. In any case, from these results it was concluded that three distinct regimes seem to exist within this system. These regimes all have their disadvantages and advantages, but may importantly allow for one to manipulate polymer properties over a vast range using one chemical system.

In the end, it seems that the results obtained allow for some pretty important details to be uncovered about the nature of the systems studied. In terms of modelling for instance, not only were models

successfully developed for both solution and dispersed processes, but they also hinted at the relevance of certain phenomenon occurring therein. The experimental evidence on the other hand illuminated the interesting transition region, between conventional and controlled polymerizations.

6.2 Recommendations

From the work carried out in this study, it is evident that some areas within this subfield of polymer research still require more attention. Below some recommendations for future studies are given.

Solution ARGET ATRP of BMA:

1. An experimental study over a large range of TCL is needed, since in the work of Payne et al. (2013) values of TCL were limited to a range of 35- 400, and only three different TCL values were used.
2. Development of a model which is able to capture the kinetic features of the ARGET ATRP of BMA in solution over a wide range of TCL is needed.

Dispersed AGET ATRP of BA:

Modelling:

1. Find a finite set of differential equations which exactly model the AGET ATRP process in dispersed systems has still not been found.
2. Continue to develop the Monte Carlo model created in this work.

Experimental:

1. Experimentally determine some of the more basic rate constants currently not available within literature such as the rate of reduction of ascorbic acid.
2. Investigate the partitioning behavior of some of the species in this system.
3. Continue to explore the different regimes observed in the AGET ATRP of BA in a two-stage dispersed system.

NOMENCLATURE

Chemical Species

Latin:

A: Activator Species (Catalyst in its lower oxidation state)

A: Activator species or metal catalyst in lower oxidized state

AGENT: Can be used to represent any of the species which establishes an equilibrium between dormant and active radicals

Br: Bromine

CuBr/BPMODA: Activators (Catalyst in its lower oxidation state for dispersed system); Ligand: BPMODA, Transition metal: Copper; Halogen atom: bromide)

CuBr: Copper (I) Bromide

$CuBr_2$/BPMODA: Deactivators (Catalyst in its higher oxidation state for dispersed system); Ligand: BPMODA, Transition metal: Copper; Halogen atom: bromide)

$CuBr_2$: Copper (II) Bromide

D: Deactivator Species or metal catalyst in oxidized state

D: Dormant Species (Catalyst in its higher oxidation state)

I: initiator (conventional)

I-Br: Initiator (Ethyl 2-bromoisobutyrate)

I-X: Initiator species (alkyl halide)

M: Monomer

M·: Monomer derived radical (monomeric radical)

M-X: Monomeric radical dormant species

P_n: are dead polymers of length n

P_n-P_m: are dead polymers of length n+m

R_0·: Primary Radical

$R_0^{\cdot}$:primary radical (no assumption about radical position)

$R_1^{\cdot}$: Radical of chain of length 1 (no assumption about radical position)

Red^{I}: Reducing agent in its first oxidation state (Ascorbic Acid)

Red^{II}: Reducing agent in its second oxidation state (Ascorbic Acid)

Red^{III}: Reducing agent in its third oxidation state (Ascorbic Acid)

Red^{II}: Reducing agent in its first oxidation state (Tin (II) 2-ethylhexanoate)

Red^{III}: Reducing agent in its second oxidation state (Tin (II) 2-ethylhexanoate)

Red^{IV}: Reducing agent in its third oxidation state (Tin (II) 2-ethylhexanoate)

$R_n^{\cdot}$: Radical of size n; where n≥1

R_n-X: Dormant species of length n

$R_{s,0}^{\cdot}$: primary radical (assumed to be a secondary radical)

$R_{s,1}^{\cdot}$: Secondary radical of chain length 1

$R_{s,n}^{\cdot}$: secondary radical of size n; where n≥1

$R_{s,n}$-Br: bromide capped secondary radical

$R_{s,n}$-X: halide capped secondary radical

$R_{t,n}^{\cdot}$: tertiary radical of size n; where n≥1

$R_{t,n}$-Br: bromide capped tertiary radical

$R_{t,n}$-X: halide capped tertiary radical

T: Transfer agent

T·: Transfer agent with radical activity

X: halogen

Greek:

μ_0: Dead polymer zeroth moment

μ_1: Dead polymer first moment

μ_2: Dead polymer second moment

δ_0: Dormant species zeroth moment

δ_1: Dormant species first moment

δ_2: Dormant species second moment

λ_0: Macromolecule radical zeroth moment

λ_1: Macromolecule radical first moment

λ_2: Macromolecule radical second moment

Parameters

Latin:

$[Cu^{I}]_{aq}$: concentration of copper (I) in the aqueous phase

$[Cu^{I}]_{org}$: concentration of copper (I) in the organic phase

$[Cu^{II}]_{aq}$: concentration of copper (II) in the aqueous phase

$[Cu^{II}]_{org}$: concentration of copper (II) in the organic phase

[M]: Monomer concentration at time T

$[M]_{aq}$: concentration of monomer in the aqueous phase

$[M]_{aq,sat}$: concentration of monomer in the aqueous phase at saturation point

$[M]_{p}$: Monomer concentration in polymer particle

$[M]_{p,sat}$: Monomer concentration in polymer particle at saturation point

[M0]: initial monomer concentration

A_{avg}: proportion of active particles

A_{H}: Activation frequency of reaction H; where H can be any of the reactions whose parameters are being found through optimization

CMC_{Brij98}: Critical micelle concentration of Brij 98

Ea_{H}: Activation Energy of reaction H; where H can be any of the reactions whose parameters are being found through optimization

F_{poly}: Mass fraction of polymer

F_{sol}: mass fraction of solids

F_{x}: initial mass fraction of compound x in solution

j: number of purges

kact: Rate constant for activation of dormant species

$kact_{0}$: Rate constant for activation of alkyl halide initatior

$kact_{s,0}$: Rate constant for activation of alkyl halide initiator which produce solely secondary radicals

$kact_{s}$: Rate constant for activation of dormant secondary macro-radical

$kact_t$: Rate constant for activation for dormant tertiary macro-radical

K_{ATRP}: Equilibrium constant for the activation/deactivation reactions

kbb: Rate constant for backbiting reaction

$K_{Cu(I)}$: partition coefficient for copper (I) species

$K_{Cu(II)}$: partition coefficient for copper (II) species

k_d: Rate constant for dissociation/decomposition of initiator

k_{deact}: Rate constant for deactivation of active radical

$k_{deact,0}$: Rate constant for deactivation of primary radical

$k_{deact,s,0}$: Rate constant for deactivation of secondary primary radicals

$k_{deact,s}$: Rate constant for deactivation of secondary macro-radical

$k_{deact,t}$: Rate constant for deactivation of tertiary macro-radical

k_i: Rate constant for initiation

k_p: Rate constant for propagation

$k_{p,s}$: Rate constant for propagation of secondary radical

$k_{p,t}$: Rate constant for propagation of tertiary radical

k_{r1}: Rate of reduction of reducing agent in first oxidation state (Reducing agent can be tin (II) ethyl hexanoate or Ascorbic acid depending on which system is being considered)

k_{r2}: Rate of reduction of reducing agent in second oxidations state (Reducing agent can be tin (II) ethyl hexanoate or Ascorbic acid depending on which system is being considered)

k_t: Overall rate constant for termination

k_{tc}: Rate constant for termination by combination

$k_{tc,ss}$: Rate constant for termination by combination for two secondary radicals

$k_{tc,st}$: Rate constant for termination by combination for one secondary and one tertiary radical

$k_{tc,tt}$: Rate constant for termination by combination for two tertiary radicals

k_{td}: Rate constant for termination by disproportionation

$k_{td,ss}$: Rate constant for termination by disproportionation for two secondary radicals

$k_{td,st}$: Rate constant for termination by disproportionation for one secondary and one tertiary radical

$k_{td,tt}$: Rate constant for termination by disproportionation for two tertiary radicals

k_{trm}: Rate constant for transfer to monomer

$k_{trm,s}$: Rate constant for transfer of radical activity to monomer from a secondary macro-radical.

$K_{trm,t}$: Rate constant for transfer of radical activity to monomer from a tertiary macro-radical.

k_{trp}: Rate constant for transfer of radical activity to polymer chain (assumed in this work to be dead polymer chain), from a secondary macro-radical

k_{trt}: Rate constant for transfer to transfer agent

$k_{trt,s}$: Rate constant for transfer of radical activity from secondary radical to transfer agent

$k_{trt,t}$: Rate constant for transfer of radical activity from tertiary radical to transfer agent

$k_{t,ss}$: Overall rate constant of termination when two secondary radicals participate in the reaction

$k_{t,tt}$: Overall rate constant of termination when two tertiary radicals participate in the reaction

M_n: Number average molecular weight

m_{poly}: mass of polymer within the particle

M_w: Weight average molecular weight

M_{wM}: molecular weight of monomer

$m_{y,cup}$: mass of cup in state y

n: chain length

n_H: Total number of moles at high pressure

n_L: Total number of moles at low pressure

$n_{agg,Brij98}$: Aggregation number for Brij 98

N_{av}: is Avogadro's number

$N_{Cu(I)}$: number of moles of copper (I) remaining in the system

$N_{Cu(II)}$: number of moles of copper (II) remaining in the system

$N_{M,0}$: initial number of moles of monomer in the system

N_M: number of moles of monomer remaining the system

P(r): Probability of adding r monomers in and interval Δt

$P(t_{react,occur})$: Probability of a given reaction occurring at time $t_{react,occur}$

PDI: Polydispersity Index

P_H: Pressure after pressurization (high pressure)

P_L: Pressure before pressurization (lower pressure)

$\bar{r}$: Average number of monomer units added to a single radical in a time interval Δt

R: Gas constant

$R_{CuBr:}$ average rate of consumption of CuBr consumption

R_{CuBr2}: average rate of $CuBr_2$ consumption

Rp_{avg}: average rate of polymerization

T: Temperature

T_H: Temperature at high pressure

T_L: Temperature at low pressure

$t_{react,avg}$: Average time until a reaction occurs

$t_{react,occur}$: Random generated time until a reaction occurred

U: random number taken from a continuous uniform distribution from 0 to 1

V: volume of the reaction loci

V_H: Volume at high pressure

V_L: Volume at low pressure

V_{aq}: volume of the aqueous phase

V_{org}: volume of the entire organic phase

$V_{p,avg}$: average volume of the particles.

$V_{p,tot}$: total volume enclosed by all the particles

V_{part}: volume of the particle

x: conversion of monomer

$y_{O2,H}$: mole fraction of oxygen at high pressure

$y_{i,experimental}$: Experimental value for the i^{th} experitment (where the output can take on the form of conversion, number average molecular weight, or polydispersity index)

$y_{i,predicted}$: Output value predicted from model for the i^{th} experiment (where the output can take on the form of conversion, number average molecular weight, or polydispersity index)

$y_{O2,j}$: mole fraction of oxygen after jth purge

$y_{O2,L}$: mole fraction of oxygen at low pressure

$y_{O2,0}$: initial mole fraction of oxygen

Δt: Time interval

Greek:

δss: proportion of termination between two secondary radicals occurring by disproportionation

δst: proportion of termination between one secondary and one tertiary radical occurring by disproportionation

δ_{tt}: proportion of termination between two tertiary radicals occurring by disproportionation.

ρ: is the rate of a particular event in mol L^{-1} s^{-1}

ρ_M: density of monomer

ρ_p: density of the polymer

ϕ_m: volume fraction of the monomer within the particle

ϕ_p: volume fraction of the polymer within the particle

$\phi_{p,sat}$: volume fraction of the polymer within the particle at saturation point

Acronyms

AA: Ascorbic Acid

ACS: American chemical society

AGET: Activators Generated by Electron Transfer

aq: Aqueous phase

ARGET: Activators Regenerated by Electron Transfer

ATRP: Atom Transfer Radical Polymerization

BA: Butyl Acrylate

BMA: Butyl Methacrylate

Brij 98: Polyoxyethylene (20) oleyl ether

CLRP: Controlled (Living) Radical Polymerization

CuBr/2dNbpy: Activators (Catalyst in its lower oxidation state for dispersed system); Ligand: dNbpy, Transition metal: Copper; Halogen atom: bromide)

CuBr: Copper (I) Bromide

$CuBr_2$/2dNbpy: Deactivators (Catalyst in its higher oxidation state for dispersed system); Ligand: dNbpy, Transition metal: Copper; Halogen atom: bromide)

$CuBr_2$: Copper (II) Bromide

dNbpy: 4,4'-Dinonyl-2,2'-dipyridyl

eATRP: Electrochemically mediated Atom Transfer Radical Polymerization

EBiB: Ethyl 2-bromoisobutyrate

GPC: Gel Permeation Chromatography

HPLC: High performance liquid chromatography

ICAR: Initiators for continuous regeneration

MWD: Molecular Weight Distribution

NMP or NMRP: Nitroxide Mediated Polymerization or Nitroxide Mediated Radical Polymerization

org: organic phase

PDI: Polydispersity

RAFT: Reversible Addition-Fragmentation Chain Transfer

RPM: Rotations per minute

SEC: Size exclusion chromatography

SR&NI: Simultaneous reverse and normal initiation

TCL: Targeted Chain Length

THF: Tetrahydrofuran

APPENDICES

Appendix A: Experimental Conditions of Payne et al. (2013)

Experiment and Temperature	Reactant	Amount (g)	Molar Ratio $[reactant]_0/[I\text{-}X]$	Amount (mol/L)
1 (70°C)*	BMA (Monomer)	35	35	5.65
	EBiB (Initiator)	1.3717	1	0.161
	$(Cu^{II}TPMABr)Br$	0.0181	0.005	0.000809
	$Sn(EH)_2$	0.1424	0.05	0.00807
2 (70°C)*	BMA (Monomer)	35	35	5.65
	EBiB (Initiator)	1.3717	1	0.161
	$(Cu^{II}TPMABr)Br$	0.0045	0.00125	0.000201
	$Sn(EH)_2$	0.0356	0.0125	0.00202
3 (70°C)*	BMA (Monomer)	35	35	5.65
	EBiB (Initiator)	1.3717	1	0.161
	$(Cu^{II}TPMABr)Br$	0.0045	0.00125	0.000201
	$Sn(EH)_2$	0.356	0.125	0.0202
4(70°C)*	BMA (Monomer)	35	50	5.72
	EBiB (Initiator)	0.9602	1	0.114
	$(Cu^{II}TPMABr)Br$	0.0032	0.00125	0.000145
	$Sn(EH)_2$	0.2493	0.125	0.0143
5(70°C)*	BMA (Monomer)	35	400	5.87
	EBiB (Initiator)	0.1200	1	0.0147
	$(Cu^{II}TPMABr)Br$	0.0032	0.001	0.000149
	$Sn(EH)_2$	0.0249	0.1	0.00147
6(90°C)*	BMA (Monomer)	35	35	5.65
	EBiB (Initiator)	1.3717	1	0.161
	$(Cu^{II}TPMABr)Br$	0.0045	0.00125	0.000201
	$Sn(EH)_2$	0.0356	0.0125	0.00202
7 (90°C)*	BMA (Monomer)	35	35	5.65
	EBiB (Initiator)	1.3717	1	0.161
	$(Cu^{II}TPMABr)Br$	0.0045	0.00125	0.000201
	$Sn(EH)_2$	0.356	0.125	0.0202

This appendix contains the experimental conditions obtained from Payne et al. (2013). *It should be noted that anisole (acting as a solvent) was part of all of these experiments having a 30 % w/w with respect to monomer.

Appendix B: Experimental conditions of Min et al. (2006)

Experiment and Temperature	Reactant	Amount (moles, mL, or mol/L)	Molar Ratio $[reactant]_0/[EBiB]_0$
1 (80°C)*	BA (Monomer) Injection 1	0.0070 moles	100
	BA (Monomer) Injection 2	0.0139 moles	200
	EBiB (Initiator)	6.97×10^{-5} moles	1
	$CuBr_2$/BPMODA (Catalyst)	3.49×10^{-5} moles	0.5
	AA (Reducing Agent)	4.83×10^{-4} mol/L	0.2
	Brij98 (Surfactant)	0.0626 mol/L	26
	Water (Continuous Phase)	28.76 mL	N.A
2 (80°C)*	BA (Monomer) Injection 1	0.00140 moles	15
	BA (Monomer) Injection 2	0.0195 moles	210
	EBiB (Initiator)	9.30×10^{-5} moles	1
	$CuBr_2$/BPMODA (Catalyst)	1.39×10^{-5} moles	0.15
	AA (Reducing Agent)	5.36×10^{-4} mol/L	0.06
	Brij98 (Surfactant)	0.0269 mol/L	3
	Water (Continuous Phase)	10.40 mL	N.A
3 (80°C)*	BA (Monomer) Injection 1	0.001045 moles	15
	BA (Monomer) Injection 2	0.019855 moles	285
	EBiB (Initiator)	6.97×10^{-5} moles	1
	$CuBr_2$/BPMODA (Catalyst)	1.04×10^{-5} moles	0.15
	AA (Reducing Agent)	4.85×10^{-4} mol/L	0.06
	Brij98 (Surfactant)	0.0257 mol/L	3.18
	Water (Continuous Phase)	8.62 mL	N.A

Appendix C: Parameters Used in the Simulation of the AGET ATRP of BA in Two-Stage Dispersed System

Parameter	Frequency Factor	Activation Energy	Papers used in Obtaining Value
Kinetic Parameters			
kt_{ss}	3.89×10^{9} mol/L s	8.4×10^{3} J/mol	(Nikitin et al., 2010)
kt_{tt}	5.30×10^{9} mol/L s	1.96×10^{4} J/mol	(Nikitin et al., 2010)
$kact_{s,0}$	6.63×10^{4} mol/L s	2.75×10^{4} J/mol	(Seeliger and Matyjaszewski, 2009; Tang and Matyjaszewski, 2007) & This work
$kdeact_{s,0}$ [1,*]	-	-	(Elsen et al., 2012; Qiu et al., 2000a; Tang et al., 2008; Wang et al., 2012) & This work
kp_{s}	2.24×10^{7} mol/L s	1.79×10^{4} J/mol	(Asua et al., 2004)
kp_{t}	1.2×10^{6} mol/L s	2.86×10^{4} J/mol	(Nikitin et al., 2010)
$kdeact_{s}$ [1,*]	-	-	(Elsen et al., 2012; Qiu et al., 2000a; Tang et al., 2008; Wang et al., 2012) & This work
$kdeact_{t}$ [2,*]	-	-	(Elsen et al., 2012; Qiu et al., 2000a; Schroeder et al., 2014; Tang et al., 2008; Wang et al., 2012) & This work
$kact_{s}$	6.63×10^{4} mol/L s	2.75×10^{4} J/mol	(Seeliger and Matyjaszewski, 2009; Tang and Matyjaszewski, 2007) &This work
$kact_{t}$ [2,*]	2.55×10^{5} mol/L s	2.75×10^{4} J/mol	(Schroeder et al., 2014; Seeliger and Matyjaszewski, 2009; Tang and Matyjaszewski, 2007) & This work
K_{ATRP}	0.02513	4.4×10^{3} J/mol	(Elsen et al., 2012; Qiu et al., 2000a; Tang et al., 2008; Wang et al., 2012)
kr1	$5.55*10^{2}$ mol/L s	1.49×10^{4} J/mol	(Payne et al., 2013), This work
kr2	1.87×10^{3} mol/L s	1.49×10^{4} J/mol	(Payne et al., 2013), This work
kbb	7.41×10^{7} mol/L s	32.7×10^{3} J/mol	(Nikitin et al., 2010)
ktrp	4.01×10^{3} mol/L s	29×10^{3} J/mol	(Nikitin et al., 2010)

Parameter	Frequency Factor	Activation Energy	Papers used in Obtaining Value
$ktrm_s$	2.9×10^5 mol/L s	32.6×10^3 J/mol	(Nikitin et al., 2010)
$ktrm_t$	2.0×10^5 mol/L s	46.1×10^3 J/mol	(Nikitin et al., 2010)
δss	0.1	N/A	(Nikitin et al., 2010)
δst	0.7	N/A	(Nikitin et al., 2010)
δtt	0.9	N/A	(Nikitin et al., 2010)
Diffusional Parameters			
$K_{Cu(I)}$	20	N/A	(Elsen et al., 2012; Qiu et al., 2000b), This work
$K_{Cu(II)}$	0.9	N/A	(Elsen et al., 2012; Qiu et al., 2000b), This work
General Properties			
ρ_M (g/L)	$\left(0.45798+\frac{417.08}{T}+\frac{-48466}{T^2}\right)10^3$	N/A	(Lyons et al., 1996)
ρ_p (g/L)	1087	N/A	
Mw_M	128.17 (g/mol)	N/A	N/A
CMC_{Brij98}	2.5×10^{-5} mol/L	N/A	(Prak et al., 2011)
$n_{agg,Brij98}$	29	N/A	(Prak et al., 2011)
$[M]_{aq,sat}$	0.0064 mol/L		(Fortuny et al., 2004)
$[M]_{p,sat}$	5.0 mol/L		(Fortuny et al., 2004)
$\phi_{p,sat}$	0.2746		(Fortuny et al., 2004)

Given above are the parameters used to simulate the two-stage dispersed system of Min et al. (2006)

Notes:

- Now while the majority of parameters above appear to be exact, they were extracted for data in bulk/solution polymerizations, and therefore only provide a first approximation to the true rate constants of the system.
- For any parameter that contains "This work" in the reference section, modifications within reasonable limits (Usually within an order of magnitude) were made from initial estimates, so as to obtain better fits of the data.

[1,*] The deactivation rate constants are obtained from their corresponding activation rate constants by dividing by K_{ATRP}

[2,*] Activation/Deactivation rates for tertiary radicals were obtained by multiplying the Activation/Deactivation rates for secondary radicals by an appropriate proportion obtained from the work of Schroeder et al. (2014)

Appendix D: Parameter Estimation

Estimation of Activation Constants:

In estimating the activation rate constants to be used for the simulation of the dispersed system of Min et al, (2006), the works (Schroeder et al., 2014; Seeliger and Matyjaszewski, 2009; Tang and Matyjaszewski, 2007) were used.

In starting this estimation process a temperature dependent expression for the activation rate of EBiB by Cu(I)Br(PMDETA) was obtained from Seeliger and Matyjaszewski (2009):

$$k_{act,PMDETA} = 12000\, e^{-27500/RT}$$

This was then used to obtain an estimate of the rate of activation of EBiB by Cu(I)Br(BPMODA) using rate constants available in the work of Tang and Matyjaszewski (2006) as follows[9]:

$$k_{act,s,0} = k_{act,BPMODA} = \left(12000\, e^{-27500/RT}\right)\left(\frac{k_{act,BPMODA,35^\circ C}}{k_{act,PMDETA,35^\circ C}}\right)$$

Finally, using the work of Seeliger and Matyjaszewski (2009) as justification, an equality was assumed to hold, and thus provided first order estimates of all the necessary parameters:

$$k_{act,s,0} = k_{act,s} = 0.26\, k_{act,t}$$

Estimation of Deactivation Constants:

In estimating the deactivation rate constants used in modelling the dispersed system of Min et al. (2006), the works (Elsen et al., 2012; Qiu et al., 2000a; Schroeder et al., 2014; Tang et al., 2008; Wang et al., 2012) were used.

In order to obtain estimates of the rates of deactivation a temperature dependent expression for K_{ATRP} needed to be found. Luckily in the work of Wang et al. (2012) an expression of this form was provided for TPMA[10]:

$$K_{ATRP,TPMA} = 0.0672 e^{-44000/T}$$

[9] It is important to note that this equation assumed that the ratio of kinetic rate constants between the two catalysts remained constant over all temperatures.

[10] Unfortunately this was for a different initiator than EBiB, but was still used as it could still at least provide an estimate of magnitude for the equilibrium constant.

Using this expression an estimate of K_{ATRP} for the BPMODA system was found through use a ratio of K_{ATRP} values collected from the works *(Elsen et al., 2012; Qiu et al., 2000a; Tang et al., 2008)*[11]:

$$K_{ATRP,s,0} = K_{ATRP,BPMODA} = \left(0.0672e^{-44000/T}\right)\left(\frac{K_{ATRP,BPMODA,50^\circ C}}{K_{ATRP,TPMA,35^\circ C}}\right)$$

This then once again could be modified using an equality suggested by the work of Seeliger and Matyjaszewski (2009) to obtain the final rate constants[12]:

$$k_{deact,s,0} = \frac{k_{act,s,0}}{K_{ATRP,s,0}} = k_{deact,s} = \frac{k_{act,s}}{K_{ATRP,s}} = 10k_{deact,t} = 10\,\frac{k_{act,s,0}}{K_{ATRP,s,0}}$$

[11] Now while a value for the TPMA equilibrium constant could be obtained directly from the work of Tang et al. (2008), an estimate of the KATRP for BPMODA had to be obtained using the E1/2 value provided by Elsen et al. (2012), and the correlation given by Qiu et al. (2000a).

[12] It is important to note that this equality requires first that the activation rate constants be obtained.

Appendix E: Estimation of Oxygen Content in Headspace

In chapter 5, within Table 5.2, a relation between the number of purges, the initial mole fraction of oxygen in the headspace, and the pressure of the headspace while pressurized and after venting is given.

In this appendix a derivation of this relation is provided, as well as a numerical example to allow the reader to better understand this relation.

Starting with the derivation, two equations can be derived from the ideal gas law relating quantities when the system is at low pressure and high pressure.

$$P_L V_L = n_L R T_L \tag{A.E.1}$$

$$P_H V_H = n_H R T_H \tag{A.E.2}$$

Further some relations exist between quantities in the system, when the vessel is being filled with inert gas, and when it is being vented, derived simply from the nature of these two processes while assuming pressurization and venting occur between a high pressure (P_H) and low pressure (P_L):

During the pressurizing phase (when the vessel is filled with inert gas):

$$V_L = V_H \tag{A.E.3}$$

$$T_L = T_H \tag{A.E.4}$$

$$n_{O_2,L} = n_{O_2,H} \tag{A.E.5}$$

During the venting phase:

$$V_L = V_H \tag{A.E.3}$$

$$T_L = T_H \tag{A.E.4}$$

$$y_{O_2,L} = y_{O_2,H} \tag{A.E.6}$$

Thus during the pressurization phase, by combing relations (A.E.1), (A.E.2), (A.E.3), (A.E.4), we can derive:

$$\frac{P_H}{P_L} = \frac{n_H}{n_L} \tag{A.E.7}$$

Multiplying the top and bottom of this expression by $n_{O_2,L}$ and using equation (A.E.5) you can obtain:

$$\frac{P_H}{P_L} = \left(\frac{n_H}{n_L}\right)\left(\frac{n_{O_2,L}}{n_{O_2,L}}\right) = \left(\frac{n_H}{n_L}\right)\left(\frac{n_{O_2,L}}{n_{O_2,H}}\right) = \left(\frac{y_{O_2,L}}{y_{O_2,H}}\right) \quad \text{(A.E.8)}$$

This relation is used to relate the mole fractions before and after pressurization, to the total pressures before and after pressurization. It therefore provides a measure of how much the mole fraction changes when an inert gas is used to pressurize the system to P_H.

Now since we know from (A.E.8) that the mole fractions during a pressurization phase changes in proportion to $\frac{P_L}{P_H}$ from their value at the start of this phase to their value at the end of this phase, and also that the mole fraction remains constant during the venting phase, as per (A.E.6), it can be seen that by creating a pressurization-venting cycle (also known as a purge) and repeating it venting j times, the following relation exists between the mole fraction after the jth cycle and the initial mole fraction.

$$y_{O_2,j} = y_{O_2,0}\left(\frac{P_L}{P_H}\right)^j \quad \text{(A.E.9)}$$

This equation was the one used in Table 5.2 to find the oxygen after j purges, which since proven here now ends our derivation process.

In terms of a numerical example illustrating the use of this equation one can be found below.

Consider a reaction vessel with a gaseous headspace of volume V and at atmospheric temperature. After five purges with a relatively pure source of nitrogen (~100% nitrogen), such that the nitrogen pressurizes the system to 20 psig and venting discharges the contents of the reaction system until it is at atmospheric pressure, what will the mole fraction of oxygen in the system be? (Assuming the oxygen content starts with a mole fraction 0.21)

Using (A.E.9) the solution to this problem is:

$$y_{O_2,5} = 0.21\left(\frac{14.7}{34.7}\right)^5 = 0.0029$$

REFERENCES

Ahmad, N. M., B. Charleux, C. Farcet, C. J. Ferguson, S. G. Gaynor, B. S. Hawkett, F. Heatley, B. Klumperman, D. Konkolewicz, P. A. Lovell, K. Matyjaszewski, and R. Venkatesh, 2009, Chain Transfer to Polymer and Branching in Controlled Radical Polymerizations of n-Butyl Acrylate: Macromolecular Rapid Communications, v. 30, p. 2002-2021.

Asua, J. M., S. Beuermann, M. Buback, P. Castignolles, B. Charleux, R. G. Gilbert, R. A. Hutchinson, J. R. Leiza, A. N. Nikitin, J. P. Vairon, and A. M. van Herk, 2004, Critically evaluated rate coefficients for free-radical polymerization, 5 - Propagation rate coefficient for butyl acrylate: Macromolecular Chemistry and Physics, v. 205, p. 2151-2160.

Ballard, N., M. Salsamendi, J. I. Santos, F. Ruiperez, J. R. Leiza, and J. M. Asua, 2014, Experimental Evidence Shedding Light on the Origin of the Reduction of Branching of Acrylates in ATRP: Macromolecules, v. 47, p. 964-972.

Beuermann, S., M. Buback, T. P. Davis, R. G. Gilbert, R. A. Hutchinson, A. Kajiwara, B. Klumperman, and G. T. Russell, 2000, Critically evaluated rate coefficients for free-radical polymerization, 3 - Propagation rate coefficients for alkyl methacrylates: Macromolecular Chemistry and Physics, v. 201, p. 1355-1364.

Braun, D., 2009, Origins and Development of Initiation of Free Radical Polymerization Processes: International Journal of Polymer Science, p. 10.

Braunecker, W. A., and K. Matyjaszewski, 2007, Controlled/living radical polymerization: Features, developments, and perspectives: Progress in Polymer Science, v. 32, p. 93-146.

Cao, X. T., Y. H. Kim, J. M. Park, and K. T. Lim, 2016, One-pot synthesis of dual-responsive core cross-linked polymeric micelles and covalently entrapped drug by click chemistry: European Polymer Journal, v. 78, p. 264-273.

Chanda, M., and S. Roy, 2009, Industrial Polymers, Specialty Polymers, and Their Applications, CRC.

Chern, C.-S., 2009, Principles and Applications of Emulsion Polymerization, Wiley.

Crowl, D. A., and J. F. Louvar, 2011, Chemical process safety : fundamentals with applications: Prentice Hall international series in the physical and chemical engineering sciences: Upper Saddle River, NJ, Prentice Hall, xxiv, 723 p. p.

Cuccato, D., E. Mavroudakis, M. Dossi, and D. Moscatelli, 2013, A Density Functional Theory Study of Secondary Reactions in n-Butyl Acrylate Free Radical Polymerization: Macromolecular Theory and Simulations, v. 22, p. 127-135.

Dadashi-Silab, S., M. A. Tasdelen, A. M. Asiri, S. B. Khan, and Y. Yagci, 2014, Photoinduced Atom Transfer Radical Polymerization Using Semiconductor Nanoparticles: Macromolecular Rapid Communications, v. 35, p. 454-459.

Destarac, M., 2010, Controlled Radical Polymerization: Industrial Stakes, Obstacles and Achievements: Macromolecular Reaction Engineering, v. 4, p. 165-179.

Elsen, A. M., J. Burdynska, S. Park, and K. Matyjaszewski, 2012, Active Ligand for Low PPM Miniemulsion Atom Transfer Radical Polymerization: Macromolecules, v. 45, p. 7356-7363.

Feeney, P. J., D. H. Napper, and R. G. Gilbert, 1984, Coagulative Nucleations and Particle-Size Distributions in Emulsion Polymerization: Macromolecules, v. 17, p. 2520-2529.

Fortuny, M., C. Graillat, and T. E. McKenna, 2004, A new technique for the experimental measurement of monomer partition coefficients: Macromolecular Chemistry and Physics, v. 205, p. 1309-1319.

Gao, J., and A. Penlidis, 2002, Mathematical modeling and computer simulator/database for emulsion polymerizations: Progress in Polymer Science, v. 27, p. 403-535.

Gody, G., R. Barbey, M. Danial, and S. Perrier, 2015, Ultrafast RAFT polymerization: multiblock copolymers within minutes: Polymer Chemistry, v. 6, p. 1502-1511.

Gozgen, A., A. Dag, H. Durmaz, O. Sirkecioglu, G. Hizal, and U. Tunca, 2009, ROMP-NMP-ATRP Combination for the Preparation of 3-Miktoarm Star Terpolymer via Click Chemistry: Journal of Polymer Science Part a-Polymer Chemistry, v. 47, p. 497-504.

Guo, J. S., E. D. Sudol, J. W. Vanderhoff, and M. S. Elaasser, 1992, Particle Nucleation and Monomer Partitioning in Styrene O/W Microemulsion Polymerization: Journal of Polymer Science Part a-Polymer Chemistry, v. 30, p. 691-702.

Jeong, J., H. Kim, S. Lee, H. Choi, H. B. Jeon, and H. J. Paik, 2015, Improved synthesis of bicyclic polystyrenes by ATRP and "click" reaction: Polymer, v. 72, p. 447-452.

Jousset, S., J. Qiu, and K. Matyjaszewski, 2001, Atom transfer radical polymerization of methyl methacrylate in water-borne system: Macromolecules, v. 34, p. 6641-6648.

Kagawa, Y., P. B. Zetterlund, H. Minami, and M. Okubo, 2007, Atom transfer radical polymerization in miniemulsion: Partitioning effects of copper(I) and copper(II) on polymerization rate, livingness, and molecular weight distribution: Macromolecules, v. 40, p. 3062-3069.

Kato, M., M. Kamigaito, M. Sawamoto, and T. Higashimura, 1995, Polymerization of methyl-methacrylate with the carbon-tetrachloride dichlorotris(triphenylphosphine)ruthenium(II) methylaluminum bis(2,6-di-tert-butylphenoxide) Initiating System- Possibility of Living Radical Polymerization: Macromolecules, v. 28, p. 1721-1723.

Kim, J. M., and C. Baig, 2016, Communication: Role of short chain branching in polymer structure and dynamics: The Journal of chemical physics, v. 144, p. 081101.

Li, X. H., W. J. Wang, B. G. Li, and S. P. Zhu, 2011, Kinetics and Modeling of Solution ARGET ATRP of Styrene, Butyl Acrylate, and Methyl Methacrylate: Macromolecular Reaction Engineering, v. 5, p. 467-478.

Li, Y., X. Zheng, Z. Xia, and M. Lu, 2016, Synthesis of fluorinated block copolymer and superhydrophobic cotton fabrics preparation: Progress in Organic Coatings, v. 97, p. 122-132.

Lyons, R. A., J. Hutovic, M. C. Piton, D. I. Christie, P. A. Clay, B. G. Manders, S. H. Kable, and R. G. Gilbert, 1996, Pulsed-laser polymerization measurements of the propagation rate coefficient for butyl acrylate: Macromolecules, v. 29, p. 1918-1927.

Magenau, A. J. D., N. Bortolamei, E. Frick, S. Park, A. Gennaro, and K. Matyjaszewski, 2013, Investigation of Electrochemically Mediated Atom Transfer Radical Polymerization: Macromolecules, v. 46, p. 4346-4353.

Mastan, E., and S. P. Zhu, 2015, Method of moments: A versatile tool for deterministic modeling of polymerization kinetics: European Polymer Journal, v. 68, p. 139-160.

Matyjaszewski, K., and N. V. Tsarevsky, 2014, Macromolecular Engineering by Atom Transfer Radical Polymerization: Journal of the American Chemical Society, v. 136, p. 6513-6533.

Maxwell, I. A., J. Kurja, G. H. J. Vandoremaele, A. L. German, and B. R. Morrison, 1992, Partial Swelling of Latex-Particles with Monomers: Makromolekulare Chemie-Macromolecular Chemistry and Physics, v. 193, p. 2049-2063.

Min, K., H. F. Gao, and K. Matyjaszewski, 2006, Development of an ab initio emulsion atom transfer radical polymerization: From microemulsion to emulsion: Journal of the American Chemical Society, v. 128, p. 10521-10526.

Min, K., and K. Matyjaszewski, 2005, Atom transfer radical polymerization in microemulsion: Macromolecules, v. 38, p. 8131-8134.

Monteiro, M. J., and M. F. Cunningham, 2012, Polymer Nanoparticles via Living Radical Polymerization in Aqueous Dispersions: Design and Applications: Macromolecules, v. 45, p. 4939-4957.

Mortimer, G. A., 1971, Effect of Short-Chain Branch Structure on Properties of Low-Density Polyethylene: Journal of Applied Polymer Science, v. 15, p. 1231-&.

Morton, M., S. Kaizerman, and M. W. Altier, 1954, Swelling of Latex Particles: Journal of Colloid Science, v. 9, p. 300-312.

Nicolas, J., Y. Guillaneuf, C. Lefay, D. Bertin, D. Gigmes, and B. Charleux, 2013, Nitroxide-mediated polymerization: Progress in Polymer Science, v. 38, p. 63-235.

Nikitin, A. N., and R. A. Hutchinson, 2009, Effect of Intramolecular Transfer to Polymer on Stationary Free Radical Polymerization of Alkyl Acrylates, 4-Consideration of Penultimate Effect: Macromolecular Rapid Communications, v. 30, p. 1981-1988.

Nikitin, A. N., R. A. Hutchinson, W. Wang, G. A. Kalfas, J. R. Richards, and C. Bruni, 2010, Effect of Intramolecular Transfer to Polymer on Stationary Free-Radical Polymerization of Alkyl Acrylates, 5-Consideration of Solution Polymerization up to High Temperatures: Macromolecular Reaction Engineering, v. 4, p. 691-706.

Oh, J. K., 2008, Recent Advances in Emulsion and in Controlled/Living Radical Polymerization Dispersion: Journal of Polymer Science Part a-Polymer Chemistry, v. 46, p. 6983-7001.

Payne, K. A., D. R. D'Hooge, P. H. M. van Steenberge, M. F. Reyniers, M. F. Cunningham, R. A. Hutchinson, and G. B. Marin, 2013, ARGET ATRP of Butyl Methacrylate: Utilizing Kinetic Modeling To Understand Experimental Trends: Macromolecules, v. 46, p. 3828-3840.

Pladis, P., A. H. Alexopoulos, and C. Kiparissides, 2014, Mathematical Modeling and Simulation of Vinylidene Fluoride Emulsion Polymerization: Industrial & Engineering Chemistry Research, v. 53, p. 7352-7364.

Prak, D. J. L., W. I. Jahraus, J. M. Sims, and A. H. R. MacArthur, 2011, An H-1 NMR investigation into the loci of solubilization of 4-nitrotoluene, 2,6-dinitrotoluene, and 2,4,6-trinitrotoluene in nonionic surfactant micelles: Colloids and Surfaces a-Physicochemical and Engineering Aspects, v. 375, p. 12-22.

Qiu, J., S. G. Gaynor, and K. Matyjaszewski, 1999, Emulsion polymerization of n-butyl methacrylate by reverse atom transfer radical polymerization: Macromolecules, v. 32, p. 2872-2875.

Qiu, J., K. Matyjaszewski, L. Thouin, and C. Amatore, 2000a, Cyclic voltammetric studies of copper complexes catalyzing atom transfer radical polymerization: Macromolecular Chemistry and Physics, v. 201, p. 1625-1631.

Qiu, J., T. Pintauer, S. G. Gaynor, K. Matyjaszewski, B. Charleux, and J. P. Vairon, 2000b, Mechanistic aspect of reverse atom transfer radical polymerization of n-butyl methacrylate in aqueous dispersed system: Macromolecules, v. 33, p. 7310-7320.

Rabea, A. M., and S. P. Zhu, 2015, Modeling the Influence of Diffusion-Controlled Reactions and Residual Termination and Deactivation on the Rate and Control of Bulk ATRP at High Conversions: Polymers, v. 7, p. 819-835.

Schroeder, H., J. Buback, J. Schrooten, M. Buback, and K. Matyjaszewski, 2014, Modeling Atom-Transfer Radical Polymerization of Butyl Acrylate: Macromolecular Theory and Simulations, v. 23, p. 279-287.

Seeliger, F., and K. Matyjaszewski, 2009, Temperature Effect on Activation Rate Constants in ATRP: New Mechanistic Insights into the Activation Process: Macromolecules, v. 42, p. 6050-6055.

Stoffelbach, F., N. Griffete, C. Bui, and B. Charleux, 2008, Use of a simple surface-active initiator in controlled/living free-radical miniemulsion polymerization under AGET and ARGET ATRP conditions: Chemical Communications, p. 4807-4809.

Tang, W., Y. Kwak, W. Braunecker, N. V. Tsarevsky, M. L. Coote, and K. Matyjaszewski, 2008, Understanding atom transfer radical polymerization: Effect of ligand and initiator structures on the equilibrium constants: Journal of the American Chemical Society, v. 130, p. 10702-10713.

Tang, W., and K. Matyjaszewski, 2006, Effect of ligand structure on activation rate constants in ATRP: Macromolecules, v. 39, p. 4953-4959.

Tang, W., and K. Matyjaszewski, 2007, Effects of initiator structure on activation rate constants in ATRP: Macromolecules, v. 40, p. 1858-1863.

Thomson, M. E., and M. F. Cunningham, 2010, Compartmentalization Effects on the Rate of Polymerization and the Degree of Control in ATRP Aqueous Dispersed Phase Polymerization: Macromolecules, v. 43, p. 2772-2779.

Tobita, H., 1995, Monte-Carlo Simulation of Emulsion Polymerization - Linear, Branched, and Cross-Linked Polymers: Acta Polymerica, v. 46, p. 185-203.

Tobita, H., 2010, Modeling Controlled/Living Radical Polymerization Kinetics: Bulk and Miniemulsion: Macromolecular Reaction Engineering, v. 4, p. 643-662.
Tobita, H., and F. Yanase, 2007, Monte Carlo simulation of controlled/living radical polymerization in emulsified systems: Macromolecular Theory and Simulations, v. 16, p. 476-488.
Treat, N. J., H. Sprafke, J. W. Kramer, P. G. Clark, B. E. Barton, J. R. de Alaniz, B. P. Fors, and C. J. Hawker, 2014, Metal-Free Atom Transfer Radical Polymerization: Journal of the American Chemical Society, v. 136, p. 16096-16101.
Van Herk, A., ed., 2013, Chemistry and Technology of Emulsion Polymerisation: Wiley.
Van Steenberge, P. H. M., D. R. D'Hooge, M. F. Reyniers, G. B. Marin, and M. F. Cunningham, 2014, 4-Dimensional Modeling Strategy for an Improved Understanding of Miniemulsion NMP of Acrylates Initiated by SG1-Macroinitiator: Macromolecules, v. 47, p. 7732-7741.
Vanzo, E., R. H. Marchessault, and V. Stannett, 1965, Solubility and Swelling of Latex Particles: Journal of Colloid Science, v. 20, p. 62-+.
Wang, J. S., and K. Matyjaszewski, 1995a, Controlled Living Radical Polymerization - Atom Transfer Radical Polymerization in the Presence of Transition-Metal Complexes: Journal of the American Chemical Society, v. 117, p. 5614-5615.
Wang, J. S., and K. Matyjaszewski, 1995b, Controlled Living Radical Polymerization - Halogen Atom-Transfer Radical Polymerization Promoted by CU(I)CU(II) Redox Process: Macromolecules, v. 28, p. 7901-7910.
Wang, Y., Y. Kwak, J. Buback, M. Buback, and K. Matyjaszewski, 2012, Determination of ATRP Equilibrium Constants under Polymerization Conditions: Acs Macro Letters, v. 1, p. 1367-1370.
Wei, Y. P., Y. Y. Jia, W. J. Wang, B. G. Li, and S. P. Zhu, 2014, Surfactant-Ligand Design for ab Initio Emulsion Atom Transfer Radical Polymerization: Macromolecules, v. 47, p. 7701-7706.
Wu, M., L. M. F. Ramirez, A. R. Lozano, D. Quemener, J. Babin, A. Durand, E. Marie, J. L. Six, and C. Nouvel, 2015, First multi-reactive dextran-based inisurf for atom transfer radical polymerization in miniemulsion: Carbohydrate Polymers, v. 130, p. 141-148.
Yu, X. R., and L. J. Broadbelt, 2012, Kinetic Study of 1,5-Hydrogen Transfer Reactions of Methyl Acrylate and Butyl Acrylate Using Quantum Chemistry: Macromolecular Theory and Simulations, v. 21, p. 461-469.
Zaremski, M. Y., C. Xin, A. P. Orlova, I. V. Blagodatskikh, and N. I. Nikonorova, 2015, Block Copolymers of Styrene and 4-Vinylpyridine: Synthesis and Structure: Polymer Science Series B, v. 57, p. 181-196.
Zetterlund, P. B., 2010, Compartmentalization in Atom Transfer Radical Polymerization to High Conversion in Dispersed Systems: Effects of Diffusion-Controlled Reactions: Macromolecules, v. 43, p. 1387-1395.